Iron dose and form both determine growth and development outcomes of excess iron supplementation in pre-weanling rats

By

SHASTA MCMILLEN

DISSERTATION

Submitted in partial satisfaction of the requirements for the degree of

DOCTOR OF PHILOSOPHY

in

NUTRITIONAL BIOLOGY

in the

OFFICE OF GRADUATE STUDIES

of the

UNIVERSITY OF CALIFORNIA

DAVIS

Approved:

Bo Lönnerdal, Chair

Patricia Oteiza

Peng Ji

Committee in Charge

2022

ACKNOWLEDGEMENTS

My mentor and advisor, Distinguished Professor Emeritus Bo Lönnerdal, gave me the opportunity to pursue this work. When I came to his lab as an undergraduate research intern, I quickly fell in love with the research process and dedicated myself to any opportunity to participate in the research. I am forever grateful to Bo for recognizing my potential as an academic, for fueling my curiosity, encouraging my independence. He selected me as his PhD student and displayed steadfast trust in me to carry the work through, even, and most importantly, when I doubted my own abilities. I am deeply humbled to be associated with Bo's incredibly successful academic career. I am deeply thankful for all of the times he told me to keep going.

While Bo provided unparalleled knowledge and guidance in the field of pediatric nutrition, I would have been hard-pressed to complete this research without the technical expertise of my lab-mates and peers. I am thankful to Xiaogu Du, MD and Rulan Jiang, PhD for assisting me and advising me in my lab work and my animal work. I am thankful to Shannon McClorry for all of the questions she answered patiently to help me gain proficiency in microbiome analysis and the use of R programming. I would also like to thank Yu Hasegawa, PhD, and the lab of Professor Carolyn Slupsky for allowing me to use their methods to extract microbial DNA and metabolites. I would also like to acknowledge Sydney Thomas and Dr. Slupsky for collaborating on my microbiome study and contributing metabolomics analyses.

I was extremely fortunate to be mentored by Eric Nonnecke, PhD, a former student of Bo's, whose experience and skillset were invaluable to me throughout my entire PhD. I am grateful to him for the many hours spent discussing study design, methods, results, and interpretation of data. I am grateful for our ongoing collaborations that allow me the opportunity to contribute microbiome analysis and deepen my skills and knowledge in this area. Like Bo, Eric encouraged me to pursue an academic career. Most importantly, I am thankful to Eric for inviting me to participate in journal club, to read and critically review

articles. I believe that the journal club discussions we've had throughout my PhD have afforded me exceptional strengths in critical thinking, and that the skill I've gained this way will only continue to benefit my career goal of becoming a professor and leading my own research lab.

I have been fortunate to have access to one of the largest and most productive nutrition departments in the country, to be a student in one of the highest ranked nutrition graduate programs. That our program is designed as a graduate group has made it easier to access expertise in neighboring departments. I am thankful to my graduate program coordinator, Alisha Bartolomucci for being a kind and accessible administrator. I am thankful to all of the professors who taught my graduate coursework, although there are too many to name. Speaking of professors, I would also like to acknowledge to several exceptional teachers I had in high school who laid the groundwork for my doctoral pursuits: Mr. Chayo, my calculus teacher, imparted problem-solving methods that I employed throughout my PhD research; I credit Mr. Carroll, Ms. Pierce, and Mr. Rowe for teaching me how to write.

I am thankful to my qualifying exam committee for their guidance: Professors Peng Ji, Gerardo Mackenzie, Patricia Oteiza, David Mills, and Melanie Gareau. I thank Peng Ji and Patricia Oteiza for also serving on my dissertation committee; along with Bo, they provided helpful feedback and comments on my work. Additionally, I am thankful to Professor Jonathan Eisen, head of the microbiome research program at UC Davis. Jon Eisen made time to meet with me because I sought his feedback on my microbiome study, and he encouraged me to publish my results.

It goes without saying that the challenges in research itself are only part of the doctoral degree journey. Finishing this dissertation demanded immense perseverance, resilience, and dedication, which would not have been possible without the love and support of my friends and family. My mother and father have always encouraged me to dream big and to work hard. I am glad to call my graduate peers my friends, and to share this journey with them. Karli Haugen, who has been my dear friend for over a

decade and is now a third-year medical student, understands the immense social, mental, and emotional challenges of being in school for a long time. I am immensely grateful for Karli's support in every step of this degree. I am thankful for all of my friends and family – they know who they are – who have believed in me and supported me, without whom I would not have completed this journey.

Finally, I thank my husband, Jared Kessler, who in my mind has earned an honorary doctoral degree for his partnership through every step of the way. Together, he and I weathered the storm of a doctoral degree; there were so many long, hard days in the lab, immense amounts grueling animal work, and then a global pandemic. Together, we have celebrated every achievement of this degree: the preliminary exam, the qualifying exam, attending an international conference, publishing my first articles. I am in constant admiration of Jared's support, and I am so thrilled to share this triumph with him.

ABSTRACT

Iron deficiency (ID) during infancy is harmful to health and development. Iron supplements such as iron drops and fortified infant formula prevent ID effectively but typically provide 10-20x more iron than breast milk and may have adverse health and development effects when provided to infants not at high risk for ID. Adverse effects on growth, gut microbiota development, trace mineral status, neurodevelopment, and risk of morbidity have been observed, but these effects have been poorly understood. These effects and the underlying mechanisms were investigated underlying utilizing a pre-weanling rat supplementation model. In the first study, Sprague Dawley rat litters were randomly assigned to receive daily vehicle control (CON) supplementation, or 10 mg iron/kg body weight (BW) (representative of the typical daily iron intake from fortified formula) as either ferrous sulfate (FS) or ferrous bis-glycinate chelate (FC), a novel bioavailable form of iron. FS and FC groups had comparable liver iron, hemoglobin, and hematocit values that were higher than CON ($p < 0.0001$) at postnatal day (PD) 15 after 2 weeks of supplementation. BW gain was unaffected by group, but FS brains were heavier than FC brains ($p < 0.05$). In the second study, short- and long-term effects of routine iron levels on gut microbiota development were assessed. Iron supplementation induced over 10,000-fold loss of *Lactobacillus* commensal bacteria in the gut compared to CON. Gut microbiome composition and diversity depended on iron form: FS and FC gut microbiome communities were distant, and while iron reduced gut microbiota diversity, FC microbiomes were even less diverse than FS as compared to CON. Long-term effects of iron were revealed when an additional cohort of groups were supplemented with FS, FC, or CON up to weaning: adult gut microbiome compositions 6 weeks after weaning depicted a 10,000-fold loss of *Lactobacillus* if they had received iron prior to weaning, and overall microbiome also which form was provided (FS or FC). The results of the first two studies concluded that iron provision prior to weaning elevates iron status beyond needs and adversely effects long-term microbiome composition. Additionally, it was concluded that microbiome and development effects depend on the

form of iron provided. A final FS dose response study sought to identify the role of the excess iron dose in adverse health and development outcomes and found that increasing daily iron supplementation to 90 mg iron/kg BW further elevated liver iron loading, reduced pre-weanling rat weight gain and brain size, elevated inflammation, and altered levels of copper and zinc in the liver. The results of the final experiment suggest that mineral interactions and inflammatory signaling are implicated in adverse growth and development effects of excess iron. In summary, results from all three studies support that excess iron disrupts growth and development, and these effects depend upon iron form and dose. The findings provide novel evidence it is likely that the gut microbiota, inflammatory signaling, and mineral interactions may play important roles in the adverse outcomes of iron provision during infancy.

TABLE OF CONTENTS

CHAPTER 1: The Adverse Effects of Iron Supplementation During Infancy

1.1. Iron Deficiency and Iron Provision During Infancy

Iron is a transition metal, one of the trace minerals essential for human life. Basic cellular reactions like energy production and DNA replication require iron. In mammals, iron also transports oxygen in the blood as hemoglobin. Insufficient iron intake to meet basic metabolic requirements leads to deficiency. Iron deficiency (ID) is the most common single nutrient deficiency and causes of approximately half of all anemia cases worldwide [1].

Infants are especially susceptible to ID and iron deficiency anemia (IDA)[2,3]. Infants suffering from ID may suffer adverse effects to long-term cognition and behavior because critical phases of brain development during infancy are adversely affected by ID. Once ID occurs in infants, evidence suggests that correcting iron status through dietary intervention prevents anemia, but does not correct disruptions to neurodevelopment [4,5]. Since the consequences of ID during infancy are harmful—and likely irreparable—sufficient iron intake is imperative for infants.

Infants who consume exogenous iron have lower risk of developing ID, and populations with better access to supplements have lower prevalence of ID [2,6]. Iron supplements, whether iron drops, multi-nutrient packets (MNPs), fortified formula, or fortified complimentary foods, are effective at preventing or treating ID in most infants. Concern about the harms of ID in infants justifies routine use of iron supplements to prevent ID [7,8]. Based on the success of iron supplements for preventing ID and IDA, the WHO recommends that iron supplements are provided to infants in populations where anemia prevalence exceeds 40% [8]. The same rationale backs the American Academy of Pediatrics' recommendations that exclusively breast-fed infants receive iron supplements beginning at 4 months, and that formula-fed infants receive iron-fortified formula [7].

The vast difference in iron intake—between the iron supplemented infant and the un-supplemented infant receiving only breast milk—is important but generally under-recognized. The Dietary Reference Intake (DRI) for iron for infants 0-6 months is 0.3 mg per day, based on the amount provided in breast milk [9]. For healthy infants born at term, liver iron stores in combination with the small amount provided in breast milk is sufficient to support healthy growth and development up to 6 mo [10–12], but most iron-fortified formulas in the USA contain 40× more iron than breast milk [13]. Even after accounting for differences in bioavailability between breast milk iron and formula iron, formula still provides around 7× more absorbable iron than breast milk. Furthermore, the AAP recommends 1 mg iron/kg daily supplementation for all exclusively or primarily breast-fed infants [7]. Following these recommendations, an iron-supplemented 5 kg infant would receive 17× more iron than what is provided in breast milk. Routine iron supplementation practices provide large amounts of exogenous iron at an early age to ensure that ID is avoided, but the long-term health impact of such practices has not been fully investigated. The WHO and AAP recommendations may lower the risk of ID, but a growing body of evidence suggests that infants who are already at low risk of ID should not receive iron supplements due to risk of adverse effects to health and development [14–18].

Routine doses may be beneficial to ID infants, or for infants at risk of developing ID before complementary foods may be safely introduced, but for most iron-replete infants, routine doses of iron are excessive. Many infants in the USA and other countries are iron-replete, yet they are receiving exogenous iron at doses that far exceed their needs, which may have adverse, multifactorial health effects that have not been fully characterized [14,15]. The mechanisms underlying these effects must be investigated so that the risks of iron for infants can be fully identified; so that it is possible to predict infants that are most vulnerable to which adverse outcomes; and, ultimately, so that iron interventions during infancy are better informed to improve the efficacy and safety of these practices [19,20].

1.2. Adverse Health & Development Effects of Iron

Iron provided to infants at routine levels has been shown to cause inflammation and gut microbiome dysbiosis [17,21–24], disrupt trace mineral status [14,25,26], lead to poorer cognitive development [16], and, heightened risk of morbidities [17,18]. It is likely that healthy infants with normal iron status at birth are susceptible to the negative effects of iron provision, but this is not fully understood. Adverse outcomes of controlled iron supplementation studies on infants are summarized below.

1.2.1. Growth

Controlled iron supplementation studies have shown that iron negatively impacts growth of iron-replete infants [26–28], but this effect has not been consistent in all studies [29,30]. A randomized placebo-controlled trial (RCT) reported reduced length-gain and head circumference-gain to 9 mo in Swedish infants who received iron from 4-9 mo [27]. A separate RCT in Indonesia found that iron provision reduced weight-for-age and length-for-age z-scores of iron-replete infants [26]. Another RCT in South-East Asia found that iron supplementation from 6 to 12 months reduced length-for-age, but only in infants who had a healthy birth weight at baseline [28]. However, a more recent RCT from our group did not find any effects on growth metrics for healthy, full term Swedish infants from 6 weeks to 6 months [31]. A systematic review and meta-analysis of randomized controlled studies in children age 4-23 months reported negative effects of iron on weight and length gain [29], while another systematic review and meta-analysis of studies in children age 6-23 months did not find an effect on growth [30]. Yet another comparable review and meta-analysis will investigate growth effects in iron-replete infants [32]. To date, there are insufficient studies on healthy, iron-replete infants to conclude the growth effect of iron supplementation in this group. Nevertheless, that iron is disruptive to growth in some cases demands further investigation into these effects.

1.2.2. Trace Mineral Interactions

Sufficient intake of other trace minerals is essential for growth and lifelong health, but excess iron may disrupt absorption and metabolism of trace minerals. In a secondary analysis of a randomized, placebo-controlled trial, serum zinc decreased in infants after 6 months of iron supplementation, but only in infants that were iron-replete at baseline (6 months) [26]. However, a study in non-anemic Kenyan infants did not find an effect on serum zinc or zinc absorption with the addition of iron in micronutrient powder [33]. Copper-zinc superoxide (CuZnSOD) dismutase activity, a marker of copper status, was reduced in iron vs. placebo-supplemented infants at 9 months; however, no effect on serum copper was observed [25]. Insufficient research exists to ascertain that excess iron influences infant zinc and copper status, but similarities in biochemistry among iron, zinc, copper, and manganese may explain how excess iron intake compromises trace mineral metabolism. Negative effects of excess iron on zinc, copper, and manganese status in a pre-weanling rat study provides additional evidence of unfavorable mineral interactions [34].

1.2.3. Gut Microbiota

A double-blind RCT of iron in micronutrient powder (MNP) in Kenyan infants found increased abundance of *Clostridium* and *Escherichia/Shigella* — including increased pathogenic strains of *E. coli* — as well as elevated calprotectin, a measure of GI inflammation [24]. An additional robustly designed, double-blinded placebo controlled trial tested the effects of iron in MNP which was provided to 6-month old Kenyan infants for 3 months. In contrast to infants who received MNP without iron, infants who consumed MNP with iron had reduced abundance of commensal bacteria *Bifidobacterium* over time, while maintaining the abundance of *Escherichia* [22]. Another study from this group that was part of a large double-blind RCT in Kenya concluded that the addition of galacto-oligosaccharides to the MNP with iron prevented its adverse effects on the microbiome. Despite the small sample size in this study, the results provide compelling evidence that iron adversely alters microbiome development by disruption colonization by commensal bacteria [21]. A separate analysis that was part of this RCT

followed gut microbiota changes and diarrhea outcomes in infants participating in the trial that had to be treated with antibiotics. Antibiotics were not as effective at suppressing the growth of enteropathogens or reducing diarrhea incidence in infants who were receiving MNP with iron, as compared to antibiotic-treated infants receiving MNP without iron [35]. These findings suggest that infants receiving iron supplements would be more susceptible to enteropathogens and have more diarrhea despite antibiotic treatment [35].Disruptions to gut microbiota development lead to adverse effects on infant health, including alterations to GI development, metabolic signaling, brain development, and immune system development [36,37]. Therefore, further studies are necessary to define how excess iron-induced alterations to gut microbiota development during infancy impact infant health and growth [14,17].

1.2.4. Neurodevelopment

Iron provision may prevent disruptions to neurodevelopment from ID, but may also be harmful to neurodevelopment of iron-replete infants leading to long-term cognitive and behavioral deficits [38,39]. Few studies investigating neurodevelopment effects of iron measure infants' iron status prior to intervention, let alone stratify results according to baseline iron status. Fewer studies have investigated cognitive and behavioral outcomes of supplementing iron-replete infants, and the findings of these studies are not consistent [16].

A double-blind RCT in Chile was designed to test the effects of different levels of iron in infant formula (12 or 2.3 mg iron/L as FS) from 6-12 mo of age on iron status, growth, and neurodevelopment of infants who were born full-term and did not have IDA at 6 mo baseline. The study was well-powered, but the design was altered part of the way through recruitment. At the start of the study, all 6 mo old infants who had been receiving at least some formula (more than 250 mL/day) were randomized to either high-iron formula or cow's milk with vitamins but no iron. Conversely, enrolled infants who had

been primarily breast-fed up to the start of the study (less than 250 mL of formula per day) were randomized to receive a multivitamin preparation with or without iron. High-iron formula and breast-fed infants receiving multivitamins with formula were pooled into an iron supplemented group, and infants who received multivitamins without iron (whether in drops or cow's milk) were pooled into the no-iron group. The results of the pooled analysis found that iron supplemented infants had improved iron status and improved metrics of behavioral and social development, indicating improved brain development with iron. It seems that ID may have been common at 6 mo in these infants despite exclusion of infants with anemia, and this may explain why brain development was improved with iron in this study. However, growth metrics were reduced with iron supplementation. Furthermore, the change in study design and the poor control of iron intake among groups muddles the interpretation of these results [40,41]. A follow-up study reported response to reward, language abilities, and motor function was scored higher in 10-year-olds who had received additional iron as infants. These findings suggest that for populations with high rates of ID at baseline, preventative iron supplementation may improve cognitive and behavior outcomes The authors found no difference in the prevalence of ID between iron and control groups at this age, but their analysis did not determine whether baseline iron status influenced behavioral outcomes of iron provision [42]. A separate follow-up of the same RCT found that baseline hemoglobin predicted the effect of iron intake from high-iron formula on development scores: infants with higher hemoglobin levels at baseline had poorer development scores at 10 years of age if they received high-iron formula, while infants with lower hemoglobin at baseline had improved development scores [38]. More recently, an additional follow-up from this group reported adverse cognitive and behavior effects in 16-year-olds who had received high-iron formula during infancy [39].

Determining whether an optimum dose of iron exists that will support healthy brain development for most infants, regardless of their baseline iron status, will undoubtedly require robust,

well-powered studies. Unfortunately, few of these studies exist to date. A double-blind RCT of iron supplementation from 1 to 6 mo of age did not affect growth or serum zinc, nor serum copper levels of Canadian infants who were iron-replete at baseline, but increased Bayley's scores, indicating improved brain development with iron. However, infants in this study were not exclusively breast-fed outside of their iron/placebo supplement, meaning that the intake of iron from iron-fortified formula intake was not controlled, and only reported based on parental records. Additionally, the sample size at the start of this study was relatively small and the dropout rate was high at 6 mo and the 12 mo follow-up [43]. Another double-blind RCT in Spain found that adding iron to cow's milk improved the iron status of infants who were already iron-replete at baseline, but did not affect mental and psychomotor development metrics [44]. Infants in this study were iron replete at baseline. However, there was a small sample of infants in the control group: only 28 low dose iron group infants were included in the final analysis. Thus, future studies must be sufficiently powered to investigate long-term development effects of infant iron supplementation while tightly controlling for iron status and iron intake.

A systematic review of iron supplementation in children aged 4-23 months performed a meta-analysis of Bayley's mental and psychomotor development scores from prior RCTs, and the effect of iron was not significant. The authors went on to find a beneficial effect of iron on Bayley scores when iron was provided to iron-deficient children, but there were an insufficient number of well-powered studies to conclude whether iron provision is beneficial or harmful to iron-replete infants [29]. An upcoming systematic review and meta-analysis may provide further insight on this matter [32]. Animal studies provide some compelling evidence that excess iron is harmful to brain development and leads to long-term cognitive and psychomotor deficits; however, more human studies are necessary to confirm these effects [16]. Furthermore, additional animal studies are needed to investigate the short-term neurodevelopment effects of iron supplementation in healthy pre-weanling animals.

1.2.5. Morbidity

Iron provision may increase the risk of diarrhea and respiratory infections [18,29]. A previous study from our group found that diarrhea frequency increased for infants in Sweden and Honduras who had normal Hb levels at baseline, while the opposite was true for infants who were anemic at baseline [27]. For many studies reporting no effect of iron supplementation on diarrhea frequency, results are not stratified according to baseline iron status (provided that baseline iron status was measured in the study) [45–50]. One recent study, described above, found that infants who were treated with antibiotics experienced greater frequency of diarrhea if they were also receiving MNP with iron, as compared to infants who were treated with antibiotics while receiving MNP without iron, as part of a larger double-blinded RCT [35]. Increased iron availability in the gut may have increased the proliferation of diarrhea-causing bacteria *Clostridium difficile* in infants receiving high-iron formula and iron drops [23]. In summary, current evidence suggests that baseline microbiota and iron status are important factors in predicting whether iron may increase morbidities in infants.

1.3. Biological Mechanisms Underlying Adverse Effects of Iron

Animal studies, particularly mammalian research models, provide valuable insight into the mechanisms behind the adverse effects of postnatal iron supplementation, including its effects on growth, mineral status, the gut microbiota, neurodevelopment, and morbidity. So far, research in animals implies several non-mutually exclusive mechanisms, described below, are likely involved in the adverse outcomes of iron.

1.3.1. Direct Iron Toxicity

1.3.1.1. Excess Iron Causes Oxidative Stress

Iron is a pro-oxidative element, and iron overload in cells disrupts the oxidative balance by generating reactive oxygen species (ROS). Iron catalyzes the conversion of hydrogen peroxide into the highly oxidizing species hydroxyl radical. Iron overload thereby causes lipid, protein, and DNA oxidation,

which can ultimately result in, which can ultimately result in cell death. This type of cell death, termed ferroptosis, is implicated in many degenerative diseases [51,52]. Iron excess is prevented through the action of hepcidin, the iron regulatory hormone, which is expressed by liver hepatocytes in response to iron sensing [53]. Hepcidin reduces iron absorption and circulating iron levels by blocking iron export through ferroportin in the small intestine, in iron-storing hepatocytes, and in spleen reticuloendothelial macrophages [54,55]. Mutations to this pathway are the cause of hereditary hemochromatosis (HH), an iron overload disease. The pathology of HH clearly exhibits the harm of iron toxicity on biological systems. During HH, iron accumulates in the liver, the iron storage organ, but once extreme iron overload initiates liver fibrosis, then cirrhosis and loss of liver function [56,57], eventually leading to complications and death if untreated [56,57]. In HH patients, liver fibrosis is believed to result from iron-induced oxidative stress [58].

One double-blinded RCT tested varying levels of iron (either lactoferrin-bound iron or FS), as well as selenium and copper (trace minerals essential for antioxidant activity) in infant formula; a breast fed (BF) infant group was included as a control [59]. Infants receiving formula with 4 mg iron/L as lactoferrin and FS, or with 4 mg iron/L as FS, had similar plasma glutathione peroxidase activity compared to BF controls and greater activity than those receiving formula with 6.9 mg iron/L as FS. However, this may have been due to higher levels of selenium in the low-iron formulas, because selenium is a component glutathione peroxidase and required for its antioxidant activity. When the high iron formula group was compared to a low iron formula group with the same amounts of selenium and copper, there was no difference in glutathione peroxidase activity. Another RCT found that iron supplementation of infants reduced plasma copper-zinc superoxide dismutase (SOD) activity, which is an antioxidant marker as well as an indicator for copper status [25]. Few other studies in human infants have reported effects on oxidative stress markers. Animal studies provide some insight into the effects

of iron on long-term oxidative stress markers in the brain, but additional studies in infants are necessary to understand how oxidative stress might play a role in the adverse effects of iron supplementation.

1.3.1.2. Infants Are More Susceptible to Iron Toxicity

Infants may not have the same regulation of iron absorption that adults have in response to excess iron [11]. Infants tend to absorb excess iron, and this means they are more vulnerable to toxicity-related injury. Iron absorption is not well-regulated during the first year of life in human infants compared to adults [10]; iron regulation develops similarly in animal models prior to weaning [60–62]. Infants under 9 months of age will absorb iron at the same rate regardless of iron status or iron dose, and the same is true for pre-weanling mice [60], rats [61,62], and piglets [63]. Animal studies show that intestinal ferroportin is hypo-responsive to hepcidin and permits elevated iron absorption during early development, despite sufficient liver iron levels [60–64]. Resistance to hepcidin may be a component of developmental iron regulation, a mechanism in place during infancy to prevent ID, but this has not been confirmed. Iron-toxicity injuries to developing organs like the liver would explain delays in growth and other adverse effects of iron supplementation [11,14]. Current research suggests that excess iron exposure in the neonatal brain is responsible for disruptions to neurodevelopment, but this has not been confirmed, nor have other mechanisms of iron toxicity-related growth delays been investigated [14,16].

1.3.1.3. Iron Toxicity in the Brain

The essential roles of iron in neurodevelopment may be highly relevant to understanding the effects of excess iron or iron toxicity on infant neurodevelopment. Iron is required not only for CNS proliferation and differentiation—which begins prenatally and continues postnatally—but also CNS-specific pathways, including neurotransmitter synthesis and myelination [65]. Certain areas of the brain import more iron than other regions to support unique metabolic needs for development and

differentiation. For example, the adult hippocampus is heavily myelinated, and the infant hippocampus requires relatively large amounts of iron because myelin synthesis is iron-demanding and peaks at this age. Myelin sheaths in the CNS are formed by oligodendrocytes, which wrap their myelin around neuronal axons, surrounding and insulating them to reduce axon resistance and accelerate signaling speed. Oligodendrocytes and their precursors must import and store sufficient iron for myelination, which is why ID leads to insufficient myelination. This may explain how ID during infancy leads to long-term cognitive and behavioral deficits; however myelination is only one of many iron-demanding processes that take place in the CNS during the first year of life [66]. This may also explain why the hippocampus is more likely to be affected by iron loading following excess iron exposure; brain regions that are programmed to import iron rapidly at this stage of life may permit excess iron loading, and this may lead to oxidative stress and damage to CNS cells and tissues.

One animal study provided pre-weanling rats with excess iron increased total iron content in the cortex, hippocampus, substantia nigra, thalamus, deep cerebellum, and pons, but not in the striatum at PD 21. In contrast, supplying rats with iron after weaning elevated iron in the hippocampus and pons at PD 35, but not in other regions. Further, pre-weanling rats that were supplemented through weaning to PD 35 had elevated iron levels in the cortex, hippocampus, pons, and superficial cerebellum [67]. These results provide strong evidence that brain iron levels vary across brain regions following iron supplementation and are more affected by pre-weaning iron supplementation than post-weaning.

A study in Sprague Dawley rats found that neonatal exposure to excess iron (through oral gavage of 120 mg iron/kg BW as carbonyl iron) did not affect the long-term measurements of oxidative stress of the cerebellum, nor was there any effect to substantia nigra iron content at PD 200. However, at PD 400, aging rats that had been exposed to excess iron as neonates had elevated substantia nigra MDA content (a marker for oxidative stress) and reduced glutathione content (a marker for antioxidant activity). These outcomes were associated with reduced dopamine neurotransmitter content in the

striatum, as well as alterations in motor behavior. The results suggest that neonatal exposure to excess iron may lead to long-term dysfunction of the nigrostriatal pathway, a brain circuit involved in controlling movement, as well as memory and response to reward [68], and may help to explain adverse effects to cognition and psychomotor behavior scores that were observed in human infants [38]. Another study investigated how the timing of excess iron exposure affected oxidative stress in various brain regions. Rats were treated with iron PD 5-7, PD 10-12, PD 19-21 (pre-weaning), or PD 30-32 (post-weaning), and brain regions were assessed for oxidative stress at 3-5 mo of age (adulthood) [69]. All pre-weanling iron treatments increased hippocampal MDA content, and all iron treatments increased superoxide content. All pre-weanling iron treatments increased superoxide dismutase in the adult cortex and the substantia nigra. Substantia nigra MDA increased with PD 12-14 and PD 19-21 iron exposure, and cortical MDA increased with PD 19-21 exposure. In contrast, striatal MDA and superoxide production decreased with pre-weanling iron treatments. Taken together, the results provide additional evidence not only that excess iron exposure affects long-term oxidative stress in the brain, but also that brain regions are differentially affected by excess iron: pre-weanling iron exposure causes oxidative stress in the hippocampus, cortex, and substantia nigra, but may reduce oxidative stress in the striatum. Furthermore, CNS oxidative stress in this study was associated with impaired recognition memory. The hippocampus is part of the brain circuitry that encodes learning and memory—including spatial mapping and social cognition—and was also the region most consistently affected by oxidative stress in this study. The results from this study [69] and recent studies from our group in piglets [63,70] suggest oxidative stress caused by iron loading in the hippocampus is a likely mechanism by which excess iron supplementation during infancy may lead to adverse long-term effects on cognitive function.

1.3.2. Mineral Interactions

A pre-weanling rat supplementation study from our group demonstrated that tissue levels of zinc, copper, and manganese were altered by excess iron supplementation [34]. In this study, the

highest iron supplementation group had elevated liver, kidney, brain, and intestine levels of zinc. Meanwhile, liver copper levels were reduced in the high iron group. Additionally small intestine manganese levels were increased. Intriguingly, prolonged supplementation with excess iron resulted in reduced manganese levels in the small intestine and spleen, reduced brain zinc and copper levels, and reduced spleen zinc and manganese, although liver zinc remained elevated. Few other studies have reported the effect of excess iron on trace mineral metabolism or storage.

The transporters DMT1, ZIP8, and ZIP14 import divalent metals including iron, copper, zinc, and manganese [62,71–73], therefore it is possible that high levels of iron may out-compete other divalent metals for import, and this may explain alterations in availability of these minerals due to excess iron supplementation. Cellular iron loading upregulates trace metal binding and storage proteins copper-zinc SOD, manganese SOD, metallothioneins (MT), and ceruloplasmin (CP). MTs, CP, and copper-zinc or manganese SODs require these metals to function as ROS scavengers. Oxidative stress and iron loading both upregulate antioxidant, metal-binding proteins including MTs, SODs, and CP. Thus, excess iron may interrupt uptake of other trace minerals while increasing demand for these trace minerals to combat oxidative stress, possibly explaining how trace mineral status is compromised by excess iron. Since zinc and copper are needed for basic metabolism, growth, and resistance to infection, disrupting their availability to growing organs and tissues would disrupt development and health [9]. However, it remains to be investigated if mineral interactions in the context of excess iron are linked to the other adverse health and development effects of excess iron.

1.3.3. **Gut Microbiota & Gut Health**

1.3.3.1. Iron and Gastrointestinal Inflammation

Low bioavailability of iron from most supplements means that the majority of iron—approximately 90% of FS iron—ingested by infants remains in the gastrointestinal (GI) tract until it is

excreted [10]. Infancy is a critical period for symbiotic gut microbiota colonization and recent studies show that iron supplements alter the gut microbiota in ways that may be unfavorable to infant health [21–24]. Alterations to the gut microbiota may explain GI distress side effects, as well as several other adverse health and development outcomes of iron. The GI distress side effects of FS iron supplements are well-established. In a systematic review and meta-analysis of GI side effects of FS for adults, after pooling data from 43 studies, the authors estimated an 11% incidence rate for nausea, 12% for constipation, and 8% for diarrhea [74]. Another systematic review and meta-analysis estimated that 1 in 3 adults who received FS supplementation experiences adverse effects [75]. It seems likely that infants would be affected similarly, but this has not been fully investigated. Enteropathogens may invade more easily during this age due to immature barrier function of the intestinal mucosa [76], leading to diarrhea or other infections, which are harmful to health and development [18,77]. Bacteria translocating across the mucosa would trigger pro-inflammatory signaling, perhaps leading to diarrhea, both of which are likely to hinder the nutrient absorption capacity of the GI tract [78]. Prolonged GI inflammation or diarrhea might therefore reduce an infant's growth rate, suggesting GI effects are mechanistically related to adverse growth and development effects of excess iron.

1.3.3.2. Iron and the Gut Microbiota

An important aspect of development involves healthy colonization of the gut with commensal microbes, because the gut microbiota provide essential roles to their host's health and development [37,79,80]. Besides maternal microbiota and birth method, the infant diet is the major determinant of gut colonization [80–83]. Breastfeeding and breast milk support healthy gut microbiota development by providing prebiotic oligosaccharides that preferentially craft the infant gut so that it is dominated by commensal *Bifidobacterium infantis*, which serves multiple health and development roles [84–87]. *Bifidobacterium infantis* has been shown to suppress the proliferation of pathogens and improve the integrity of the mucosal barrier, preventing inflammation and diarrhea [87]. Multiple studies have

shown that iron reduces the abundance of commensal bacteria (including *Bifidobacterium infantis*) and elevates pathogen-associated bacteria [17,22,35]. These alterations to the gut microbiota were associated with GI inflammation for Kenyan infants, but this result has not yet been confirmed in other studies [24]. Since commensal gut bacteria are so important for health and development, disrupting healthy colonization with commensals might explain some adverse outcomes of iron [21,36,37]. Iron-replete infant gut microbiomes may be more adversely affected by iron, but only one study has investigated gut microbiota outcomes in healthy, iron-replete infants [23].

Considering that infant gut microbiota development is so important for overall development and that increased iron levels in the gut may cause adverse GI side effects and gut microbiota dysbiosis, it seems likely that the gut microbiota is implicated in the adverse development effects of excess iron. Additional studies in animal models should characterize effects of excess iron on gut microbiota development and generate hypotheses about iron-induced alterations to the microbiota that may be causing adverse health and development outcomes.

1.4. Rationale Statement

The capacity of exogenous iron provision, at routine levels, to disrupt health and development of otherwise healthy infants who are iron-replete is unclear. Further, translationally optimized animal models are necessary to investigate the mechanisms behind adverse effects to infant health. Excess iron provision may delay growth, neurodevelopment, and increase susceptibility to disease and infection, and it is likely that iron toxicity, mineral interactions, and the gut microbiota are behind these outcomes.

A pre-weanling rat supplementation model developed by our group was used to study excess iron supplementation outcomes and their underlying mechanisms. Effects of iron dose and form on growth, neurodevelopment, and the gut microbiota were investigated, with the goal of informing iron supplementation practices for infants.

1.5. References

1. Miller, J.L. Iron Deficiency Anemia: A Common and Curable Disease. *Cold Spring Harbor Perspectives in Medicine* **2013**, *3*, a011866–a011866, doi:10.1101/cshperspect.a011866.
2. Burke, R.; Leon, J.; Suchdev, P. Identification, Prevention and Treatment of Iron Deficiency during the First 1000 Days. *Nutrients* **2014**, *6*, 4093–4114, doi:10.3390/nu6104093.
3. Yang, Z.; Lönnerdal, B.; Adu-Afarwuah, S.; Brown, K.H.; Chaparro, C.M.; Cohen, R.J.; Domellöf, M.; Hernell, O.; Lartey, A.; Dewey, K.G. Prevalence and Predictors of Iron Deficiency in Fully Breastfed Infants at 6 Mo of Age: Comparison of Data from 6 Studies. *The American Journal of Clinical Nutrition* **2009**, *89*, 1433–1440, doi:10.3945/ajcn.2008.26964.
4. Lozoff, B.; Beard, J.; Connor, J.; Barbara, F.; Georgieff, M.; Schallert, T. Long-Lasting Neural and Behavioral Effects of Iron Deficiency in Infancy. *Nutr Rev* **2006**, *64*, S34-43; discussion S72-91, doi:10.1301/nr.2006.may.s34-s43.
5. East, P.; Doom, J.R.; Blanco, E.; Burrows, R.; Lozoff, B.; Gahagan, S. Iron Deficiency in Infancy and Neurocognitive and Educational Outcomes in Young Adulthood. *Developmental Psychology* **2021**, *57*, 962–975, doi:10.1037/dev0001030.
6. *Worldwide Prevalence of Anaemia 1993-2005: WHO Global Database on Anemia*; De Benoist, B., McLean, E., Egli, I., Cogswell, M.E., Eds.; World Health Organization: Geneva, 2008; ISBN 978 92 4 159665 7.
7. Shelov, S.P.; American Academy of Pediatrics *Caring for Your Baby and Young Child: Birth to Age Five*; Bantam: New York, 2009; ISBN 978-0-553-38630-1.
8. World Health Organization *Iron Deficiency Anaemia: Assessment, Prevention, and Control. A Guide for Programme Managers.*; World Health Organization: Geneva, 2001;
9. *DRI: Dietary Reference Intakes for Vitamin A, Vitamin K, Arsenic, Boron, Chromium, Copper, Iodine, Iron, Manganese, Molybdenum, Nickel, Silicon, Vanadium, and Zinc: A Report of the Panel on Micronutrients ... and the Standing Committee on the Scientific Evaluation of Dietary Reference Intakes, Food and Nutrition Board, Institute of Medicine*; Institute of Medicine (U.S.), Ed.; National Academy Press: Washington, D.C, 2001; ISBN 978-0-309-07279-3.
10. Domellöf, M.; Lönnerdal, B.; Abrams, S.A.; Hernell, O. Iron Absorption in Breast-Fed Infants: Effects of Age, Iron Status, Iron Supplements, and Complementary Foods. *The American Journal of Clinical Nutrition* **2002**, *76*, 198–204, doi:10.1093/ajcn/76.1.198.
11. Lönnerdal, B. Development of Iron Homeostasis in Infants and Young Children. *Am J Clin Nutr* **2017**, *106*, 1575S-1580S, doi:10.3945/ajcn.117.155820.
12. Lönnerdal, B.; Georgieff, M.K.; Hernell, O. Developmental Physiology of Iron Absorption, Homeostasis, and Metabolism in the Healthy Term Infant. *The Journal of Pediatrics* **2015**, *167*, S8–S14, doi:10.1016/j.jpeds.2015.07.014.
13. Lönnerdal, B. Iron, Zinc, Copper, and Manganese in Infant Formulas. *Arch Pediatr Adolesc Med* **1983**, *137*, 433, doi:10.1001/archpedi.1983.02140310015003.
14. Lönnerdal, B. Excess Iron Intake as a Factor in Growth, Infections, and Development of Infants and Young Children. *Am J Clin Nutr* **2017**, *106*, 1681S-1687S, doi:10.3945/ajcn.117.156042.
15. Wessling-Resnick, M. Excess Iron: Considerations Related to Development and Early Growth. *Am J Clin Nutr* **2017**, *106*, 1600S-1605S, doi:10.3945/ajcn.117.155879.
16. Agrawal, S.; Berggren, K.L.; Marks, E.; Fox, J.H. Impact of High Iron Intake on Cognition and Neurodegeneration in Humans and in Animal Models: A Systematic Review. *Nutr Rev* **2017**, *75*, 456–470, doi:10.1093/nutrit/nux015.

17. Paganini, D.; Zimmermann, M.B. The Effects of Iron Fortification and Supplementation on the Gut Microbiome and Diarrhea in Infants and Children: A Review. *Am J Clin Nutr* **2017**, *106*, 1688S-1693S, doi:10.3945/ajcn.117.156067.
18. Ghanchi, A.; James, P.T.; Cerami, C. Guts, Germs, and Iron: A Systematic Review on Iron Supplementation, Iron Fortification, and Diarrhea in Children Aged 4–59 Months. *Current Developments in Nutrition* **2019**, *3*, doi:10.1093/cdn/nzz005.
19. Allen, L.H. Iron Supplements: Scientific Issues Concerning Efficacy and Implications for Research and Programs. *J Nutr* **2002**, *132*, 813S-9S, doi:10.1093/jn/132.4.813S.
20. Dietary Guidelines Advisory Committee *Scientific Report of the 2020 Dietary Guidelines Advisory Committee: Advisory Report to the Secretary of Agriculture and the Secretary of Health and Human Services*; U.S. Department of Agriculture, Agricultural Research Service: Washington, DC, 2020; p. 786;.
21. Paganini, D.; Uyoga, M.A.; Kortman, G.A.M.; Cercamondi, C.I.; Moretti, D.; Barth-Jaeggi, T.; Schwab, C.; Boekhorst, J.; Timmerman, H.M.; Lacroix, C.; et al. Prebiotic Galacto-Oligosaccharides Mitigate the Adverse Effects of Iron Fortification on the Gut Microbiome: A Randomised Controlled Study in Kenyan Infants. *Gut* **2017**, *66*, 1956–1967, doi:10.1136/gutjnl-2017-314418.
22. Tang, M.; Frank, D.N.; Hendricks, A.E.; Ir, D.; Esamai, F.; Liechty, E.; Hambidge, K.M.; Krebs, N.F. Iron in Micronutrient Powder Promotes an Unfavorable Gut Microbiota in Kenyan Infants. *Nutrients* **2017**, *9*, doi:10.3390/nu9070776.
23. Simonyté Sjödin, K.; Domellöf, M.; Lagerqvist, C.; Hernell, O.; Lönnerdal, B.; Szymlek-Gay, E.A.; Sjödin, A.; West, C.E.; Lind, T. Administration of Ferrous Sulfate Drops Has Significant Effects on the Gut Microbiota of Iron-Sufficient Infants: A Randomised Controlled Study. *Gut* **2019**, *68*, 2095–2097, doi:10.1136/gutjnl-2018-316988.
24. Jaeggi, T.; Kortman, G.A.M.; Moretti, D.; Chassard, C.; Holding, P.; Dostal, A.; Boekhorst, J.; Timmerman, H.M.; Swinkels, D.W.; Tjalsma, H.; et al. Iron Fortification Adversely Affects the Gut Microbiome, Increases Pathogen Abundance and Induces Intestinal Inflammation in Kenyan Infants. *Gut* **2015**, *64*, 731–742, doi:10.1136/gutjnl-2014-307720.
25. Domellöf, M.; Dewey, K.G.; Cohen, R.J.; Lönnerdal, B.; Hernell, O. Iron Supplements Reduce Erythrocyte Copper-Zinc Superoxide Dismutase Activity in Term, Breastfed Infants. *Acta Paediatr* **2005**, *94*, 1578–1582, doi:10.1080/08035250500252674.
26. Lind, T.; Seswandhana, R.; Persson, L.-A.; Lönnerdal, B. Iron Supplementation of Iron-Replete Indonesian Infants Is Associated with Reduced Weight-for-Age. *Acta Paediatr* **2008**, *97*, 770–775, doi:10.1111/j.1651-2227.2008.00773.x.
27. Dewey, K.G.; Domellöf, M.; Cohen, R.J.; Landa Rivera, L.; Hernell, O.; Lönnerdal, B. Iron Supplementation Affects Growth and Morbidity of Breast-Fed Infants: Results of a Randomized Trial in Sweden and Honduras. *The Journal of Nutrition* **2002**, *132*, 3249–3255, doi:10.1093/jn/132.11.3249.
28. Dijkhuizen, M.A.; Winichagoon, P.; Wieringa, F.T.; Wasantwisut, E.; Utomo, B.; Ninh, N.X.; Hidayat, A.; Berger, J. Zinc Supplementation Improved Length Growth Only in Anemic Infants in a Multi-Country Trial of Iron and Zinc Supplementation in South-East Asia. *J Nutr* **2008**, *138*, 1969–1975, doi:10.1093/jn/138.10.1969.
29. Pasricha, S.-R.; Hayes, E.; Kalumba, K.; Biggs, B.-A. Effect of Daily Iron Supplementation on Health in Children Aged 4-23 Months: A Systematic Review and Meta-Analysis of Randomised Controlled Trials. *Lancet Glob Health* **2013**, *1*, e77–e86, doi:10.1016/S2214-109X(13)70046-9.
30. Petry, N.; Olofin, I.; Boy, E.; Donahue Angel, M.; Rohner, F. The Effect of Low Dose Iron and Zinc Intake on Child Micronutrient Status and Development during the First 1000 Days of Life: A Systematic Review and Meta-Analysis. *Nutrients* **2016**, *8*, doi:10.3390/nu8120773.

31. Björmsjö, M.; Hernell, O.; Lönnerdal, B.; Berglund, S.K. Reducing Iron Content in Infant Formula from 8 to 2 Mg/L Does Not Increase the Risk of Iron Deficiency at 4 or 6 Months of Age: A Randomized Controlled Trial. *Nutrients* **2020**, *13*, 3, doi:10.3390/nu13010003.
32. Hare, D.J.; Braat, S.; Cardoso, B.R.; Morgan, C.; Szymlek-Gay, E.A.; Biggs, B.-A. Health Outcomes of Iron Supplementation and/or Food Fortification in Iron-Replete Children Aged 4–24 Months: Protocol for a Systematic Review and Meta-Analysis. *Syst Rev* **2019**, *8*, 253, doi:10.1186/s13643-019-1185-3.
33. Esamai, F.; Liechty, E.; Ikemeri, J.; Westcott, J.; Kemp, J.; Culbertson, D.; Miller, L.V.; Hambidge, K.M.; Krebs, N.F. Zinc Absorption from Micronutrient Powder Is Low but Is Not Affected by Iron in Kenyan Infants. *Nutrients* **2014**, *6*, 5636–5651, doi:10.3390/nu6125636.
34. Leong, W.-I.; Bowlus, C.L.; Tallkvist, J.; Lönnerdal, B. Iron Supplementation during Infancy—Effects on Expression of Iron Transporters, Iron Absorption, and Iron Utilization in Rat Pups. *The American Journal of Clinical Nutrition* **2003**, *78*, 1203–1211, doi:10.1093/ajcn/78.6.1203.
35. Paganini, D.; Uyoga, M.A.; Kortman, G.A.M.; Cercamondi, C.I.; Winkler, H.C.; Boekhorst, J.; Moretti, D.; Lacroix, C.; Karanja, S.; Zimmermann, M.B. Iron-Containing Micronutrient Powders Modify the Effect of Oral Antibiotics on the Infant Gut Microbiome and Increase Post-Antibiotic Diarrhoea Risk: A Controlled Study in Kenya. *Gut* **2019**, *68*, 645–653, doi:10.1136/gutjnl-2018-317399.
36. Xu, J.; Gordon, J.I. Honor Thy Symbionts. *Proceedings of the National Academy of Sciences* **2003**, *100*, 10452–10459, doi:10.1073/pnas.1734063100.
37. Dominguez-Bello, M.G.; Godoy-Vitorino, F.; Knight, R.; Blaser, M.J. Role of the Microbiome in Human Development. *Gut* **2019**, *68*, 1108–1114, doi:10.1136/gutjnl-2018-317503.
38. Lozoff, B. Iron-Fortified vs Low-Iron Infant Formula: Developmental Outcome at 10 Years. *Arch Pediatr Adolesc Med* **2012**, *166*, 208, doi:10.1001/archpediatrics.2011.197.
39. Gahagan, S.; Delker, E.; Blanco, E.; Burrows, R.; Lozoff, B. Randomized Controlled Trial of Iron-Fortified versus Low-Iron Infant Formula: Developmental Outcomes at 16 Years. *J Pediatr* **2019**, *212*, 124-130.e1, doi:10.1016/j.jpeds.2019.05.030.
40. Lozoff, B.; De Andraca, I.; Castillo, M.; Smith, J.B.; Walter, T.; Pino, P. Behavioral and Developmental Effects of Preventing Iron-Deficiency Anemia in Healthy Full-Term Infants. *Pediatrics* **2003**, *112*, 846–854.
41. Walter, T.; Pino, P.; Pizarro, F.; Lozoff, B. Prevention of Iron-Deficiency Anemia: Comparison of High- and Low-Iron Formulas in Term Healthy Infants after Six Months of Life. *J Pediatr* **1998**, *132*, 635–640, doi:10.1016/s0022-3476(98)70352-x.
42. Lozoff, B.; Castillo, M.; Clark, K.M.; Smith, J.B.; Sturza, J. Iron Supplementation in Infancy Contributes to More Adaptive Behavior at 10 Years of Age. *J Nutr* **2014**, *144*, 838–845, doi:10.3945/jn.113.182048.
43. Friel, J.K.; Aziz, K.; Andrews, W.L.; Harding, S.V.; Courage, M.L.; Adams, R.J. A Double-Masked, Randomized Control Trial of Iron Supplementation in Early Infancy in Healthy Term Breast-Fed Infants. *J Pediatr* **2003**, *143*, 582–586, doi:10.1067/S0022-3476(03)00301-9.
44. Iglesias Vázquez, L.; Canals, J.; Voltas, N.; Jardí, C.; Hernández, C.; Bedmar, C.; Escribano, J.; Aranda, N.; Jiménez, R.; Barroso, J.M.; et al. Does the Fortified Milk with High Iron Dose Improve the Neurodevelopment of Healthy Infants? Randomized Controlled Trial. *BMC Pediatr* **2019**, *19*, 315, doi:10.1186/s12887-019-1679-0.
45. Lind, T.; Lönnerdal, B.; Stenlund, H.; Gamayanti, I.L.; Ismail, D.; Seswandhana, R.; Persson, L.-A. A Community-Based Randomized Controlled Trial of Iron and Zinc Supplementation in Indonesian Infants: Effects on Growth and Development. *Am J Clin Nutr* **2004**, *80*, 729–736, doi:10.1093/ajcn/80.3.729.

46. Nagpal, J.; Sachdev, H.P.S.; Singh, T.; Mallika, V. A Randomized Placebo-Controlled Trial of Iron Supplementation in Breastfed Young Infants Initiated on Complementary Feeding: Effect on Haematological Status. *J Health Popul Nutr* **2004**, *22*, 203–211.
47. Bora, R.; Ramasamy, S.; Brown, B.; Wolfson, J.; Rao, R. Effect of Iron Supplementation from Neonatal Period on the Iron Status Of6-Month-Old Infants at-Risk for Early Iron Deficiency: A Randomized Interventional Trial. *J Matern Fetal Neonatal Med* **2019**, 1–9, doi:10.1080/14767058.2019.1638358.
48. Ermis, B.; Demirel, F.; Demircan, N.; Gurel, A. Effects of Three Different Iron Supplementations in Term Healthy Infants after 5 Months of Life. *J Trop Pediatr* **2002**, *48*, 280–284, doi:10.1093/tropej/48.5.280.
49. Smuts, C.M.; Dhansay, M.A.; Faber, M.; van Stuijvenberg, M.E.; Swanevelder, S.; Gross, R.; Benadé, A.J.S. Efficacy of Multiple Micronutrient Supplementation for Improving Anemia, Micronutrient Status, and Growth in South African Infants. *J Nutr* **2005**, *135*, 653S-659S, doi:10.1093/jn/135.3.653S.
50. Silva, D.G.; Franceschini, S. do C.C.; Sigulem, D.M. Growth in Non-Anemic Infants Supplemented with Different Prophylactic Iron Doses. *J Pediatr (Rio J)* **2008**, *84*, 365–372, doi:10.2223/JPED.1817.
51. Chen, X.; Yu, C.; Kang, R.; Tang, D. Iron Metabolism in Ferroptosis. *Front. Cell Dev. Biol.* **2020**, *8*, 590226, doi:10.3389/fcell.2020.590226.
52. Li, J.; Cao, F.; Yin, H.; Huang, Z.; Lin, Z.; Mao, N.; Sun, B.; Wang, G. Ferroptosis: Past, Present and Future. *Cell Death Dis* **2020**, *11*, 88, doi:10.1038/s41419-020-2298-2.
53. Wang, C.-Y.; Babitt, J.L. Liver Iron Sensing and Body Iron Homeostasis. *Blood* **2019**, *133*, 18–29, doi:10.1182/blood-2018-06-815894.
54. Billesbølle, C.B.; Azumaya, C.M.; Kretsch, R.C.; Powers, A.S.; Gonen, S.; Schneider, S.; Arvedson, T.; Dror, R.O.; Cheng, Y.; Manglik, A. Structure of Hepcidin-Bound Ferroportin Reveals Iron Homeostatic Mechanisms. *Nature* **2020**, *586*, 807–811, doi:10.1038/s41586-020-2668-z.
55. Nemeth, E. Hepcidin Regulates Cellular Iron Efflux by Binding to Ferroportin and Inducing Its Internalization. *Science* **2004**, *306*, 2090–2093, doi:10.1126/science.1104742.
56. Niederau, C.; Fischer, R.; Sonnenberg, A.; Stremmel, W.; Trampisch, H.J.; Strohmeyer, G. Survival and Causes of Death in Cirrhotic and in Noncirrhotic Patients with Primary Hemochromatosis. *N Engl J Med* **1985**, *313*, 1256–1262, doi:10.1056/NEJM198511143132004.
57. Deugnier, Y.M.; Loréal, O.; Turlin, B.; Guyader, D.; Jouanolle, H.; Moirand, R.; Jacquelinet, C.; Brissot, P. Liver Pathology in Genetic Hemochromatosis: A Review of 135 Homozygous Cases and Their Bioclinical Correlations. *Gastroenterology* **1992**, *102*, 2050–2059, doi:10.1016/0016-5085(92)90331-R.
58. Houglum, K.; Ramm, G.A.; Crawford, D.H.; Witztum, J.L.; Powell, L.W.; Chojkier, M. Excess Iron Induces Hepatic Oxidative Stress and Transforming Growth Factor ?1 in Genetic Hemochromatosis. *Hepatology* **1997**, *26*, 605–610, doi:10.1002/hep.510260311.
59. Lönnerdal, B.; Hernell, O. Iron, Zinc, Copper and Selenium Status of Breast-Fed Infants and Infants Fed Trace Element Fortified Milk-Based Infant Formula. *Acta Paediatrica* **1994**, *83*, 367–373, doi:10.1111/j.1651-2227.1994.tb18121.x.
60. Frazer, D.M.; Wilkins, S.J.; Darshan, D.; Mirciov, C.S.G.; Dunn, L.A.; Anderson, G.J. Ferroportin Is Essential for Iron Absorption During Suckling, But Is Hyporesponsive to the Regulatory Hormone Hepcidin. *Cellular and Molecular Gastroenterology and Hepatology* **2017**, *3*, 410–421, doi:10.1016/j.jcmgh.2016.12.002.
61. Darshan, D.; Wilkins, S.J.; Frazer, D.M.; Anderson, G.J. Reduced Expression of Ferroportin-1 Mediates Hyporesponsiveness of Suckling Rats to Stimuli That Reduce Iron Absorption. *Gastroenterology* **2011**, *141*, 300–309, doi:10.1053/j.gastro.2011.04.012.

62. Leong, W.-I.; Bowlus, C.L.; Tallkvist, J.; Lönnerdal, B. DMT1 and FPN1 Expression during Infancy: Developmental Regulation of Iron Absorption. *American Journal of Physiology-Gastrointestinal and Liver Physiology* **2003**, *285*, G1153–G1161, doi:10.1152/ajpgi.00107.2003.
63. Ji, P.; Lönnerdal, B.; Kim, K.; Jinno, C.N. Iron Oversupplementation Causes Hippocampal Iron Overloading and Impairs Social Novelty Recognition in Nursing Piglets. *J Nutr* **2019**, *149*, 398–405, doi:10.1093/jn/nxy227.
64. McMillen, S.; Lönnerdal, B. Postnatal Iron Supplementation with Ferrous Sulfate vs. Ferrous Bis-Glycinate Chelate: Effects on Iron Metabolism, Growth, and Central Nervous System Development in Sprague Dawley Rat Pups. *Nutrients* **2021**, *13*, 1406, doi:10.3390/nu13051406.
65. McCann, S.; Perapoch Amadó, M.; Moore, S.E. The Role of Iron in Brain Development: A Systematic Review. *Nutrients* **2020**, *12*, 2001, doi:10.3390/nu12072001.
66. Todorich, B.; Pasquini, J.M.; Garcia, C.I.; Paez, P.M.; Connor, J.R. Oligodendrocytes and Myelination: The Role of Iron. *Glia* **2009**, *57*, 467–478, doi:10.1002/glia.20784.
67. Piñero, D.J.; Li, N.-Q.; Connor, J.R.; Beard, J.L. Variations in Dietary Iron Alter Brain Iron Metabolism in Developing Rats. *The Journal of Nutrition* **2000**, *130*, 254–263, doi:10.1093/jn/130.2.254.
68. Chen, H.; Wang, X.; Wang, M.; Yang, L.; Yan, Z.; Zhang, Y.; Liu, Z. Behavioral and Neurochemical Deficits in Aging Rats with Increased Neonatal Iron Intake: Silibinin's Neuroprotection by Maintaining Redox Balance. *Front Aging Neurosci* **2015**, *7*, 206, doi:10.3389/fnagi.2015.00206.
69. de Lima, M.N.M.; Polydoro, M.; Laranja, D.C.; Bonatto, F.; Bromberg, E.; Moreira, J.C.F.; Dal-Pizzol, F.; Schröder, N. Recognition Memory Impairment and Brain Oxidative Stress Induced by Postnatal Iron Administration. *Eur J Neurosci* **2005**, *21*, 2521–2528, doi:10.1111/j.1460-9568.2005.04083.x.
70. Ji, P.; B Nonnecke, E.; Doan, N.; Lönnerdal, B.; Tan, B. Excess Iron Enhances Purine Catabolism Through Activation of Xanthine Oxidase and Impairs Myelination in the Hippocampus of Nursing Piglets. *J Nutr* **2019**, *149*, 1911–1919, doi:10.1093/jn/nxz166.
71. Liu, Q.; Barker, S.; Knutson, M.D. Iron and Manganese Transport in Mammalian Systems. *Biochimica et Biophysica Acta (BBA) - Molecular Cell Research* **2021**, *1868*, 118890, doi:10.1016/j.bbamcr.2020.118890.
72. Aydemir, T.B.; Cousins, R.J. The Multiple Faces of the Metal Transporter ZIP14 (SLC39A14). *The Journal of Nutrition* **2018**, *148*, 174–184, doi:10.1093/jn/nxx041.
73. Wang, C.-Y.; Jenkitkasemwong, S.; Duarte, S.; Sparkman, B.K.; Shawki, A.; Mackenzie, B.; Knutson, M.D. ZIP8 Is an Iron and Zinc Transporter Whose Cell-Surface Expression Is Up-Regulated by Cellular Iron Loading. *Journal of Biological Chemistry* **2012**, *287*, 34032–34043, doi:10.1074/jbc.M112.367284.
74. Tolkien, Z.; Stecher, L.; Mander, A.P.; Pereira, D.I.A.; Powell, J.J. Ferrous Sulfate Supplementation Causes Significant Gastrointestinal Side-Effects in Adults: A Systematic Review and Meta-Analysis. *PLoS ONE* **2015**, *10*, e0117383, doi:10.1371/journal.pone.0117383.
75. Cancelo-Hidalgo, M.J.; Castelo-Branco, C.; Palacios, S.; Haya-Palazuelos, J.; Ciria-Recasens, M.; Manasanch, J.; Pérez-Edo, L. Tolerability of Different Oral Iron Supplements: A Systematic Review. *Current Medical Research and Opinion* **2013**, *29*, 291–303, doi:10.1185/03007995.2012.761599.
76. Chin, A.M.; Hill, D.R.; Aurora, M.; Spence, J.R. Morphogenesis and Maturation of the Embryonic and Postnatal Intestine. *Seminars in Cell & Developmental Biology* **2017**, *66*, 81–93, doi:10.1016/j.semcdb.2017.01.011.
77. Black, R.E.; Heidkamp, R. Causes of Stunting and Preventive Dietary Interventions in Pregnancy and Early Childhood. In *Nestlé Nutrition Institute Workshop Series*; Colombo, J., Koletzko, B., Lampl, M., Eds.; S. Karger AG, 2018; Vol. 89, pp. 105–113 ISBN 978-3-318-06351-6.
78. Brown, K.H. Diarrhea and Malnutrition. *The Journal of Nutrition* **2003**, *133*, 328S-332S, doi:10.1093/jn/133.1.328S.

79. Koenig, J.E.; Spor, A.; Scalfone, N.; Fricker, A.D.; Stombaugh, J.; Knight, R.; Angenent, L.T.; Ley, R.E. Succession of Microbial Consortia in the Developing Infant Gut Microbiome. *Proceedings of the National Academy of Sciences* **2011**, *108*, 4578–4585, doi:10.1073/pnas.1000081107.
80. Moore, R.E.; Townsend, S.D. Temporal Development of the Infant Gut Microbiome. *Open Biol.* **2019**, *9*, 190128, doi:10.1098/rsob.190128.
81. Mueller, N.T.; Bakacs, E.; Combellick, J.; Grigoryan, Z.; Dominguez-Bello, M.G. The Infant Microbiome Development: Mom Matters. *Trends in Molecular Medicine* **2015**, *21*, 109–117, doi:10.1016/j.molmed.2014.12.002.
82. Nielsen, S.; Nielsen, D.S.; Lauritzen, L.; Jakobsen, M.; Michaelsen, K.F. Impact of Diet on the Intestinal Microbiota in 10-Month-Old Infants. *J Pediatr Gastroenterol Nutr* **2007**, *44*, 613–618, doi:10.1097/MPG.0b013e3180406a11.
83. O'Sullivan, A.; He, X.; McNiven, E.M.S.; Haggarty, N.W.; Lönnerdal, B.; Slupsky, C.M. Early Diet Impacts Infant Rhesus Gut Microbiome, Immunity, and Metabolism. *J. Proteome Res.* **2013**, *12*, 2833–2845, doi:10.1021/pr4001702.
84. Zivkovic, A.M.; German, J.B.; Lebrilla, C.B.; Mills, D.A. Human Milk Glycobiome and Its Impact on the Infant Gastrointestinal Microbiota. *Proceedings of the National Academy of Sciences* **2011**, *108*, 4653–4658, doi:10.1073/pnas.1000083107.
85. Bode, L. Human Milk Oligosaccharides: Every Baby Needs a Sugar Mama. *Glycobiology* **2012**, *22*, 1147–1162, doi:10.1093/glycob/cws074.
86. Pacheco, A.R.; Barile, D.; Underwood, M.A.; Mills, D.A. The Impact of the Milk Glycobiome on the Neonate Gut Microbiota. *Annu. Rev. Anim. Biosci.* **2015**, *3*, 419–445, doi:10.1146/annurev-animal-022114-111112.
87. Fukuda, S.; Toh, H.; Hase, K.; Oshima, K.; Nakanishi, Y.; Yoshimura, K.; Tobe, T.; Clarke, J.M.; Topping, D.L.; Suzuki, T.; et al. Bifidobacteria Can Protect from Enteropathogenic Infection through Production of Acetate. *Nature* **2011**, *469*, 543–547, doi:10.1038/nature09646.

CHAPTER 2: Postnatal Iron Supplementation with Ferrous Sulfate vs. Ferrous Bis-Glycinate Chelate: Effects on Iron Metabolism, Growth, and Central Nervous System Development in Sprague Dawley Rat Pups

ABSTRACT

Iron-fortified formulas and iron drops (both usually ferrous sulfate, FS) prevent early life iron deficiency, but may delay growth and adversely affect neurodevelopment by providing excess iron. We used a rat pup model to investigate iron status, growth, and development outcomes following daily iron supplementation (10 mg iron/kg body weight, representative of iron-fortified formula levels) with FS or an alternative, bioavailable form of iron, ferrous bis-glycinate chelate (FC). On postnatal day (PD) 2, sex-matched rat litters (n = 3 litters, 10 pups each) were randomly assigned to receive FS, FC, or vehicle control until PD 14. On PD 15, we evaluated systemic iron regulation and CNS mineral interactions and we interrogated iron loading outcomes in the hippocampus, in search of mechanisms by which iron may influence neurodevelopment. Body iron stores were elevated substantially in iron-supplemented pups. All pups gained weight normally, but brain size on PD 15 was dependent on iron source. This may have been associated with reduced hippocampal oxidative stress but was not associated with CNS mineral interactions, iron regulation, or myelination, as these were unchanged with iron supplementation. Additional studies are warranted to investigate iron form effects on neurodevelopment so that iron recommendations can be optimized for all infants.

2.1. INTRODUCTION

Postnatal iron deficiency (ID) adversely affects both physical and cognitive development and should be prevented [1–5]. The American Academy of Pediatrics recommends infants receive iron through liquid supplements or fortified formula to prevent ID [6]. Iron-fortified formulas prevent postnatal ID effectively but provide, on average, 20 times the adequate intake (AI) for infants 0–6

months of age [7,8]. Excess iron can also be harmful to infants, and recent studies report adverse effects of iron supplementation in infants who are not ID [9–14]. In response to rising concern regarding the efficacy of blanket iron supplementation in infants, pediatric nutrition researchers as well as expert committees have recommended reevaluation of iron recommendations and stressed the need for postnatal iron supplementation research to identify adverse outcomes and define their biological mechanisms [15–22].

Previous studies on infants have reported reduced growth and deleterious cognitive outcomes due to iron supplementation [9–14]. In a randomized controlled trial (RCT), iron-sufficient infants who had received standard iron formula (12.7 mg iron/L) had poorer cognitive outcomes at 10 and 16 years of age [10,11] compared to those who had received low-iron formula (2.3 mg iron/L). Comparable cognitive effects were observed in both rodents and pigs [23–26]. In these studies, several biological mechanisms may have contributed to the cognitive outcomes, including but not limited to iron under-regulation, iron–mineral interactions, or CNS iron overload-induced oxidative stress.

Iron can compete with other essential trace minerals for absorption and transport and iron loading causes oxidative stress in biological environments through generation of reactive oxygen species (ROS). Systemic and cellular regulators of iron homeostasis work to ensure that the diverse iron needs of all tissues are met and still prevent iron toxicity. In early development, however, iron homeostasis might not be as responsive to elevated body iron stores. Indeed, postnatal iron supplementation increases body iron stores even in iron-replete infants [8,27], and under-regulation of iron metabolism in early life is further supported by postnatal iron regulation studies in humans [28], rats [29,30], mice [31], and piglets [25]. It is possible that under-regulation of iron homeostasis would permit iron overload in the CNS with increased iron intake, and iron uptake in the CNS may also be under-regulated postnatally, as previously indicated in rats [30]. Dysregulation of iron metabolism and iron loading contribute to neurodegeneration by causing oxidative stress [32,33]. Removal of iron from the CNS through iron

chelation may even be a promising new therapy for those suffering cognitive effects of neurodegeneration [34]. Studies in rodents have concluded that neonatal iron exposure can promote neurodegenerative disease progression later in life, and this may be a result of neonatal CNS oxidative stress [19,24,26,35–37]. In neonatal pigs, increased iron supplementation led to iron loading in the hippocampus, the region that forms memories, as well as markers of lipid peroxidation (a form of oxidative stress), and impaired social behavior after weaning [25]. It was concluded that iron loading in the hippocampus might disrupt cognitive development directly through oxidative stress injury. Cognitive effects of iron supplementation have also been associated with reduced expression of myelin basic protein (MBP) in the hippocampus [38]. In summary, due to under-regulation of iron in early life, postnatal iron supplementation might lead to iron loading, and in the CNS, this could lead to oxidative stress and disrupt myelination, thereby explaining deficits in cognitive development.

The existence of a causal link between early life CNS iron exposure and neurodegenerative disease can only be speculated, but this possibility only highlights the need to study the effects of postnatal iron supplementation [19]. Previous studies in animals have relied on a range of iron intervention designs, but none have closely modeled routine postnatal interventions nor have they accounted for differences in milk iron intake be- tween humans and model species [23,25,35,38,39]. Moreover, the vast majority all studies reporting adverse neurodevelopment effects of iron supplementation in humans have used ferrous sulfate (FS), whereas alternative chemical forms of iron have rarely been explored. Therefore, in addition to FS, we investigated the effects of ferrous bis-glycinate (FC), an amino acid chelated form of iron, which due to its unique absorptive fate may be less likely to cause the adverse effects attributed to FS [40]. FC has been shown to be effective and safe for use in infants as a bioavailable source of iron [41]. Herein, we characterized FS and FC iron supplementation effects on growth, iron status, iron regulation, and neurodevelopment in healthy,

nursing rat litters, providing new insight into the activities of exogenous iron during one of the critical windows of development.

2.2. MATERIALS & METHODS

2.2.1. Animals

The use of animal models is essential for advancing infant nutrition knowledge because a multitude of ethical and procedural limitations preclude this research in humans. Rats are often preferred for postnatal nutrition research because regular handling of pups is comparatively well-tolerated [42,43]. The use of rats for studying outcomes of postnatal iron supplementation is also reinforced by evidence that mechanisms of iron homeostasis across stages of development are consistent between rats and humans [26–28].

Animal procedures for this study were approved by the University of California Davis Institutional Animal Care and Use Committee. Sprague Dawley rats between 8 and 10 weeks of age were obtained from Charles River Laboratories (Wilmington, MA, USA) and maintained on standard 18% protein rodent chow (200 mg Fe/kg diet; 2018, Teklad Diets, Madison, WI, USA) in clear polycarbonate hanging cages at constant temperature (22 ◦C) and humidity (63%) with standard 12 h light cycles; these conditions applied during habituation, breeding, and throughout the entire postnatal experimental period. Rats were habituated to the vivarium for one week prior to breeding. There were 11 nulliparous female breeders and 9 of them had litters, all of which were used for the experiment. Original litter sizes ranged between 10 to 15 pups. In order to normalize growth between litters, newborn pups born within the same 24 h period were randomly assigned to sex- matched litters of 10 pups. All litters nursed freely throughout the experiment, except for a brief period during daily supplementation. On postnatal day (PD) 2, litters were randomly assigned to supplementation groups (n = 3 litters, 10 pups each) to receive 10% sucrose vehicle control (CON) or iron as either ferrous sulfate heptahydrate (Cat#215422-250G,

Sigma-Aldrich, St. Louis, MO, USA) or ferrous bis-glycinate chelate (Albion Minerals Ferrochel®, Balchem Inc., New Hampton, NY, USA). Littermates were assigned to the same treatment group to avoid coprophagic iron transfer across treatment groups, which would be highly confounding.

Pups were weighed every other day beginning PD 2, and litter average body weight (BW) was used to calculate the supplement volume, which provided 10 mg Fe/kg BW· day. This experimental iron dose for postnatal supplementation was designed to represent the daily iron intake of an exclusively formula-fed infant, after adjusting for known differences in milk iron and iron absorption efficiency between humans and rats. References and calculations for iron dose determination are shown in Table 1 and Equation (1) (below). Iron supplements were prepared in acid-washed glassware by dissolving FS or FC in sterile 10% w/v sucrose at 6 mg iron/mL. Supplementation was performed by hand-pipetting, at the same time each day from PD 2 through PD 14. To deliver calculated volume, a sterile pipette was placed gently on the roof of the mouth to stimulate natural suckling, and solution was dispensed slowly, allowing swallowing at intervals. On PD 15, pups were fasted for 6 h and euthanized by cardiac venipuncture under deep anesthesia (100 mg ketamine × 10 mg xylazine/kg BW). Hippocampi were dissected immediately from fresh brains and all hippocampi were dissected by the same researcher for consistency.

$$\text{Rat Pup Supplementation Dose} = RM \cdot (IF/HM) = [6.4\text{-}14] \approx 10 \text{ mg iron/kg BW} \quad (1)$$

2.2.2. Blood Measurements

Whole blood (n = 20 per group) was collected in EDTA tubes (Safe-T-Fill Capillary Blood Collection Systems, RAM Scientific, Nashville, TN), and blood measurements were performed on the day of collection. Hemoglobin was measured by the cyanmethemoglobin method using a commercially available kit (Cat#MAK115-1KT, Sigma-Aldrich, St. Louis, MO, USA). For hematocrit measurement, whole

blood (n = 20) was collected in heparinized capillary tubes (Fisher Scientific, Pittsburgh, PA, USA), centrifuged, and measured in a hematocrit reader.

2.2.3. Tissue Iron, Zinc, Copper, and Manganese

Tissues (liver, n = 12 per group; whole brains, n = 12 per group) were flash frozen at time of collection and stored at −20 ◦C. Sample weights were recorded prior to digestion in HNO3 (16 mol/L) at room temperature for 7 d. The HNO3 was evaporated at sub-boiling temperatures for 6–8 h [52], and remaining tissue ash was rehydrated with ultrapure water (Milli-Q®, Millipore Sigma, Burlington, MA, USA) for quantification of iron, zinc, copper, and manganese by atomic absorption spectrometry (Model Smith-Heifjie 4000, Thermo Jarrell Ash Corporation, Franklin, MA, USA).

2.2.4. Histology

At the time of collection, liver tissue (n = 6 per group) and whole brains (n = 6 per group) were immersion-fixed in 4% w/v PFA at 4 ◦C for 24 h. Tissues were then washed in 1× PBS three times, stored in 70% ethanol at 4 ◦C, and submitted to the UC Davis School of Veterinary Medicine Anatomic Pathology Laboratory for embedding by standard protocols. Tissue sections were stained for iron by Perls' Prussian blue method with nuclear fast red counterstain.

2.2.5. Real-Time PCR

Tissue samples (liver, n = 7 per group; hippocampus, n = 7 per group) were stored in RNAlater® (Sigma-Aldrich, St.Louis, MO, USA) solution at time of collection, kept at 4 ◦C for 24 h, and then stored at −20 ◦C until extraction by the TRIzolTM protocol (InvitrogenTM, Carlsbad, CA, USA). RNA was reverse transcribed to cDNA using a High-Capacity cDNA Reverse Transcription Kit with RNase Inhibitor (Cat#4374966, Applied BiosystemsTM, Foster City, CA, USA) as outlined by the manufacturer. RT-PCR reactions were performed using a CFX96 Real-Time PCR System (Cat#1725121, Bio-Rad, Hercules, CA,

USA) with iTaq Universal SYBR® Green Supermix to determine relative expression of target transcripts. The fold change in target gene expression was calculated and normalized to *Actb* expression using the $2^{\Delta\Delta Ct}$ method. Primer sequences for target and housekeeping genes are listed in Table 2.

2.2.6. Western Blotting

Tissues (duodenum, n = 4 per group; hippocampus, n = 6 per group) were flash frozen in liquid nitrogen immediately after collection and stored at −80 ◦C. Frozen tissue samples were homogenized by bead beating with 5 mm stainless steel beads (Qiagen, Valencia, CA, USA) in Pierce® RIPA Buffer (Cat#PI89900, Thermo Fisher ScientificTM, Waltham, MA, USA) with Roche cOmpleteTM protease inhibitor cocktail (Cat#NC0969110, Sigma- Aldrich, St. Louis, MO, USA) in a TissueLyser II (Qiagen, Valencia, CA, USA). Following quantification of tissue lysate protein by the Bradford assay, 30 ug protein samples diluted in Laemmli buffer were loaded onto 10% TGX Stain-FreeTM polyacrylamide gels (Bio-Rad, Hercules, CA, USA) and separated by electrophoresis under reducing conditions (5% 2-mercaptoethanol). Protein was transferred to nitrocellulose membranes using a Trans-Blot Turbo Transfer System (Bio-Rad). Stain-FreeTM blot images were captured using a ChemiDoc MP (Bio-Rad, Hercules, CA, USA) and membranes were blocked with 5% non-fat milk (Sigma-Aldrich, St. Louis, MO, USA) in 0.1% Tween®20 PBS (PBST) buffer for 1 h. Blots were washed in PBST and resuspended in primary antibody solution for overnight incubation at 4 ◦C. Primary antibody solutions were prepared according to the following ratios: rabbit 1:1000 rabbit anti-4-HNE (Cat#ab46545; Abcam, Cambridge, MA, USA), 1:1000 rabbit anti-Slc40a1 (Cat#ab58695; Abcam, Cambridge, MA, USA), and 1:100 mouse anti-Fth1 (Cat#sc-376594; Santa Cruz Biotechnologies, Santa Cruz, CA, USA). Following overnight incubation blots were washed thoroughly with PBST and then treated with horseradish peroxidase-conjugated secondary antibody (1:5000 anti-rabbit or anti- mouse, Sigma-Aldrich, St. Louis, MO, USA) in blocking solution. After a final wash in PBST, SuperSignalTM West Femto Maximum Sensitivity Substrate (Thermo Scientific, Fisher ScientificTM, Waltham, MA, USA) was used for chemiluminescent detection of

Slc40a1 and 4- HNE protein bands and ECL Plus Reagent (Thermo Scientific, Fisher ScientificTM, Waltham, MA, USA) was used for detection of Fth1. Blot images were captured on the ChemiDocTM MP (Bio-Rad, Hercules, CA, USA). Total adjusted band densities of target proteins were analyzed by Image Lab Software (Bio-Rad, Hercules, CA, USA) and normalized to total lane protein using Stain-FreeTM blot images [58–60].

2.2.7. Protein Carbonyl Content

Protein carbonyl content was quantified in hippocampi (n = 6 per group) using an OxiSelectTM Protein Carbonyl ELISA kit (Cat#STA-310; Cell Biolabs, Inc., San Diego, CA, USA) according to the manufacturer's instructions.

2.2.8. Statistical Analysis

Data were analyzed and plotted in GraphPad Prism (Version 8). A repeated-measures two-way ANOVA with Geisser–Greenhouse correction was used to test for treatment group effect on body weight across the supplementation period. Litters were analyzed as biological replicates, with respective pups as technical replicates when testing for effects on growth. Significant differences in gene and protein expression with treatment were detected with a one-way ANOVA with post hoc Tukey's test. The Shapiro–Wilk test was used to check for normality, and Kruskal–Wallis tests were used with Dunn's multiple comparison's test to detect group differences in nonparametric data. Individual data points representing biological replicates are plotted with the mean ± SEM, except for growth data, where, for clarity purposes, only the mean ± SD was plotted. Significance was determined at $p \leq 0.05$.

2.3. RESULTS

2.3.1. Iron Status

We provided daily ferrous sulfate (FS) or ferrous bis-glycinate chelate (FC) iron supplements to rat pups from postnatal day (PD) 2–14 to investigate outcomes of postnatal iron supplementation. Supplements were delivered based on 10 mg iron/kg body weight (BW), a dose we designed to represent the estimated routine iron intake of an infant fed exclusively iron-fortified infant formula (Table 1 and Equation (1)). We interrogated hemoglobin and hepatic iron pools to evaluate body iron stores at PD 15 following supplementation. Initially, we tested whether differences in liver iron, hemoglobin, and hematocrit may be due to sex. We did not detect any effects on these metrics due to sex, so this variable was dropped when testing for differences among iron supplementation groups. Hemoglobin and hematocrit were 15% higher in iron-supplemented pups (FS and FC) over CON (p < 0.0001; Figure 1a,b). Substantial liver iron loading was also observed in all iron supplemented pups (Figure 1c,d). Liver iron concentration following FS or FC supplementation was around 100x CON liver iron levels (p < 0.0001; Figure 1a), and marked ferric iron deposition blue was clearly visible with Perls' Prussion blue iron staining in both FS and FC liver sections while nearly undetectable in CON livers (Figure 1d). No differences in hemoglobin (p = 0.087; Figure 1a), hematocrit (p = 0.27; Figure 1b), or liver iron concentration (p = 0.93; Figure 1c) was found between FS vs. FC groups (p = 0.93), suggesting that both iron forms elevated boy iron levels similarly following daily supplementation.

2.3.2. Growth and Development

Iron supplementation can delay growth when provided to iron-sufficient infants [12–14], and therefore we recorded BW every two days across this study to investigate the influence of supplementation on growth. Litter average BW increased steadily in all litters from postnatal day (PD) 2 to PD 15 (Figure 2a) and all individual pup weights fell within normal growth curve percentiles for Sprague Dawley rats (individual values not plotted for clarity). Litter averages were analyzed as biological replicates when testing for treatment effects on BW. A repeated-measures two-way ANOVA

of litter average BW detected a significant effect of time ($p < 0.0001$) but not litter group ($p = 0.18$), suggesting that postnatal BW gain was not affected by iron.

Organ weights were measured on PD 15 at time of collection to detect organ toxicity effects [61]. No effect of sex on liver or brain weight was detected at this age. Treatment influenced brain weight, but results of pairwise comparisons were affected when raw brain weight values were normalized to BW. Mean FS brain weight (raw weight in g) was greater than in the FC and CON groups ($p < 0.05$; Figure 2c). However, mean FS brain weight (% BW) was not different from CON, and FC brain weight (% BW) was significantly lower than both FS ($p < 0.01$) and CON ($p < 0.05$; Figure 2e). With or without normalization, FS brains were significantly heavier than FC brains. Liver weight, in contrast, was not different between groups ($p = 0.10$; Figure 2b), and this remained true when values were normalized to body weight ($p = 0.99$; Figure 2d). Overall, brain development was affected by iron supplement form and this effect does not appear to be related to iron status, since iron status was similar between the FS and FC groups (Figure 1a–d).

2.3.3. Systemic Iron Homeostasis

When iron stores become elevated in healthy individuals, the liver releases the iron regulator hepcidin to prevent iron overload [62,63]. Hepcidin reduces dietary iron uptake by blocking activity of the iron exporter ferroportin in enterocytes [62,64] and inherited disruptions to this pathway result in hemochromatosis (i.e., iron overload) [65–69]. We assessed liver hepcidin (Hamp) and duodenal ferroportin (Slc40a1) expression in rats at PD 15 to observe systemic iron homeostasis following daily postnatal iron supplementation, and to test for differences between FS and FC. Hamp was increased by at least 1000-fold in FS and FC pups ($p < 0.0001$; Figure 3a), but no difference was found between iron groups. We did not observe a treatment effect on duodenal Slc40a1 expression ($p = 0.09$; Figure 3b), in support of findings suggesting that iron absorption is under-regulated in early life [25,28,30,31]. It

appears that duodenal Slc40a1 trended toward increased expression with iron supplementation, but due to the small sample size (n = 4 per group), it is possible that our Slc40a1 analysis was underpowered to detect a significant change. Further, Iron homeostasis outcomes of iron supplementation may not depend upon iron form.

2.3.4. Iron and Trace Minerals in the Central Nervous System

Next, we measured iron levels in the CNS at PD 15 to determine whether postnatal iron supplementation led to sustained brain iron loading, but in spite of increased overall iron status this was not the case. Indeed, no difference was found in whole brain iron concentrations among groups (p = 0.91), suggesting that, in contrast to the liver, the CNS may be protected from iron loading following postnatal supplementation at physiological doses.

We suspected that iron supplementation might reduce availability of other trace mineral sin the CNS, as iron can disrupt the metabolism of other essential trace minerals through mineral-mineral interactions [15,20]. To test whether availability of these minerals was altered in the CNS following postnatal iron supplementation, zinc (Zn), copper (Cu), and manganese (Mn) concentrations were also quantified in whole brains. Congruent with brain iron results, brain zinc (p = 0.28), manganese (p = 0.84), and copper (p = 0.34) concentrations were unaffected by iron supplementation at this age.

2.3.5. Iron Regulation in the Hippocampus

Iron must be tightly regulated in the CNS to sustain basic cellular functions, neurotransmitter synthesis, and myelination. The hippocampus—a CNS region known for its central role in learning and memory—is considered highly sensitive to changes in iron availability during early development and aging. Hippocampal iron deficiency (ID) can permanently disrupt cognitive development, while hippocampal iron overload is a key component in Alzheimer's Disease pathophysiology. We assessed

iron loading and iron regulation in the hippocampus at PD 15 to observe whether the hippocampus had sustained iron loading following postnatal iron supplementation. Ferric iron deposits were undetectable in hippocampal sections (representative slides shown in Figure 4a), and no effect on hippocampal ferritin heavy chain protein (Fth1) expression was observed ($p = 0.07$; Figure 4c). This suggests iron loading did not occur in the hippocampus following iron supplementation, because iron is stored in ferritin and its components are upregulated in response to increased iron [70–72]. In addition to storing iron as Ft, the CNS can prevent iron overload during increased iron status by downregulating transferrin-bound iron uptake by transferrin receptor (Tfr1) or by increasing iron export via Slc40a1; transferrin is also upregulated in the CNS to quench free iron molecules during cellular iron overload or oxidative stress [54,73,74]. We found no differences in *Tfr1* ($p = 0.42$; Figure 4b) or *Tf* ($p = 0.27$; Figure 4d) mRNA expression among groups, nor did we observe changes in Slc40a1 protein ($p = 0.24$; Figure 4e). Taken together, these data do not ind1i0caofte18sustained iron loading had occurred in the hippocampus following postnatal iron supplementation.

2.3.6 Oxidative Stress in the Hippocampus

Iron induces oxidative damage in the CNS, including the hippocampus, and this may cause neurodegeneration [32], so we reasoned that postnatal iron supplementation might elevate oxidative stress in the hippocampus even in the absence of sustained iron loading effects, as this may occur through transient increases in CNS iron undetected by our study design. Hippocampal oxidative stress was quantified by measuring 4-hydroxynonenal (4HNE), a known product of lipid peroxidation [75]. The quantity of 4HNE modified proteins, assessed by Western blot, did not differ among groups ($p = 0.54$; Figure 5a); however, a slight effect on protein carbonyl content, a stable byproduct of protein oxidation, was observed [76]. Less oxidized protein was detected in the hippocampus of FS pups compared to the other groups, suggesting reduced hippocampal oxidative stress in this group ($p = 0.04$; Figure 5b).

2.3.7. Myelination in the Hippocampus

Myelination occurs mainly during postnatal development in rats and synthesis of myelin peaks beginning PD14 until PD 34 [77]. Iron accumulation causes oxidative stress and cell death in oligodendrocytes, which myelinate neurons in the CNS [78]. In piglets, iron supplementation reduced hippocampal myelination gene expression [38]. We sought to determine if hippocampal myelination was impacted by daily postnatal iron supplementation in rats, so we measured expression of several major myelin genes in the hippocampus, including Mag, Mbp, and Plp (Figure 6). Myelin associated glycoportien (Mag) signals myelin and axonal formation, while myelin basic protein (Mbp) ad proteolipid protein (Plp) play major structural roles in myelination [79]. We found no difference in expression of Mag, Mbp, or Plp mRNA in the hippocampus at PD 15, suggesting that myelination was not impacted by either iron supplement (p = 0.69; Figure 6).

2.4. DISCUSSION

Ferrous sulfate (FS) supplementation and formula fortification prevent postnatal iron deficiency (ID) [4,6], but may be harmful to iron-replete infants [15,18,20]. Excess iron intake through high-iron formula or iron drops can lead to growth delays, and adverse cognitive and behavioral outcomes [9–11,19]. Infants may be especially susceptible to these adverse effects, because under-regulation of iron in early life permits excessive iron absorption and this may lead to iron loading in the developing central nervous system (CNS) [8,25,31]. Adverse neurodevelopment outcomes [23–25] and oxidative stress of the CNS [25,38] have been observed in animals supplemented with iron postnatally. Research on the effects of postnatal iron supplementation in healthy subjects is limited and existing animal studies have often not been designed to mimic routine iron administration. We developed a translationally-optimized iron supplementation experiment in rat pups (Table 1 and Equation (1)) to compare effects of ferrous

bis-glycinate chelate (FC) or ferrous sulfate (FS) on development, systemic iron regulation, CNS trace mineral content, and hippocampus-specific markers of iron regulation, oxidative stress, and myelination.

First, we characterized iron status following supplementation with FS or FC. Hemoglobin, hematocrit, and liver iron content were all substantially increased in iron-supplemented pups at PD 15 (Figure 1). Liver iron concentration is more sensitive and specific to excess body iron loading than blood indices for iron status. Excess body iron is taken up by the liver for storage, and in turn, the liver controls body iron homeostasis to prevent overload. Before being assigned to treatment groups on PD 2, litters were culled to age-matched litters of 10, a normal litter size for Sprague Dawley rats. Therefore, it can be assumed that CON pups received sufficient dietary iron via milk feeding and should not have required additional iron. Yet, we observed large effects on hemoglobin, hematocrit, and liver iron content when pups were supplemented with iron, and this is probably due to under-regulation of iron absorption (Figure 3). When liver iron increases, the liver makes hepcidin, the iron systemic iron regulator that downregulates intestinal iron absorption by blocking the iron exporter, ferroportin (Slc40a1) [20–22]. Infant iron absorption was previously reported to be unaffected by dose, mode of delivery, or infant iron status [27,80], and in previous experiments in rodents [29–31] and piglets [25] intestinal ferroportin was hypo-responsive to hepcidin following iron supplementation. One study investigating this early life phenomenon in rats concluded that hypo-responsiveness of ferroportin protein to hepcidin during suckling may be explained by elevated iron-regulatory element (IRE+) Slc40a1 transcripts, which allow for upregulation of Slc40a1 in response to elevated enterocyte iron levels [29]. That study demonstrated that weanling and adult rats mainly express an Slc40a1 transcript variant lacking IRE (IRE−) in the duodenum. Expression of IRE− Slc40a1 in weanling and adult rats allows enterocytes to avoid translational regulation by iron regulatory proteins (IRPs); enterocyte Slc40a1 protein is primarily controlled by hepcidin after weaning. However, in pre-weanling pups expressing higher levels of IRE+ Slc40a1 transcripts, translation of Slc40a1 is upregulated in response to iron; Slc40a1 remains elevated

even in the presence of elevated hepcidin levels. The authors concluded that elevated IRE+ Slc40a1 during suckling may help to maximize the supply of iron during a critical period of increased iron demands [29]. In our study, liver iron concentrations in FS and FC pups were 100x control (CON) levels (Figure 1c), and liver hepcidin expression was 1000-fold CON expression, but we found no change in intestinal ferroportin protein (Figure 3). Indeed, there was a trend toward increased ferroportin expression (Figure 3b); however, our duodenal Western blot analysis may have been underpowered to detect a significant increase. Therefore, our results are consistent with previous findings that infants receiving iron through iron supplements or iron-fortified formula absorb iron unmitigatedly and may be at increased risk for iron overload. Both FS and FC supplementation comparably increased iron levels, hemoglobin, hematocrit (Figure 1), and similar liver Hamp expression and duodenal ferroportin protein expression was detected between FS and FC groups (Figure 3). Indeed, neither iron status nor iron homeostasis outcomes were affected by iron form; both forms elevated body iron stores to levels far beyond that of CON pups.

Iron deficiency and iron toxicity are both harmful, and both inhibit growth and proliferation of cells [81]. A limited number of studies have investigated whether postnatal iron supplementation benefits long-term growth and development [18,82–84]. Iron supplementation of iron-sufficient infants might delay growth but this is not consistent [9,12,14,82,83,85]. We observed no effect of iron supplementation on litter weight gain (Figure 2a), suggesting that neither FS nor FC iron affects short-term weight gain in early life when provided at routine levels. Similar findings have been reported in previous animals studies, which have used both lower and higher daily doses of FS: in pre-weanling pigs—where the same daily dose of FS was used (10 mg iron/kg BW) from PD2–21—weight gain was not affected, nor was weight gain affected with 50 mg iron/kg BW [25], and BW was not affected in pre-weaning rats following supplementation with either 30 or 150 μg iron per day [30]. In these studies, increasing the dose of iron increased iron status but did not change growth. Thus, our results are

consistent with previous experiments in animals. We also analyzed liver and brain weights following iron supplementation in rats, because organ weight is often measured to detect neonatal toxicity in rodent models [61]. Liver size typically decreases with exposure to environmental toxins [86]. We observed no difference in liver weight following iron supplementation, indicating an absence of toxic effects in the liver (Figure 2b,d). Nevertheless, brain weight was affected depending on iron form (Figure 2c,e). Data are shown as brain weight and brain % BW because current research has not determined which is more meaningful in terms of postnatal neurodevelopment [61]. In both analyses (Figure 2c,e), FS brains were heavier than FC brains. Therefore, we conclude that brain weight effects following postnatal iron supplementation are dependent upon the form of iron. Additional studies with more specific indicators of neurodevelopment are needed to determine whether functional differences may arise related to brain weight or iron source.

Previous studies have observed iron loading in the CNS following iron supplementation [25,30] and this may also alter availability of other trace metals through iron–mineral interactions [15,20]. We reasoned that differences in brain size between the iron forms might be explained by differences in iron loading or trace metal availability between FS and FC groups, but neither iron, zinc, copper, nor manganese levels were different between these groups in our study. Regarding the negative cognitive and behavioral outcomes that were observed in infants given iron-fortified formula, these results suggest dietary iron intake from iron-fortified formula is unlikely to have caused sustained brain iron loading or disruptions to zinc, copper, or manganese availability in the CNS. Furthermore, these findings do not support the hypothesis that long-term cognitive outcomes of postnatal iron supplementation are due to direct effects of iron loading or iron–mineral interactions in the CNS. Neither does it appear likely that sustained iron loading nor changes in iron regulation had occurred specifically in the hippocampus, as we had suspected it would (Figure 4). Postnatal CNS iron loading might happen transiently, or after exceptionally high oral doses are used as previously reported [25,30]. Considering that brain trace

minerals were not altered and considering that overall iron status was similar between FS and FC groups, it is unclear how FS brains became heavier than FC brains. These results provide novel evidence that iron form might influence neurodevelopment outcomes of iron supplementation.

Iron loading causes oxidative stress in the brain and this appears to be a central mechanism in neurodegenerative pathologies [32,33]. Oxidative stress has also been observed in the CNS following neonatal iron exposure [87]. Iron loading initiates pro-oxidative reactions in cells and this can be toxic to the CNS [78,88,89]. Recently in piglets, iron supplementation at 50 mg iron/kg BW as FS from PD 2 to PD 21 increased hippocampal lipid peroxidation compared to 10 mg iron/kg and control groups, but this was not statistically significant [25]. In the present experiment, we used 10 mg iron/kg BW. No change in hippocampal lipid peroxidation was observed, and only borderline less hippocampal protein oxidation was seen in the FS group, suggesting that neither iron treatment induced hippocampal oxidative stress (Figure 5). Protein oxidation was not different among the iron groups in the hippocampus, so we further conclude that differences in brain size cannot be explained by differences in oxidative stress outcomes between iron forms. Congruent to both these and the CNS mineral loading results, we also did not detect changes in myelination gene expression (Figure 6).

There are inherent limitations to extending the findings of this study to all healthy, iron-sufficient infants in spite of our optimization efforts. We believe that 10 mg iron/kg BW is representative of the iron intake of iron-fortified formula-fed infants, but dietary iron intake may vary widely in healthy infants. It is possible that many infants may be exposed to significantly more iron (e.g., preterm infants) or less iron (mixed-fed infants) than the average formula-fed infant. It is likely that significantly increasing or decreasing the dose used in our study would lead to different iron status and development outcomes. Future studies should define the dose–response relationship between postnatal iron intake, iron status, growth, and neurodevelopment at this stage of life.

In conclusion, specific development effects of postnatal iron supplementation at routine levels may not be clearly related to iron status effects and instead dependent upon indirect mechanisms related to iron form. The long-term functional consequences of these effects remain to be elucidated. The differential effects on brain growth between FS- and FC-supplemented pups provides evidence that iron impacts postnatal development in a form dependent manner. Additional studies in this area are warranted to optimize dose, timing, and form of iron for infants such that any negative health outcomes are identified and prevented without compromising risk for iron deficiency.

2.5. REFERENCES

1. Black, R.E.; Heidkamp, R. Causes of Stunting and Preventive Dietary Interventions in Pregnancy and Early Childhood. In Nestlé Nutrition Institute Workshop Series; Colombo, J., Koletzko, B., Lampl, M., Eds.; S. Karger AG: Basel, Switzerland, 2018; Volume 89, pp. 105–113. ISBN 978-3-318-06351-6.
2. McCann, J.C.; Ames, B.N. An Overview of Evidence for a Causal Relation between Iron Deficiency during Development and Deficits in Cognitive or Behavioral Function. Am. J. Clin. Nutr. 2007, 85, 931–945.
3. Baker, R.D.; Greer, F.R. The Committee on Nutrition Diagnosis and Prevention of Iron Deficiency and Iron-Deficiency Anemia in Infants and Young Children (0–3 Years of Age). Pediatrics 2010, 126, 1040–1050.
4. Guideline: Daily Iron Supplementation in Infants and Children; WHO Guidelines Approved by the Guidelines Review Committee; World Health Organization: Geneva, Switzerland, 2016; ISBN 978-92-4-154952-3.
5. Pasricha, S.-R.; Drakesmith, H.; Black, J.; Hipgrave, D.; Biggs, B.-A. Control of Iron Deficiency Anemia in Low- and Middle-Income Countries. Blood 2013, 121, 2607–2617.
6. Shelov, S.P.; American Academy of Pediatrics. Caring for Your Baby and Young Child: Birth to Age Five; Bantam: New York, NY, USA, 2009; ISBN 978-0-553-38630-1.
7. Lönnerdal, B.O.; Keen, C.L.; Ohtake, M.; Tamura, T. Iron, Zinc, Copper, and Manganese in Infant Formulas. *Am. J. Dis. Children* 1983, *137*, 433–437.
8. Lönnerdal, B. Development of Iron Homeostasis in Infants and Young Children. *Am. J. Clin. Nutr.* 2017, *106*, 1575S–1580S.
9. Dewey, K.G.; Domellöf, M.; Cohen, R.J.; Landa Rivera, L.; Hernell, O.; Lönnerdal, B. Iron Supplementation Affects Growth and Morbidity of Breast-Fed Infants: Results of a Randomized Trial in Sweden and Honduras. *J. Nutr.* 2002, *132*, 3249–3255.
10. Lozoff, B. Iron-Fortified vs Low-Iron Infant Formula: Developmental Outcome at 10 Years. *Arch. Pediatr. Adolesc. Med.* 2012, *166*, 208.
11. Gahagan, S.; Delker, E.; Blanco, E.; Burrows, R.; Lozoff, B. Randomized Controlled Trial of Iron-Fortified versus Low-Iron Infant Formula: Developmental Outcomes at 16 Years. *J. Pediatr.* 2019, *212*, 124–130.e1.
12. Lind, T.; Seswandhana, R.; Persson, L.-Å.; Lönnerdal, B. Iron Supplementation of Iron-Replete Indonesian Infants Is Associated with Reduced Weight-for-Age. *Acta Paediatr. Oslo Nor. 1992* 2008, *97*, 770–775.

13. Idjradinata, P.; Watkins, W.E.; Pollitt, E. Adverse Effect of Iron Supplementation on Weight Gain of Iron-Replete Young Children. *Lancet Lond. Engl.* 1994, *343*, 1252–1254.
14. Majumdar, I.; Paul, P.; Talib, V.H.; Ranga, S. The Effect of Iron Therapy on the Growth of Iron-Replete and Iron-Deplete Children. *J. Trop. Pediatr.* 2003, *49*, 84–88.
15. Lonnerdal, B. Excess Iron Intake as a Factor in Growth, Infections, and Development of Infants and Young Children. *Am. J. Clin. Nutr.* 2017, *106*, 1681S–1687S.
16. Hare, D.J.; Arora, M.; Jenkins, N.L.; Finkelstein, D.I.; Doble, P.A.; Bush, A.I. Is Early-Life Iron Exposure Critical in Neurodegenera- tion? *Nat. Rev. Neurol.* 2015, *11*, 536–544.
17. Hare, D.J.; Cardoso, B.R.; Szymlek-Gay, E.A.; Biggs, B.-A. Neurological Effects of Iron Supplementation in Infancy: Finding the Balance between Health and Harm in Iron-Replete Infants. *Lancet Child Adolesc. Health* 2018, *2*, 144–156.
18. Hare, D.J.; Braat, S.; Cardoso, B.R.; Morgan, C.; Szymlek-Gay, E.A.; Biggs, B.-A. Health Outcomes of Iron Supplementation and/or Food Fortification in Iron-Replete Children Aged 4–24 Months: Protocol for a Systematic Review and Meta-Analysis. *Syst. Rev.* 2019, *8*, 253.
19. Agrawal, S.; Berggren, K.L.; Marks, E.; Fox, J.H. Impact of High Iron Intake on Cognition and Neurodegeneration in Humans and in Animal Models: A Systematic Review. *Nutr. Rev.* 2017, *75*, 456–470.
20. Wessling-Resnick, M. Excess Iron: Considerations Related to Development and Early Growth. *Am. J. Clin. Nutr.* 2017, *106*, 1600S–1605S.
21. Georgieff, M.K.; Krebs, N.F.; Cusick, S.E. The Benefits and Risks of Iron Supplementation in Pregnancy and Childhood. *Annu. Rev. Nutr.* 2019, *39*, 121–146.
22. Dietary Guidelines Advisory Committee. *Scientific Report of the 2020 Dietary Guidelines Advisory Committee: Advisory Report to the Secretary of Agriculture and the Secretary of Health and Human Services*; U.S. Department of Agriculture, Agricultural Research Service: Washington, DC, USA, 2020; p. 786.
23. Alexeev, E.E.; He, X.; Slupsky, C.M.; Lönnerdal, B. Effects of Iron Supplementation on Growth, Gut Microbiota, Metabolomics and Cognitive Development of Rat Pups. *PLoS ONE* 2017, *12*, e0179713.
24. Fredriksson, A.; Schröder, N.; Eriksson, P.; Izquierdo, I.; Archer, T. Neonatal Iron Exposure Induces Neurobehavioural Dysfunc- tions in Adult Mice. *Toxicol. Appl. Pharmacol.* 1999, *159*, 25–30.
25. Ji, P.; Lönnerdal, B.; Kim, K.; Jinno, C.N. Iron Oversupplementation Causes Hippocampal Iron Overloading and Impairs Social Novelty Recognition in Nursing Piglets. *J. Nutr.* 2019, *149*, 398–405.
26. Fredriksson, A.; Schröder, N.; Eriksson, P.; Izquierdo, I.; Archer, T. Neonatal Iron Potentiates Adult MPTP-Induced Neurodegen- erative and Functional Deficits. *Parkinsonism Relat. Disord.* 2001, *7*, 97–105.
27. Domellöf, M.; Lönnerdal, B.; Abrams, S.A.; Hernell, O. Iron Absorption in Breast-Fed Infants: Effects of Age, Iron Status, Iron Supplements, and Complementary Foods. *Am. J. Clin. Nutr.* 2002, *76*, 198–204.
28. Lönnerdal, B.; Georgieff, M.K.; Hernell, O. Developmental Physiology of Iron Absorption, Homeostasis, and Metabolism in the Healthy Term Infant. *J. Pediatr.* 2015, *167*, S8–S14.
29. Darshan, D.; Wilkins, S.J.; Frazer, D.M.; Anderson, G.J. Reduced Expression of Ferroportin-1 Mediates Hyporesponsiveness of Suckling Rats to Stimuli That Reduce Iron Absorption. *Gastroenterology* 2011, *141*, 300–309.
30. Leong, W.-I.; Bowlus, C.L.; Tallkvist, J.; Lönnerdal, B. Iron Supplementation during Infancy—Effects on Expression of Iron Transporters, Iron Absorption, and Iron Utilization in Rat Pups. *Am. J. Clin. Nutr.* 2003, *78*, 1203–1211.

31. Frazer, D.M.; Wilkins, S.J.; Darshan, D.; Mirciov, C.S.G.; Dunn, L.A.; Anderson, G.J. Ferroportin Is Essential for Iron Absorption During Suckling, But Is Hyporesponsive to the Regulatory Hormone Hepcidin. *Cell. Mol. Gastroenterol. Hepatol.* 2017, *3*, 410–421.
32. Li, J.; Cao, F.; Yin, H.; Huang, Z.; Lin, Z.; Mao, N.; Sun, B.; Wang, G. Ferroptosis: Past, Present and Future. *Cell Death Dis.* 2020, *11*, 88. [CrossRef]
33. Carocci, A.; Catalano, A.; Sinicropi, M.S.; Genchi, G. Oxidative Stress and Neurodegeneration: The Involvement of Iron. *Biometals Int. J. Role Met. Ions Biol. Biochem. Med.* 2018, *31*, 715–735.
34. Nuñez, M.T.; Chana-Cuevas, P. New Perspectives in Iron Chelation Therapy for the Treatment of Neurodegenerative Diseases. *Pharmaceuticals* 2018, *11*, 109.
35. Dornelles, A.S.; Garcia, V.A.; de Lima, M.N.M.; Vedana, G.; Alcalde, L.A.; Bogo, M.R.; Schröder, N. MRNA Expression of Proteins Involved in Iron Homeostasis in Brain Regions Is Altered by Age and by Iron Overloading in the Neonatal Period. *Neurochem. Res.* 2010, *35*, 564–571.
36. Fernandez, L.L.; de Lima, M.N.M.; Scalco, F.; Vedana, G.; Miwa, C.; Hilbig, A.; Vianna, M.; Schröder, N. Early Post-Natal Iron Administration Induces Astroglial Response in the Brain of Adult and Aged Rats. *Neurotox. Res.* 2011, *20*, 193–199.
37. Fernandez, L.L.; Carmona, M.; Portero-Otin, M.; Naudi, A.; Pamplona, R.; Schröder, N.; Ferrer, I. Effects of Increased Iron Intake during the Neonatal Period on the Brain of Adult AbetaPP/PS1 Transgenic Mice. *J. Alzheimers Dis. JAD* 2010, *19*, 1069–1080.
38. Ji, P.; Nonnecke, E.B.; Doan, N.; Lönnerdal, B.; Tan, B. Excess Iron Enhances Purine Catabolism Through Activation of Xanthine Oxidase and Impairs Myelination in the Hippocampus of Nursing Piglets. *J. Nutr.* 2019, *149*, 1911–1919.
39. Figueiredo, L.S.; de Freitas, B.S.; Garcia, V.A.; Dargél, V.A.; Köbe, L.M.; Kist, L.W.; Bogo, M.R.; Schröder, N. Iron Loading Selectively Increases Hippocampal Levels of Ubiquitinated Proteins and Impairs Hippocampus-Dependent Memory. *Mol. Neurobiol.* 2016, *53*, 6228–6239.
40. Hertrampf, E.; Olivares, M. Iron Amino Acid Chelates. *Int. J. Vitam. Nutr. Res.* 2004, *74*, 435–443.
41. Pineda, O.; Ashmead, H.D. Effectiveness of Treatment of Iron-Deficiency Anemia in Infants and Young Children with Ferrous Bis-Glycinate Chelate. *Nutrition* 2001, *17*, 381–384.
42. Puiman, P.; Stoll, B. Animal Models to Study Neonatal Nutrition in Humans. *Curr. Opin. Clin. Nutr. Metab. Care* 2008, *11*, 601–606.
43. Pérez-Cano, F.J.; Franch, À.; Castellote, C.; Castell, M. The Suckling Rat as a Model for Immunonutrition Studies in Early Life. *Clin. Dev. Immunol.* 2012, *2012*, 1–16.
44. Domellöf, M.; Lönnerdal, B.; Dewey, K.G.; Cohen, R.J.; Hernell, O. Iron, Zinc, and Copper Concentrations in Breast Milk Are Independent of Maternal Mineral Status. *Am. J. Clin. Nutr.* 2004, *79*, 111–115.
45. Fiorotto, M.L.; Burrin, D.G.; Perez, M.; Reeds, P.J. Intake and Use of Milk Nutrients by Rat Pups Suckled in Small, Medium, or Large Litters. *Am. J. Physiol.-Regul. Integr. Comp. Physiol.* 1991, *260*, R1104–R1113.
46. Keen, C.L.; Lönnerdal, B.; Clegg, M.; Hurley, L.S. Developmental Changes in Composition of Rat Milk: Trace Elements, Minerals, Protein, Carbohydrate and Fat. *J. Nutr.* 1981, *111*, 226–236.
47. Krˇížova, E.; Imek, V.S.; Abelenda, M.; Puerta, M. Food Intake and Body Weight in Rats with Daily Food-Availability Restrictions. *Physiol. Behav.* 1996, *60*, 791–794.
48. National Research Council (US) Subcommittee on Laboratory Animal Nutrition. Nutrient Requirements of the Laboratory Rat. In *Nutrient Requirements of Laboratory Animals*, 4th ed.; National Academies Press (US): Washington, DC, USA, 1995; p. 32.
49. Swain, J.H.; Newman, S.M.; Hunt, J.R. Bioavailability of Elemental Iron Powders to Rats Is Less than Bakery-Grade Ferrous Sulfate and Predicted by Iron Solubility and Particle Surface Area. *J. Nutr.* 2003, *133*, 3546–3552.

50. Atarashi, M.; Izawa, T.; Mori, M.; Inai, Y.; Kuwamura, M.; Yamate, J. Dietary Iron Overload Abrogates Chemically-Induced Liver Cirrhosis in Rats. *Nutrients* 2018, *10*, 1400.
51. Mori, M.; Izawa, T.; Inai, Y.; Fujiwara, S.; Aikawa, R.; Kuwamura, M.; Yamate, J. Dietary Iron Overload Differentially Modulates Chemically-Induced Liver Injury in Rats. *Nutrients* 2020, *12*, 2784.
52. Clegg, M.S.; Keen, C.L.; Lönnerdal, B.; Hurley, L.S. Influence of Ashing Techniques on the Analysis of Trace Elements in Animal Tissue: I. Wet Ashing. *Biol. Trace Elem. Res.* 1981, *3*, 107–115.
53. Li, Y.; Yu, P.; Chang, S.-Y.; Wu, Q.; Yu, P.; Xie, C.; Wu, W.; Zhao, B.; Gao, G.; Chang, Y.-Z. Hypobaric Hypoxia Regulates Brain Iron Homeostasis in Rats. *J. Cell. Biochem.* 2017, *118*, 1596–1605.
54. Yang, W.M.; Jung, K.J.; Lee, M.O.; Lee, Y.S.; Lee, Y.H.; Nakagawa, S.; Niwa, M.; Cho, S.S.; Kim, D.W. Transient Expression of Iron Transport Proteins in the Capillary of the Developing Rat Brain. *Cell. Mol. Neurobiol.* 2011, *31*, 93–99.
55. Ghiani, C.A.; Ying, Z.; de Vellis, J.; Gomez-Pinilla, F. Exercise Decreases Myelin-Associated Glycoprotein Expression in the Spinal Cord and Positively Modulates Neuronal Growth. *Glia* 2007, *55*, 966–975.
56. Paintlia, M.K.; Paintlia, A.S.; Barbosa, E.; Singh, I.; Singh, A.K. N-Acetylcysteine Prevents Endotoxin-Induced Degeneration of Oligodendrocyte Progenitors and Hypomyelination in Developing Rat Brain. *J. Neurosci. Res.* 2004, *78*, 347–361.
57. Ueno, T.; Ito, J.; Hoshikawa, S.; Ohori, Y.; Fujiwara, S.; Yamamoto, S.; Ohtsuka, T.; Kageyama, R.; Akai, M.; Nakamura, K.; et al. The Identification of Transcriptional Targets of Ascl1 in Oligodendrocyte Development. *Glia* 2012, *60*, 1495–1505.
58. Dittmer, A.; Dittmer, J. β-Actin Is Not a Reliable Loading Control in Western Blot Analysis. *Electrophoresis* 2006, *27*, 2844–2845.
59. Gilda, J.E.; Gomes, A.V. Stain-Free Total Protein Staining Is a Superior Loading Control to β-Actin for Western Blots. *Anal. Biochem.* 2013, *440*, 186–188.
60. Colella, A.D.; Chegenii, N.; Tea, M.N.; Gibbins, I.L.; Williams, K.A.; Chataway, T.K. Comparison of Stain-Free Gels with Traditional Immunoblot Loading Control Methodology. *Anal. Biochem.* 2012, *430*, 108–110.
61. Bailey, S.A.; Zidell, R.H.; Perry, R.W. Relationships Between Organ Weight and Body/Brain Weight in the Rat: What Is the Best Analytical Endpoint? *Toxicol. Pathol.* 2004, *32*, 448–466.
62. Nemeth, E. Hepcidin Regulates Cellular Iron Efflux by Binding to Ferroportin and Inducing Its Internalization. *Science* 2004, *306*, 2090–2093.
63. Muckenthaler, M.U.; Rivella, S.; Hentze, M.W.; Galy, B. A Red Carpet for Iron Metabolism. *Cell* 2017, *168*, 344–361.
64. Billesbølle, C.B.; Azumaya, C.M.; Kretsch, R.C.; Powers, A.S.; Gonen, S.; Schneider, S.; Arvedson, T.; Dror, R.O.; Cheng, Y.; Manglik, A. Structure of Hepcidin-Bound Ferroportin Reveals Iron Homeostatic Mechanisms. *Nature* 2020, *586*, 807–811.
65. Chiu, M.K.; Davey, A.M. Neonatal Hemochromatosis. *Clin. Pediatr. (Phila.)* 1997, *36*, 607–610.
66. Corradini, E.; Buzzetti, E.; Pietrangelo, A. Genetic Iron Overload Disorders. *Mol. Asp. Med.* 2020, *75*, 100896.
67. Joshi, R.; Shvartsman, M.; Morán, E.; Lois, S.; Aranda, J.; Barqué, A.; Cruz, X.; Bruguera, M.; Vagace, J.M.; Gervasini, G.; et al. Functional Consequences of Transferrin Receptor-2 Mutations Causing Hereditary Hemochromatosis Type 3. *Mol. Genet. Genom. Med.* 2015, *3*, 221–232.
68. Yun, S.; Vincelette, N.D. Update on Iron Metabolism and Molecular Perspective of Common Genetic and Acquired Disorder, Hemochromatosis. *Crit. Rev. Oncol. Hematol.* 2015, *95*, 12–25.
69. Bardou-Jacquet, E.; Brissot, P. Diagnostic Evaluation of Hereditary Hemochromatosis (HFE and Non-HFE). *Hematol. Oncol. Clin. N. Am.* 2014, *28*, 625–635.
70. Kajarabille, N.; Latunde-Dada, G.O. Programmed Cell-Death by Ferroptosis: Antioxidants as Mitigators. *Int. J. Mol. Sci.* 2019, *20*, 4968.

71. Focht, S.J.; Snyder, B.S.; Beard, J.L.; Van Gelder, W.; Williams, L.R.; Connor, J.R. Regional Distribution of Iron, Transferrin, Ferritin, and Oxidatively-Modified Proteins in Young and Aged Fischer 344 Rat Brains. *Neuroscience* 1997, *79*, 255–261.
72. Erikson, K.M.; Pinero, D.J.; Connor, J.R.; Beard, J.L. Regional Brain Iron, Ferritin and Transferrin Concentrations during Iron Deficiency and Iron Repletion in Developing Rats. *J. Nutr.* 1997, *127*, 2030–2038.
73. Bradbury, M.W. Transport of Iron in the Blood-Brain-Cerebrospinal Fluid System. *J. Neurochem.* 1997, *69*, 443–454.
74. Siddappa, A.J.M.; Rao, R.B.; Wobken, J.D.; Leibold, E.A.; Connor, J.R.; Georgieff, M.K. Developmental Changes in the Expression of Iron Regulatory Proteins and Iron Transport Proteins in the Perinatal Rat Brain. *J. Neurosci. Res.* 2002, *68*, 761–775.
75. Houglum, K.; Filip, M.; Witztum, J.L.; Chojkier, M. Malondialdehyde and 4-Hydroxynonenal Protein Adducts in Plasma and Liver of Rats with Iron Overload. *J. Clin. Investig.* 1990, *86*, 1991–1998.
76. Stadtman, E.R. Metal Ion-Catalyzed Oxidation of Proteins: Biochemical Mechanism and Biological Consequences. *Free Radic. Biol. Med.* 1990, *9*, 315–325.
77. Downes, N.; Mullins, P. The Development of Myelin in the Brain of the Juvenile Rat. *Toxicol. Pathol.* 2014, *42*, 913–922.
78. Roth, A.D.; Núñez, M.T. Oligodendrocytes: Functioning in a Delicate Balance Between High Metabolic Requirements and Oxidative Damage. In *Glial Cells in Health and Disease of the CNS*; von Bernhardi, R., Ed.; Advances in Experimental Medicine and Biology; Springer International Publishing: Cham, Switzerland, 2016; Volume 949, pp. 167–181. ISBN 978-3-319-40762-3.
79. Stassart, R.M.; Möbius, W.; Nave, K.-A.; Edgar, J.M. The Axon-Myelin Unit in Development and Degenerative Disease. *Front. Neurosci.* 2018, *12*, 467.
80. Szymlek-Gay, E.A.; Domellöf, M.; Hernell, O.; Hurrell, R.F.; Lind, T.; Lönnerdal, B.; Zeder, C.; Egli, I.M. Mode of Oral Iron Administration and the Amount of Iron Habitually Consumed Do Not Affect Iron Absorption, Systemic Iron Utilisation or Zinc Absorption in Iron-Sufficient Infants: A Randomised Trial. *Br. J. Nutr.* 2016, *116*, 1046–1060.
81. Camaschella, C.; Nai, A.; Silvestri, L. Iron Metabolism and Iron Disorders Revisited in the Hepcidin Era. *Haematologica* 2020, *105*, 260–272.
82. Pasricha, S.-R.; Hayes, E.; Kalumba, K.; Biggs, B.-A. Effect of Daily Iron Supplementation on Health in Children Aged 4-23 Months: A Systematic Review and Meta-Analysis of Randomised Controlled Trials. *Lancet Glob. Health* 2013, *1*, e77–e86.
83. Petry, N.; Olofin, I.; Boy, E.; Donahue Angel, M.; Rohner, F. The Effect of Low Dose Iron and Zinc Intake on Child Micronutrient Status and Development during the First 1000 Days of Life: A Systematic Review and Meta-Analysis. *Nutrients* 2016, *8*, 773.
84. Lozoff, B.; Beard, J.; Connor, J.; Barbara, F.; Georgieff, M.; Schallert, T. Long-Lasting Neural and Behavioral Effects of Iron Deficiency in Infancy. *Nutr. Rev.* 2006, *64*, S34–S43.
85. Gahagan, S.; Yu, S.; Kaciroti, N.; Castillo, M.; Lozoff, B. Linear and Ponderal Growth Trajectories in Well-Nourished, Iron-Sufficient Infants Are Unimpaired by Iron Supplementation. *J. Nutr.* 2009, *139*, 2106–2112.
86. Uemitsu, N.; Nishimura, C.; Nakayoshi, H. Evaluation of Liver Weight Changes Following Repeated Administration of Carbon Tetrachloride in Rats and Body-Liver Weight Relationship. *Toxicology* 1986, *40*, 181–190.
87. Berggren, K.L.; Chen, J.; Fox, J.; Miller, J.; Dodds, L.; Dugas, B.; Vargas, L.; Lothian, A.; McAllum, E.; Volitakis, I.; et al. Neonatal Iron Supplementation Potentiates Oxidative Stress, Energetic Dysfunction and Neurodegeneration in the R6/2 Mouse Model of Huntington's Disease. *Redox Biol.* 2015, *4*, 363–374.

88. Miwa, C.P.; de Lima, M.N.M.; Scalco, F.; Vedana, G.; Mattos, R.; Fernandez, L.L.; Hilbig, A.; Schröder, N.; Vianna, M.R.M. Neonatal Iron Treatment Increases Apoptotic Markers in Hippocampal and Cortical Areas of Adult Rats. *Neurotox. Res.* 2011, *19*, 527–535.
89. Rathnasamy, G.; Murugan, M.; Ling, E.-A.; Kaur, C. Hypoxia-Induced Iron Accumulation in Oligodendrocytes Mediates Apoptosis by Eliciting Endoplasmic Reticulum Stress. *Mol. Neurobiol.* 2016, *53*, 4713–4727.

FIGURES

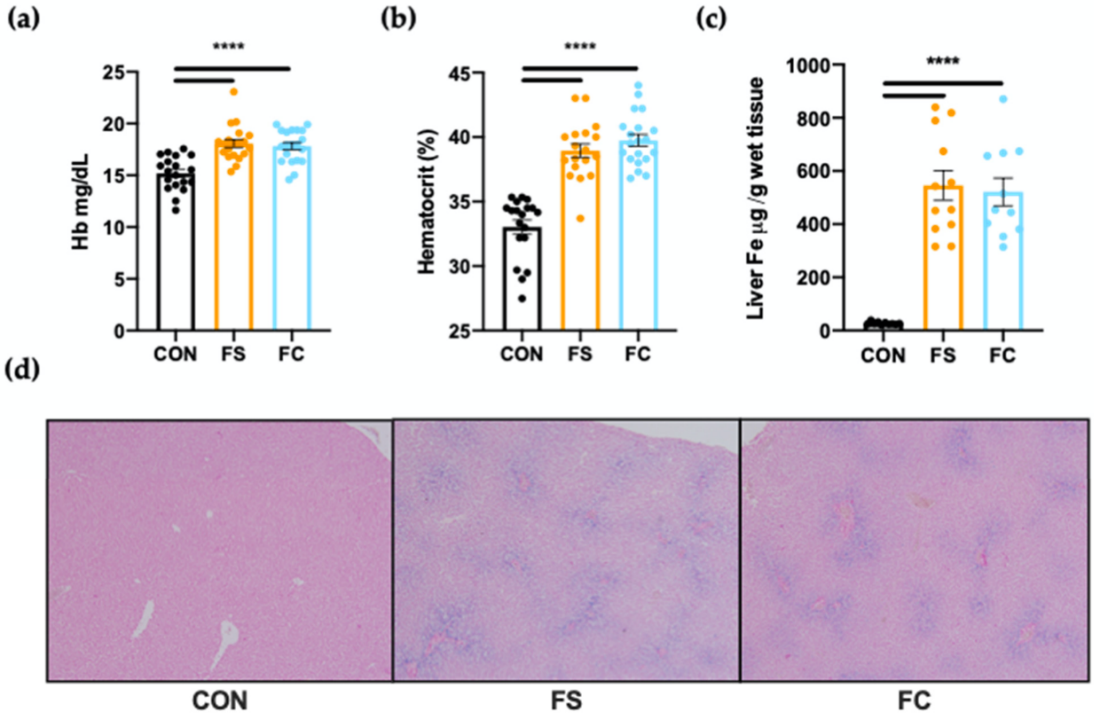

Figure 1. Iron status on postnatal day (PD) 15 following daily ferrous sulfate (FS), ferrous bis-glycinate chelate (FC), or vehicle control (CON) supplementation in rats from PD 2–14. (**a**) Hemoglobin and (**b**) hematocrit were measured from fresh whole blood (*n* = 20/group). (**c**) Liver iron concentrations were quantified by atomic absorption spectrometry (*n* = 12/group). Values are plotted as means ± SEM. (**d**) Representative microscope images of liver sections stained with Perls' Prussian blue for the detection of ferric iron deposits were captured using a 10× objective lens (n = 6/group). *p*-value summary: ****, $p < 0.0001$.

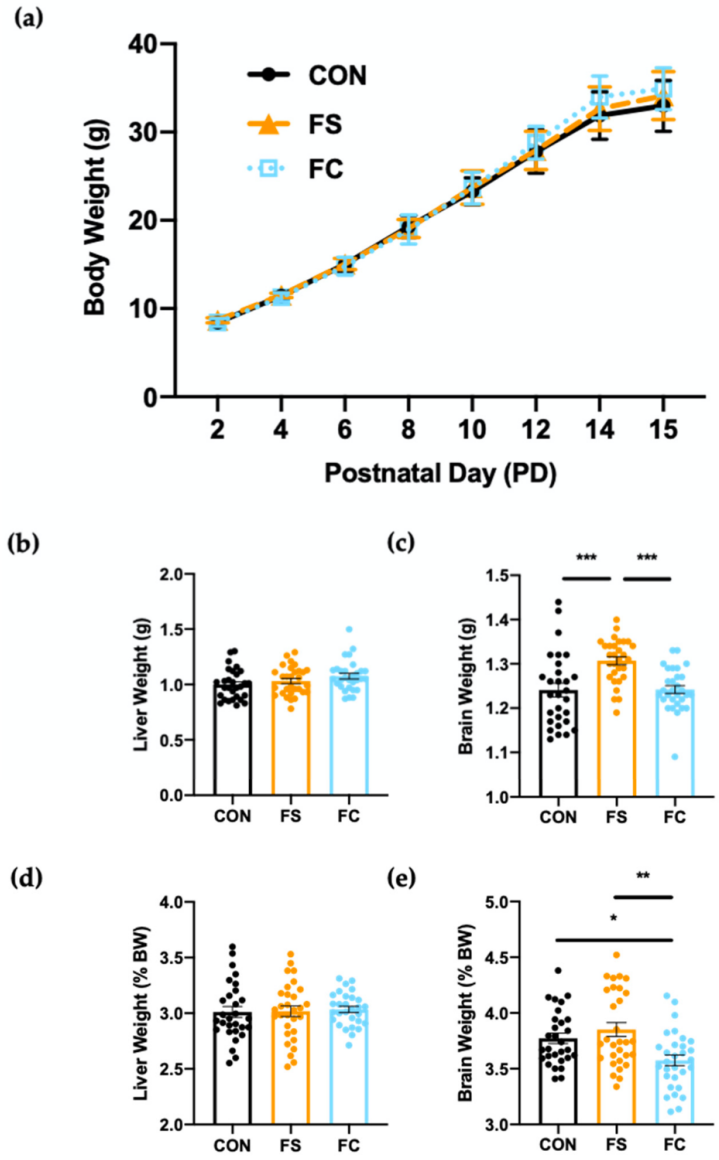

Figure 2. Weight gain and organ development with daily postnatal FS or FC supplementation in rats. (**a**) Pup body weights (*n* = 3 litters/group, 10 pups each litter) were recorded across the supplementation period from postnatal day (PD) 2–15; litter averages were analyzed as biological replicates and plotted as mean ± SD. Group and time effects were assessed by repeated-measures two- way ANOVA with Geisser–Greenhouse correction. (**b**) Liver and (**c**) brain weights were recorded at time of collection on PD 15 and normalized to body weight (**d,e**). Organ weight values are plotted as the means ± SEM. *p*-value summary: *, $p < 0.05$; **, $p < 0.01$; ***, $p < 0.001$.

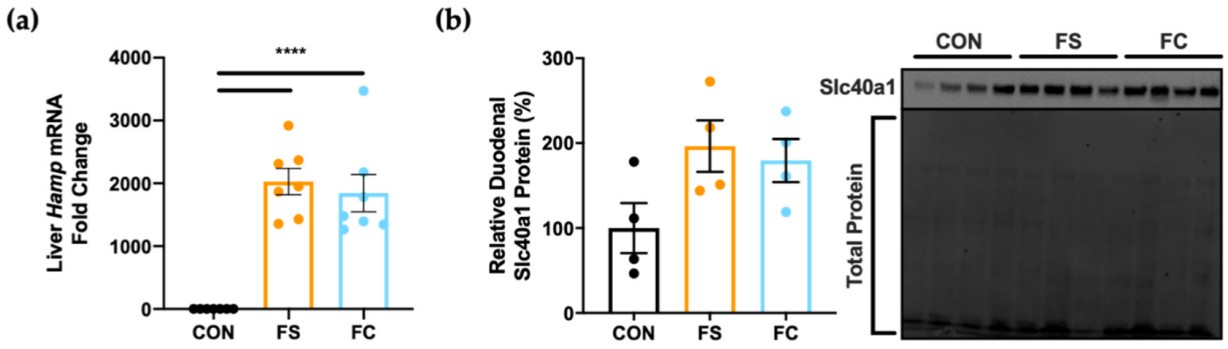

Figure 3. Changes in systemic iron regulation at PD 15. (**a**) Liver hepcidin (Hamp) mRNA expression was assessed by real-time PCR (*n* = 7–8/group). Values with the mean ± SEM are plotted as fold change relative to CON means. (**b**) Relative expression of the iron exporter protein, ferroportin (Slc40a1), was assessed in the proximal small intestine (*n* = 4/group). Adjusted Sllc40a1 band density was normalized to total protein with the Stain-Free™ method, and values are plotted relative to CON expression (%) as means ± SEM. *p*-value summary: ****, $p < 0.0001$.

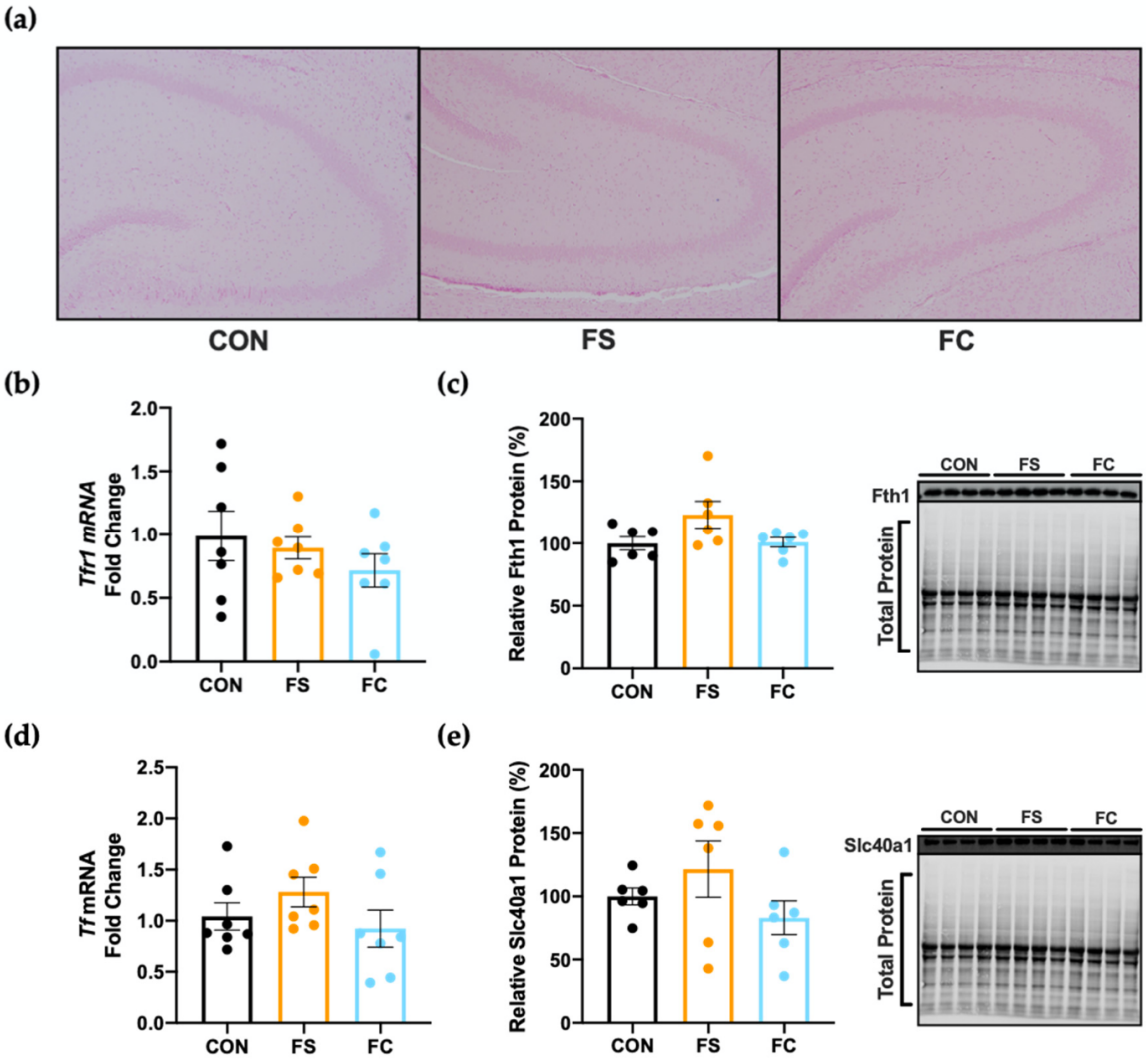

Figure 4. Hippocampal iron loading and regulation on PD 15. (**a**) Representative microscope images of hippocampal sections stained with Perls' Prussian blue stain for ferric iron detection, captured with 10x objective lens (*n* = 5–6/group). (**b**) Transferrin receptor (*Tfr1*) and (**d**) transferrin (*Tf*) mRNA expression in hippocampal tissue, shown as fold change relative to CON (*n* = 7/group). (**c**) Hippocampal expression of ferritin heavy chain (Fth1) subunit, and (**e**) iron exporter protein ferroportin (Slc40a1) expression were normalized to total protein using the Stain-Free™ method and plotted relative (%) to CON expression (*n* = 6/group). Representative blots shown on the right with total protein. Values are shown as the means ± SEM.

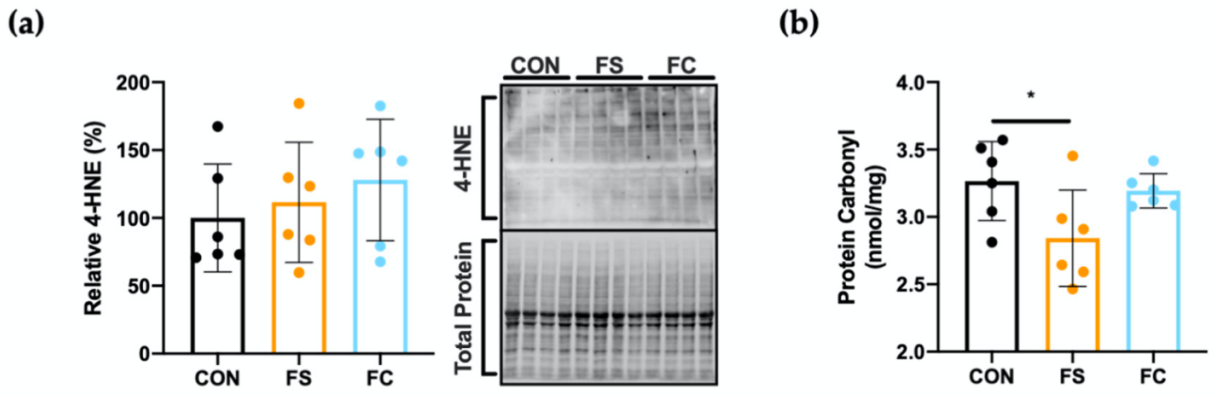

Figure 5. Hippocampal oxidative stress at PD 15. (**a**) To detect lipid peroxidation effects, 4-hydroxynonenal (4HNE) modified proteins were quantified by Western blot (*n* = 6/group), normalized to total protein using the Stain-Free™ method, and values with the mean ± SEM are plotted relative to mean CON expression (%). A representative blot with Stain-Free™ total protein blot is shown to the right. (**b**) Protein carbonyl content, a marker of protein oxidation, was quantified in hippocampal tissue lysates by enzyme-linked immunosorbent assay (ELISA; *n* = 6/group). Values are plotted as the means ± SEM. *p*-value summary: *, $p < 0.05$.

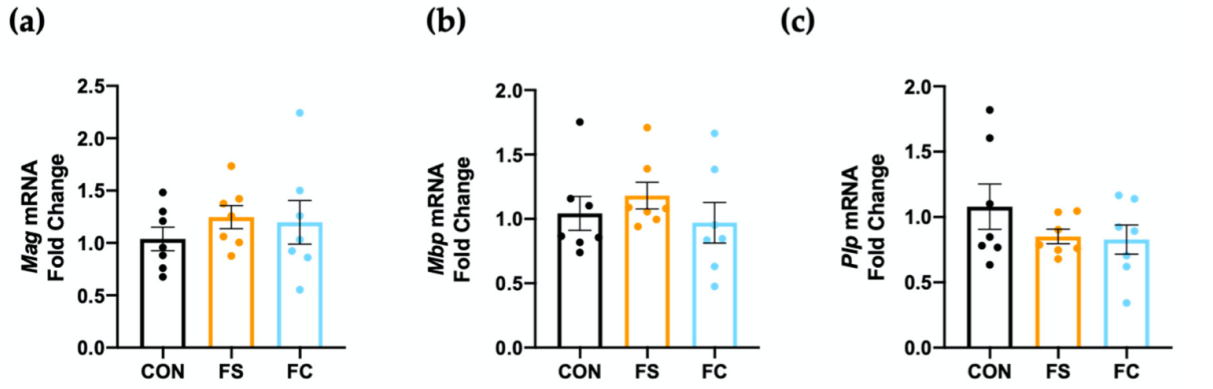

Figure 6. Hippocampal myelination gene expression at PD 15. Expression of major myelin components, (**a**) myelin-associated glycoprotein (*Mag*), (**b**) myelin basic protein (*Mbp*), and (**c**) myelin proteolipid protein (*Plp*) as assessed in hippocampal tissue by real-time PCR (*n* = 7/group). Values are plotted as fold change relative to CON as the means ± SEM.

TABLES

Table 1. Suckling rat iron over-supplementation dose determination.

Species	Diet	Feeding Volume (mL/day)	Dietary Iron (mg/L)	Daily Iron Intake[1] (mg/kg Body Weight)	Iron Absorption (%)	Adjusted Daily Iron Intake[2] (mg/ kg Body Weight)
Human	Breast milk	600-800 [6]	0.35 [32]	0.04-0.07	50 [21]	HM = 0.02-0.035
Human	Iron-fortified formula	600-800 [6]	12 [7]	1.4	10 [22]	HF = 0.14
Rat	Rat milk	4-10 [33]	5 [34]	1.6-2.0	100 [24]	RM = 1.6-2.0
Daily Iron Dose = RM • (HF/HM) = [6.4 – 14] mg Iron / kg Body Weight ≈ 10 mg Iron / kg Body Weight						

[1] Based on 5-7 kg infant; 10–30 g rat pup; [2] Adjusted for iron absorption

Table 2. Real-time PCR primer sequences.

Gene	Primer Sequence[1]	Reference
Actb	F: GAAATCGTGCGTGACATTAAAGAG R: GCGGCAGTGGCCATCTC	[36]
Hamp	F: GCTGCCTGTCTCCTGCTTCT R: CTGCAGAGCCGTAGTCTGTCTCGTC	[23]
Tf	F: GCATCAGACTCCAGCATCAA R: CAGGACAGTCTGGTGCTTCA	[37]
TfR1	F: GAGTTCACTGACATCATCAA R: GCAATCCAGATGACTGAGAT	[36]
Mag	F: TGTGTAGCTGAGAAGGAGTATGG R: ACAGTGCGATTCCAGAAGGATTAT	[38]
Mbp	F: CTCTGGCAAGGACTCACACAC R: TCTGCTGAGGGACAGGCCTCTC	[39]
Plp	F: GTGTTCTCCCATGGAATGCT R: TGAAGGTGAGCAGGGAAACT	[40]

CHAPTER 3: Gut microbiome alterations following postnatal iron supplementation depend on iron form and persist into adulthood

ABSTRACT

he gut microbiota is implicated in the adverse developmental outcomes of postnatal iron supplementation. To generate hypotheses on how changes to the gut microbiota by iron adversely affect development, and to determine whether the form of iron influences microbiota outcomes, we characterized gut microbiome and metabolome changes in Sprague-Dawley rat pups given oral supplements of ferrous sulfate (FS), ferrous bis-glycinate chelate (FC), or vehicle control (CON) on postnatal day (PD) 2–14. Iron supplementation reduced microbiome alpha-diversity ($p < 0.0001$) and altered short-chain fatty acids (SCFAs) and trimethylamine (TMA) in a form-dependent manner. To investigate the long-term effects of iron provision in early life, an additional cohort was supplemented with FS, FC, or CON until PD 21 and then weaned onto standard chow. At ~8 weeks of age, young adult (YA) rats that received FS exhibited more diverse microbiomes com-pared to CON ($p < 0.05$), whereas FC microbiomes were less diverse ($p < 0.05$). Iron provision resulted in 10,000-fold reduced abundance of Lactobacilli in pre-weanling and YA animals provided iron in early life ($p < 0.0001$). Our results suggest that in pre-weanling rats, supplemental iron form can generate differential effects on the gut microbiota and microbial metabolism that persist into adulthood.

3.1. INTRODUCTION

Iron deficiency (ID)—which affects approximately 10–40% of infants worldwide—can irreversibly disrupt neurodevelopment [1–4]. Iron supplements and iron-fortified foods are widely used during infancy to prevent ID [5,6]; however, iron provision is not without risks [7–9]. Iron provision can have adverse effects in infants, including inflammation [10], growth delay [7,11–13], long-term cognitive

deficits [14–16], and morbidities [11,17–19]. The mechanisms underlying these adverse effects are not fully known [8,9,20].

Recent evidence suggests that iron alters development of the gut microbiota in in- fants [8,19]. The developing microbiota confers an array of health benefits for the infant, such as improved intestinal barrier function and nutrient absorption, as well as infection re- sistance [21–25]. The development of the microbiota is influenced by the infant's diet [26,27]. Iron salts, such as ferrous sulfate (FS), are commonly used in supplements and infant for- mula, despite relatively low bioavailability—only 10% of FS iron is absorbed by infants [28]. Unabsorbed iron in the gut may exert effects on the microbiota [10,19,29–31]. Postnatal iron administration has been shown to suppress typical populations comprising the commensal bacteria and promote pathogen-associated bacteria, which may consequently potentiate adverse development outcomes [10,29–32].

The microbiota can influence their host by producing metabolites that guide nutrient absorption [33], infection resistance [34], and immune regulation [35,36], as well as brain development [37] and behavior [38]. There are few studies on the impact of iron on the metabolism of intestinal microbiota. Furthermore, existing microbiome studies in infants have used different iron forms that may exert differential effects on the microbiota [19].

In the present study, we developed an iron supplementation model in pre-weanling rats to mimic the effects of routine iron administration in healthy, term infants [39]. Rat pups received either FS or ferrous bis-glycinate chelate (Ferrochel®; FC), a novel, bioavailable form of iron [40]. Herein, we show that both forms of iron—FS and FC—caused intestinal iron loading and altered the gut microbiome and metabolites in a form-dependent manner.

3.2. MATERIALS & METHODS

3.2.1. Animal Experiments

The University of California Institutional Animal Care and Use Committee approved all animal experiments. The postnatal rat iron supplementation model methods have been described in detail previously [39], including rationale for iron dosage. Sprague- Dawley rat litters (n = 3 litters per group, culled to 10 pups per litter) were kept with dams and allowed to nurse *ad libitum*, except for during a brief daily supplementation period. Daily supplementation occurred during PD 2–14 according to random treatment group assignment to vehicle control (CON, 10% sucrose) or 10 mg iron/kg body weight (BW) as ferrous sulfate (FS) or ferrous bis-glycinate chelate (Ferrochel®, FC). To determine whether postnatal iron supplementation induced lasting changes to the rat microbiome, additional litters (n = 4 litters per group, culled to 10 pups per litter on PD 2) were randomly assigned to FS, FC, or CON groups on PD 2. These litters received daily supplements from PD 2–20 and were weaned on PD 21. All weanling rats were housed with 1–4 littermates and received standard chow (200 mg iron/kg diet as ferrous sulfate; 2018, Teklad Diets, Madison, WI, USA) ad libitum for approximately 6 weeks.

For necropsy of pre-weanling rats, tissues, cecal content, and blood were collected from 4–6 h-fasted animals on postnatal day (PD) 15. For necropsy of adult rats, blood, tissue, and cecal content samples were collected and body, brain, and liver weight were recorded following 4–6 h fasting, on PD 58 ± 4. This age group is referred to as the young adult (YA) group.

3.2.2. Iron Analysis and Hemoglobin

Distal small intestine iron concentration was determined by nitric acid wet-ashing and atomic absorption spectrometry (n = 7/group), as previously described [39]. Liver (n = 8–10/group) and spleen (n = 11–12/group) iron concentrations were also measured in YA rats using this method. For histological evaluation, fresh tissue was perfused with 1× PBS and immersion-fixed in 4% w/v paraformaldehyde (PFA) for 24 h at 4 ◦C, washed in three changes of 1× PBS, and stored in 70% ethanol at 4 ◦C. Fixed issues were embedded in paraffin, sectioned, and stained with Perls' Prussian blue for iron detection (n =

6/group, 3 litters/group) at the UC Davis School of Veterinary Medicine Anatomic Pathology Laboratory. Hemoglobin was measured in fresh, whole blood collected from YA rats using a kit (Cat#MAK115-1KT, Sigma-Aldrich, St. Louis, MO, USA).

3.2.3. Distal Small Intestine Morphology

Following PFA-fixation and paraffin embedding, as described above, two 1 cm distal sections of intestine from each pup (n = 6/group, 3 litters/group) were stained with H&E by UC Davis School of Veterinary Medicine Anatomic Pathology Laboratory for morphological evaluation. Microscope images (20× objective lens) were analyzed using ImageJ software (v1.51; [41]) to quantify villus height and crypt depth. All images were obtained in a blinded fashion. Data represent means of 20 villi and 20 neighboring crypts for each biological replicate.

3.2.4. Distal Small Intestine Gene Expression

Approximately 1 cm distal intestine was collected during necropsy, perfused with 1× PBS, and stored in RNA*later*® (Thermo Fisher Scientific™, Waltham, MA, USA) for 24 h at room temperature, and then at −20 ◦C until RNA extraction. RNA was extracted from intestine using TRIzol (Invitrogen™, Carlsbad, CA, USA) according to the manufacturer's instructions. RNA was reverse transcribed using the High-Capacity cDNA Archive Kit (Applied Biosystems™, Cat#4374966, Applied Biosystems™, Foster City, CA, USA), according to the manufacturer's instructions. Real-Time quantitative PCR was performed using a Bio-Rad CFX96 Real-Time machine with iTaq Universal SYBR Green Supermix (Cat#1725121, Bio-Rad, Hercules, CA, USA). Fold-change in mRNA gene expression was calculated using the $2^{\Delta\Delta Ct}$, with *Actb* serving as the housekeeping gene. Primer sequences are listed in Table S1. Intron-spanning primers were designed using MacVector v18.0.1 (74) software (MacVector Inc., Apex, NC, USA).

3.2.5. Cecal DNA & Metabolite Extraction

Cecal content was collected in sterile tubes and flash frozen in liquid nitrogen and stored at −80 ◦C. DNA and metabolites were extracted from the same samples, under the same thaw cycle. All surfaces and equipment used during extraction were cleaned with 70% ethanol and decontaminated with DNA Away (Cat#2123628, Thermo Fisher Scientific™, Waltham, MA, USA). Cecal content was thawed on ice, weighed, and homogenized in 1.5 mL of sterile, ice cold 1× PBS. Samples rested on ice at intervals during homogenization. Following homogenization, samples were pelleted by centrifugation at 14k rcf. DNA was extracted from the pellet, and metabolites were isolated from the supernatant. Each sample of supernatant was filtered through a 0.22 um syringe and then loaded onto a pre-washed 3 kDa Amicon Ultra Centrifugal Filter Unit (Cat# UFC500396, Millipore Sigma, Burlington, MA, USA) to remove contaminants prior to storage at −80 ◦C. DNA was extracted from the sample pellet using the DNeasy PowerLyzer PowerSoil Kit (QIAGEN, Hilden, Germany) according to manufacturer's instructions, with the following modifications: sample pellets were vortexed with beads and bead solution and incubated for 10 min at 65 ◦C, followed by 10 min at 95 ◦C prior to bead beating for 2 min at 6.5 m/s to ensure complete lysis of bacterial cells. Extracted DNA was stored at −80 ◦C.

3.2.6. 16s rRNA Library Construction, Sequencing, and Processing

Barcoded primers with Illumina sequencing adapters (Table S1) were combined with GoTaq® Master Mix for PCR (Promega Corporation, Madison, WI, USA) to amplify the variable region 4 (V4) of the prokaryotic 16S rRNA gene in the cecal DNA samples (primer sequences in Table S1). Libraries were constructed from PCR products that had been pre-checked for quality on an agarose gel with SYBR TM Safe (Thermo Fisher Scientific™, Waltham, MA, USA) and purified using a kit (QIAGEN, Hilden, Germany). Libraries were sequenced with an Illumina MiSeq platform at the DNA Technologies and Expression Analysis Core Laboratory at UC Davis.

A total of 17 million paired-end Illumina reads passed initial filtering with an overall Q30 of >80%. Reads were imported into QIIME 2, v2020.2 [42] and demultiplexed using the emp-paired plugin [43,44]. Demultiplexed reads were filtered and denoised with the DADA2 plugin to identify unique 16S amplicon sequence variants (ASVs) [45]. To optimize read quality, forward and reverse sequences were trimmed to 240 bp and 200 bp, respectively, and reads were filtered to allow a maximum of two expected errors. In the PD 15 age group (n = 27–29 per treatment group), a total of 3.3 million reads passed quality filtering and were merged, and 1111 ASVs were identified; in the YA age group (n = 22–23 per treatment), 4.0 million reads passed quality filtering and were merged, and 1889 ASV's were identified. Features (ASV's) and their representative sequences were applied to the phylogeny align-to-tree-mafft-fasttree pipeline to construct a phylogenetic tree. Rarefaction plotting and computation of alpha-diversity indices were performed using the alpha-rarefaction plugin. ASV's were assigned to taxonomy using the feature-classifier plugin [46] with a Bayes classifier that was pretrained on a Silva 138 V4 reference database [47–50]. Finally, the ASV table, representative sequence table, and constructed phylogenetic tree were imported into R (v4.1.0) using the qiime2R package for beta diversity, relative abundance, and statistical analysis, described in further detail below.

3.2.7. NMR Metabolomics

Cecal filtrate was mixed with EDTA/K_2HPO_4 buffer (pH 8.07) such that the final concentrations were 2 mM/10 mM, respectively. To this cecal mixture (CM), an internal standard (IS) containing 5 mM 3-trimethylsilyl-1-propanesulfonic acid-d6 (DSS-d6), in 99% deuterium oxide (D_2O) and 0.2% sodium azide (NaN_3) (Chenomx; AB, Canada) was added in a 1:10 IS:CM ratio. Sample pH was adjusted to between 6.95 and 7.10 using HCl or NaOH, and samples were then placed into 3 mm NMR tubes and maintained at 4 ◦C prior to acquisition. NMR spectra were recorded on a 600 MHz AVANCE system (Bruker, Billerica, MA, USA) equipped with a SampleJet using the noesypr1D pulse sequence at 25 ◦C, as

described in [51]. The corresponding spectra were analyzed using Chenomx NMRSuite Professional v.8.5 [52], and output as concentrations.

3.2.8. Statistical Analysis

Statistical analysis and plotting were performed using GraphPad Prism (v8), and R (v4.1.0) with the following core packages: ggplot2 (v3.3.3), phyloseq (v1.36.0), microbiome (v1.14.0), qiime2R (v0.99.6), car (v3.0-10), dunn.test (v1.3.5), pairwiseAdonis (v0.0.1), and DESeq2 (v1.32.0). p-values < 0.05 were considered significant.

Differences in iron concentration were detected among treatments with Kruskal– Wallis and Dunn's tests. Differences in hemoglobin, intestinal morphology, and gene expression among treatment groups were detected with one-way ANOVA and Tukey's tests. Differences in body, brain, and liver weight among groups in male and female YA rats were also detected with one-way ANOVA and Tukey's tests.

For the 16S rRNA amplicon sequencing library analysis, a total of 153 samples were sequenced from both age groups of the original 162 (90 pups and 72 YA rats) planned for collection. Two CON cecal samples were not collected during necropsy in error, and four samples (three from FS and one from FC) yielded poor quality DNA due to a small cecal sample size, leaving 84 pup samples to be sequenced (n = 27–29/group, 3 litters/group). Three YA rats were not sequenced: one CON was not collected at necropsy in error, and one each from FS and FC were lost in error during DNA extraction, leaving 69 YA samples to be sequenced (n = 23/group, 3 litters each group). Following sequencing, four additional samples were excluded from microbiome analyses due to zero reads following filtering and denoising. These samples were from YA rats in the FC group, and for unknown reasons produced only poor-quality reads during sequencing that were then filtered out.

Alpha-diversity was assessed by rarefying at depths from 1–10,000 sequences. Three different metrics of alpha-diversity were estimated at each sampling depth: Faith's Phylogenetic Diversity Index, Shannon's H Index, and richness (amplicon sequence variant, ASV, count). For each alpha-diversity metric, sample values were calculated by taking the mean of 10 iterations at that sampling depth. Significant differences in each alpha-diversity metric due to treatment and among treatment groups were detected at each depth by Kruskal–Wallis test, and Dunn's post-hoc test, respectively. Beta-diversity was assessed by log-transforming ASV counts and by using principal coordinate analyses (PCoA's) to evaluate three beta-diversity metrics per age group: Weighted UniFrac, Unweighted UniFrac, and Bray–Curtis. In each age group and for each beta-diversity metric, PERMANOVA's were used detect the effects of treatment, sex, litter, and variable interactions on community heterogeneity. For each PERMANOVA, 10,000 randomizations were performed to test for significance. For differential phylum and genus abundance, ASV counts were aggregated to Phylum or Genus level, respectively, and pseudo-counts of 1 were added to all ASV's to remove 0 values. Differential abundance due to treatment was assessed at both taxonomic ranks for both ages using DESeq2 [53,54]. Pairwise results were extracted and plotted as $\log_2$[Fold-Change], and FDR-adjusted p-values < 0.05 were considered to be a significantly different change between groups.

One cecal metabolite extract sample belonging to the pup CON group was removed due to excess zeros and lack of confidence in quantification using Chenomx (see metabolite methods above). Metabolite concentrations were converted to nmol/g wet weight by multiplying the concentration by the volume of buffer each was extracted into and dividing by the wet weight of the cecal content before extraction. Sex and litter effects were assessed separately using the multivariate approach of PCoA followed by PLS-DA; both methods demonstrated uninfluential overlap within the metabolome. Metabolites were analyzed using Kruskal-Wallis followed by Dunn's multiple comparison test in Prism GraphPad v 6.0c.

3.3. RESULTS

3.3.1. Effects of Postnatal Iron Supplementation on the Distal Small Intestine in Pups

3.3.1.1. Distal Small Intestine Iron Loading

Iron concentration was measured in the distal small intestine of ferrous sulfate (FS) iron, ferrous bis-glycinate chelate (FC) iron, and vehicle-control supplemented (CON) pups, where tissue darkening was observed in samples collected from iron-supplemented pups (Figure 1B; top row). Both FS and FC treatments increased tissue iron concentration in the distal small intestine ($p < 0.01$; Figure 1A), an effect independent of iron form ($p = 0.26$). Perls' Prussian blue staining for iron in fixed distal small intestine sections confirmed mucosal iron loading (Figure 1B; middle and bottom rows).

3.3.1.2. Distal Small Intestine Morphology

Previous studies have reported cytotoxic effects of iron loading in the gastrointestinal mucosa leading to tissue necrosis and atrophy of intestinal villi [55,56]. Despite marked iron loading in the distal small intestine with iron treatment, no alterations were observed in villus height, crypt depth, or villus height/crypt depth ratio (Figure S1).

3.3.1.3. Distal Small Intestine Gene Expression

In adult animals, interleukin 22 (Il22) is constitutively expressed by intestinal immune cells and regulates the mucosal barrier and intestinal inflammation. Pro-inflammatory signaling upregulates Il22, which then signals epithelial cell survival and proliferation to promote mucosal barrier integrity [57]. Il22 also promotes intestinal antimicrobial activity. Anti-microbial genes *Lcn2*, *Reg3g*, and *Lyz* are modulated by Il22 signaling [58–61]. A decrease in *Il22* mRNA expression in the distal small intestine was found for both iron treatment groups ($p < 0.01$;

Figure 1C). No differences in expression of *Lcn2*, *Lyz*, or *Reg3g* were found among treatment groups.

Ferroptosis is an iron-dependent form of cell death that may be initiated in iron-loaded cells [62]. It is currently unclear if iron loading alone can increase ferroptotic activity in the various cells comprising the small intestine [63]. *Gpx4* expression was elevated in the FS group but not in the FC group compared to CON ($p < 0.01$; Figure 1D). Increased *Gpx4* expression in FS-treated samples is suggestive of an antioxidant, anti-ferroptotic response. *Gpx4* enzymatic activity mitigates damage by lipid peroxidation and is suppressed during ferroptosis [64]. No effect of treatment was observed in *Nox4* or *p22-phox*, genes involved in NADPH oxidase, suggesting ferroptosis was not induced due to iron loading [62,65].

3.3.2. Effect of FS vs. FC on Cecal Microbiome in Pups

3.3.2.1. Cecal Microbiome Diversity

Iron supplementation reduced alpha diversity at all sampling depths >1 in all metrics ($p < 0.0001$; Figures 2 and S2); this effect was greater in the FC group (FC vs CON, $p < 0.001$; FC vs. FS, $p < 0.05$). Faith's Phylogenetic Diversity (FPD, Figure 2A) and ASV count (species richness, Figure S2) diversity were lower in the FS group compared to CON ($p < 0.01$); but Shannon's H Index, an alpha-diversity metric that assesses both richness and evenness, was similar between FS and CON (Figure S2).

Cecal bacterial community dissimilarity (beta-diversity) effects were observed due to treatment and litter, but no effect of sex on beta-diversity was observed across metrics. There were effects of treatment on Bray Curtis and unweighted UniFrac distances (Figure S2; $p < 0.0001$) as well as treatment:litter interaction ($p < 0.0001$). Effects of treatment:sex and treatment:sex:litter interactions on unweighted UniFrac distance were also found ($p < 0.01$).

Pairwise analysis of Bray Curtis and unweighted UniFrac results revealed separation of iron treatment groups from CON ($p < 0.01$) and separation between iron groups ($p < 0.01$). No effect of treatment was found on weighted UniFrac distance (Figure 2B; $p = 0.08$). These and the alpha-diversity results indicate that the overall gut microbiome community was altered by iron treatment while specific effects depended upon litter (i.e., baseline microbiome). The microbiome shifts observed with this early iron treatment support that exogenous iron may be disruptive to early microbiome colonization. P-values from alpha- and beta-diversity analyses in pups are listed in Table S2.

3.3.2.2. Cecal Microbiome Differential Abundance

In general, relative phyla abundance was comparable to what has been reported previously at this developmental stage [66]. Dominant phyla included Proteobacteria and Firmicutes, as well as Bacteroidetes, Actinobacteria, and Verrucomicrobia (Figure 2C). Relative abundance of bacterial phyla was altered with iron supplementation according to iron form (Figure 2C-D, Figure S3). In FC-treated pups we found a 100-fold lower abundance of Bacteroidetes ($p < 0.0001$) and lower Firmicutes ($p < 0.05$) compared to CON; Verrucomicrobia were over 6-fold elevated ($p < 0.001$). Relative abundances of Bacteroidetes, Firmicutes, and Verrucomicrobia were similar between FS and CON. Conversely, Tenericutes abundance was elevated with FS treatment compared to CON ($p < 0.0001$) while it was similar between FC and CON.

Loss of Bacteroidetes and Firmicutes with FC treatment suggest potential adverse effects on health with this form of iron. A high-fat diet or high-fat, high-sugar diet in mice can lower Bacteroidetes abundance and this is associated with metabolic dysfunction. Similarly, low fiber intake also results in decreased Bacteroidetes abundance in mice. The lower abundance of

Firmicutes in FC is unlikely to be beneficial to the host, as Firmicutes generate SCFA and other metabolites that may be beneficial to the host [67]. Statistical results of phylum differential abundance in pups are listed in Table S3.

We identified 73 differentially abundant genera among CON, FS, and FC pups (Figures 3 and S3). Iron-treated pups had a 10,000-fold lower abundance of *Lactobacilli* compared to CON pups ($p < 0.0001$); this effect was the largest we observed in all the 73 differentially abundant genera. *Bifidobacteria* were also less abundant in iron-treated pups ($p < 0.05$), as were *Turcibacter* ($p < 0.0001$), while *Ruminococcus 2* relative abundance was elevated ($p < 0.0001$). *Bacteroides* were *Parabacteroides* were 100-fold less abundant ($p < 0.0001$) in FC compared to CON, but these were uninfluenced by FS treatment. No changes in *Escherichia-Shigella* abundance was observed among treatment groups. Abundance of *Clostridium sensu stricto 1* was increased in FS compared to CON ($p < 0.0001$) but was comparable between CON and FC.

Lactobacillus and *Bifidobacterium* are considered beneficial, so their reduced abundance with iron treatment could imply adverse health and development effects [19,21,67]. These results also imply that FC changes are potentially less adverse than FS-induced microbiome changes, since *Bacteroides* is reduced with FC and *Clostridium* is increased with FS. Bacteroides are associated with metabolic dysfunction and *Clostridium* are associated with more pathogenic activity [67]. Statistical results of genus differential abundance in pups are listed in Table S4.

3.3.3. Effects of FS or FC on Cecal Metabolites in Pups

A total of 25 metabolites were identified and quantified from rat pup cecal extracts. These metabolites included short-chain fatty acids (SCFA): acetate, butyrate, propionate, valerate, and isovalerate; amino acids: alanine, arginine, glutamate, glycine, isoleucine, leucine,

methionine, proline, and valine; organic acids: 2-oxoglutarate, 3-hydroxybutyrate, 4-aminobutyrate, 5-aminopentanoate, formate, lactate, pyruvate, succinate; as well as methanol, trimethylamine (TMA), and sialic acid (Figures 4 & S4). Metabolites that differed between the groups were: acetate (p = 0.0002), butyrate (p = 0.002), propionate (p = 0.03), isovalerate (p = 0.03)), succinate (p = 0.01), and TMA (p = 0.003). Interestingly, differences in metabolite concentrations were largely due to FS treatment, including acetate (higher in FS, p = 0.0001), butyrate (higher in FS, p = 0.002), propionate (higher in FS, p = 0.04), isovalerate (higher in FS, p = 0.02) and succinate (lower in FS, p = 0.01)). Only two metabolite concentrations differed between CON and FC treatment groups: acetate (higher in FC, p = 0.03), and TMA (higher in FC, p = 0.003) (Figure 4). Comparison of the concentrations of the remaining 19 metabolites is shown in Figure S4.

3.3.4. Long-term Effects of FS vs. FC in Young Adult Rats

3.3.4.1. Body, Brain, & Liver Weight, and Iron Status

We measured body, liver, and brain weight in YA rats (n = 22-23/group). We also measured hemoglobin, liver iron concentration, and spleen iron to assess iron status. Male and female results were separated, then tested for treatment effects. Iron treatment did not affect these parameters (Table S5).

3.3.4.2. Cecal Microbiome Diversity

Postnatal supplementation with both iron forms modified alpha-diversity in YA rats with all metrics at all sampling depths > 1 (p < 0.0001; Figures 5A, S4A,C). Direction of effect depended on iron form; FS increased diversity compared to CON (p < 0.05), while FC decreased diversity (p < 0.05).

3.3.4.3. Cecal Microbiome Composition

In YA rats, we observed an effect of treatment on bacterial community dissimilarity with all three metrics ($p < 0.01$; Figures 5B, S4B,D). Effects of treatment:litter interaction on Bray-Curtis and unweighted UniFrac distances were also observed ($p < 0.0001$; Figures S5B,D). Pairwise analysis of treatment groups revealed separation of iron-treated groups from CON, and separation between iron groups ($p < 0.05$), indicating that postnatal iron supplementation and iron form affected YA cecal bacterial community composition. These and the alpha-diversity results indicate differential effects on the overall microbiome community with FS vs. FC iron treatment in early life. Indeed, FS and FC-treated microbiomes appeared more distinct from each other than from CON. This suggests different forms of iron used for supplementation in early life may initiate divergent adult gut microbiome phenotypes. P-values from alpha- and beta-diversity analyses in YA rats are listed in Table S6.

3.3.4.4. Cecal Microbiome Differential Abundance

A lower abundance (~10-fold) of Proteobacteria was found in YA rats that were treated with FS and FC ($p < 0.0001$; Figure 5D). Consistent with the results in pups, FC-treated YA rats had less Bacteroidetes than CON ($p < 0.0001$) and elevated Verrucomicrobia ($p < 0.01$); however, parallel changes did not occur in FS-treated rats. In YA rats, but not pups, Patescibacteria ($p < 0.05$) and Cyanobacteria ($p <0.01$) increased in abundance in FC compared to CON, and Actinobacteria was decreased ($p < 0.0001$), while these were unchanged in the FS group. Unidentified organisms ($p < 0.01$) were decreased with FS compared to CON but were unaffected by FC. As in pups, the reduced abundance of Bacteroidetes due to FC treatment in early life may suggest adverse effects to health and metabolism [67]. However, the reduced Proteobacteria abundance with iron treatment may have beneficial effects, since this phylum

contains many pathogenic gram-negative bacteria and elevated abundance may cause dysbiosis [68]. Statistical results of phylum differential abundance in YA rats are listed in Table S7.

We identified 95 differentially abundant genera among YA rat treatment groups (Figure 6 & S6). Consistent with results in pups, iron-treated rats had more than 10,000-fold lower abundance of *Lactobacillus* compared to CON rats ($p < 0.0001$); the largest effect observed in all the 95 differentially abundant genera in YA rats. *Turicibacter* abundance was 1,000-fold lower in iron-treated rats ($p < 0.0001$). In iron-treated YA rats but not in pups, abundance of *Escherichia-Shigella* was around 10-fold lower than CON ($p < 0.0001$), and this effect was similar between FS and FC. Also consistent with pups: *Bifidobacterium* abundance in FC rats was over 100-fold lower than CON ($p < 0.0001$), although it was similar between FS and CON; Bacteroides abundance was over 100-fold lower in FC rats compared to CON ($p < 0.0001$) and was comparable between FS and CON. The reduction of *Escherichia-Shigella* bacteria with early life iron treatment is suggestive of beneficial effects but the reduction of *Lactobacillus* is inconsistent with that notion. Reduced *Bacteroides* with FC treatment may be beneficial, but reduced *Bifidobacterium* is un likely to be beneficial to health [67]. Statistical results of genus differential abundance in YA rats are listed in Table S8.

3.4. DISCUSSION

Current research suggests that supplemental iron causes unfavorable changes to the infant gut microbiota [8,19], which may explain how iron can adversely affect infant health [11,17,69], growth [11,12], and development [14,15,70–72]. Few studies have examined the effects of iron on the microbiota of healthy, term infants, despite evidence that iron- replete infants may experience more adverse effects of exogenous iron [11,12,14,17,69,73]. It has been unclear if iron effects on the microbiota persist beyond weaning, or whether the iron form influences such outcomes. We gave pre-

weanling Sprague-Dawley rats either FS or FC iron (10 mg iron/kg body weight per day; representative of formula iron intake), or a vehicle control (CON) to model the outcomes of iron supplementation in healthy infants [39]. Iron treatment altered the pre-weanling microbiome and its associated metabolites, and long-term microbiome effects in adult animals were also observed. Micro- biome alterations depended upon the form of iron—FS or FC. These findings will generate hypotheses regarding how iron can disrupt health and development in infants.

A recent systematic review concluded that iron supplementation can cause diarrhea in infants—the authors indicated this phenotype may be a direct effect of iron toxicity on host cells or alternatively due to deleterious alterations in the microbiota [18]. To our knowledge, we are the first to report outcomes of iron supplementation in early life on distal small intestine morphology (Figure S1) and ferroptosis (Figure 1D), where iron was provided at physiologically appropriate levels. We did not observe signs of intestinal necrosis or mucosal atrophy in iron-treated pups, despite marked iron loading (Figure 1A,B). This iron loading, combined with the absence of mucosal atrophy, may suggest that the distal small intestine exhibits additional resistance to iron excess. Because we did not report on diarrhea or intestinal iron absorption activity, more experiments are required to understand the role of distal small intestine iron loading on the health and morbidity outcomes of iron supplementation. Our results suggest that, in specific pathogen free rats, iron supplementation at physiological levels does not induce direct cytotoxic effects on the intestine. It is therefore likely that alterations in the gut microbiota may be mediating adverse gastrointestinal outcomes of iron. Future work may assess how baseline microbiome and pathogen burden impact the risk of diarrhea following iron supplementation.

In our study (Figure 2), iron supplementation was found to alter the pre-weanling gut microbiome, including significant heterogeneity of the microbiome communities (beta-diversity) and significantly lower species richness (alpha-diversity). Additionally, microbiome effects were found in adult rats that received iron from PD 2 up to weaning (Figure 5), despite adherence to normal rat chow

for ~six weeks prior to sample collection—a timeframe spanning the sexual maturation of the animal. Adult animals treated with FC prior to weaning had microbiomes that were distinct from FS-treated animals. Our results confirm previous reports that iron supplementation alters the gut microbiota [10,30,31,74]. The findings in adult animals suggest lasting effects of early-life iron supplementation; however, a longitudinal study is necessary to determine the influence of age and weaning on the persistence of microbiome alterations from early-life iron provision. The changes in bacterial abundance at the phylum and genus levels at both ages imply potential adverse effects to health [67]. The differential effects of FS and FC on gut bacterial abundance align with recent evidence that the form of iron is relevant when considering health outcomes of iron provision [75,76].

The gut microbiota can be easily disturbed in early life before the community stabilizes into an adult-like composition, at around 2–3 years of age [22,24,77]. Breastfeeding provides key probiotics and prebiotics for the developing gut, and a growing number of studies suggest long-term health disparities caused by formula-feeding may be attributed to the disruption of early gut microbiota [21,23,78,79]. The typical infant formula provides approximately twenty-fold more iron than breast milk [80]. Early introduction of formula or weaning foods—often fortified with FS iron—disrupts the natural temporal development of the gut microbiota, which has negative implications for infant health and development [23,77,78]. Host-microbe interactions between humans (or other mammals) and milk-associated microbes *Bifidobacterium* or *Lactobacillus* typically protect health and guide development [27,81–83]. *Bifidobacteria* predominate in the breast-fed infant gut, gradually subsiding as gut communities become more diverse upon introduction of complementary foods [21,22,27,77]. *Lactobacilli* predominance in nursing rat pups is thought to be symbiotic and supported by rat milk [82,84,85], and much like *Bifidobacteria* in humans, relative abundance is reduced at weaning [84]. Although various effects of iron provision were observed, the greatest effect was a reduction of *Lactobacilli* in both pre- weanling and YA rats (Figures 3 and 6). Moreover, we also observed lower *Bifidobacterium* and enriched

Ruminococcus genera due to iron. These results reflect previous microbiome outcomes in controlled iron studies [10,29,31,74], as well as the effects of formula on the gut microbiota [51,79]. It remains plausible that iron supplementation causes adverse health effects in infants by precluding symbiotic, milk-associated microbes in the developing gut. Considering the difference in iron content between iron-fortified formula [80] and human [84,86] or rat milk [87] and the similar effects of iron and iron-fortified formula on the microbiome [19,79], future studies should define the role of iron in formula-induced changes in the gut microbiota.

Various constituents of foodstuffs in the gut lumen are metabolized by the microbiota, forming a complex metabolic network that contributes to the metabolism of the host. Microbial-derived metabolites are essential for proper development of immunity and cognitive functions, as well as for healthy metabolic function [34,37,88,89]. In agreement with the changes to microbial taxa and with previous iron-metabolite studies [90], we found that iron increased cecal concentrations of acetate, butyrate, and propionate (Figure 4)—all three of these SCFAs have important roles in host-microbe interactions. Microbial-derived butyrate, produced by *Clostridia*, is essential for Treg cell differentiation in the colon and protects against colitis [88]. Butyrate and propionate derived from soluble fiber improve metabolic function in a gut-brain communication loop [89]. Conversely, microbial acetate elevated in the context of a high-fat diet promotes metabolic syndrome by activating the parasympathetic nervous system to stimulate ghrelin and insulin secretion [38]. However, acetate produced by *Bifidobacteria* protected mice from enterotoxic *E. coli* [34]. Our results that oral iron increases SCFA production indicate several possible host-microbe crosstalk mechanisms by which iron supplementation affects development.

It is crucial to note that cecal metabolites following iron supplementation depended on iron form. Although both iron forms increased cecal acetate, only FS increased butyrate, propionate, and isovalerate (a branched SCFA), and only FC increased TMA, a metabolite that is associated with

cardiovascular health. These differences reflect delineating alterations in microbial taxonomy between iron treatments. Compared to CON, the relative abundance of the butyrate-producer *Ruminococcus* was higher in the FS group, consistent with the elevation of butyrate in the FC group. Conversely, other producers of SCFAs (e.g., *Akkermansia*) were higher after FC treatment, which generated acetate, not butyrate or propionate. Moreover, levels of Firmicutes, known producers of TMA [91,92], were lower, but TMA was elevated in the FC group compared to CON. Iron serves as a cofactor for numerous metabolic reactions in both humans and microorganisms. Therefore, these metabolite differences may be reflective of both microbial and host metabolic function, as modulated via iron availability.

It is unclear how FC and FS exert differential effects, but it is possible that these iron forms are absorbed and metabolized by bacteria with different efficiencies. Consistent with our study, differences in microbiome composition were found previously between FS and FC iron groups; luminal iron levels were elevated but comparable between iron groups, challenging the idea that microbiome differences between forms arose from differences in iron availability [76]. In our study, differential effects of FS and FC on alpha-diversity were found in YA rats. A recent study in adult mice found that microbiome Shannon diversity effects differed according to iron form—FS or Sucrosomial® iron—but observed that species richness increased similarly. A reduction in *Lactobacillaceae* was observed only in Sucrosomial® iron-treated mice [75].

Exactly how iron supplementation alters the gut microbiota is also unclear. Previous experiments have shown that oral iron increases iron availability in the gastrointestinal lumen, and this may have direct or indirect effects on the gut microbiota. Certain bacteria, such as *Lactobacillus*, do not require iron, and this provides a competitive advantage in low-iron environments, while others, such as *E. coli*, gain an ecological niche in high-iron conditions [93,94]. The aforementioned study also reported that increasing dietary iron in adult mice increased luminal iron, shifted microbial communities and metabolism, and reduced the abundance of *Lactobacillus* [76]. Likewise, our data support the idea that

Lactobacillus, which does not require iron for growth, is sensitive to exogenous iron in the pre-weanling gut.

Iron may affect the gut microbial community indirectly by affecting distal small intestine gene expression: Il22, a major regulator of mucosal immunity [57], was suppressed in iron-treated intestine (Figure 1C). To our knowledge, no studies have measured intestinal Il22 regulation in nursing rats treated with oral iron. It is possible that distal intestine iron loading may have altered the microbiota by causing a shift in mucosal immunity and antimicrobial activity [57,60]. Another possibility is that the change in Il22 expression was mediated by microbes, suggesting that iron affects host immunity by altering the gut microbiota. *Lactobacillus* bacteria upregulate Il22 in the intestine [35,36,95]; therefore, iron may cause lower intestinal Il22 expression by reducing the abundance of *Lactobacilli* in the distal intestine. In the small intestine, Il22 expression increases rapidly with weaning and is relatively low during the pre-weaning period compared to adult expression [96]. The functional impact of iron suppressing Il22 expression in the intestine during this developmental period remains unclear.

Our pre-weanling rat supplementation model has several strengths that increase relevance to human infant nutrition. Our dose is well within the physiological range and was specifically designed to represent the average iron intake from iron formula in a healthy, term infant [39]. Similar to human infants [28], iron absorption in rat pups is unregulated during early infancy [97], but it becomes regulated in late infancy. Further, the mechanisms regulating iron absorption during early life are similar in humans and in rat pups [98]. The rat litters were culled to control for growth and separated by treatment to avoid coprophagic iron/microbiota transfer. We used a moderate sample size of outbred rats—at least three litters for each treatment, allowing for assessment of litter and sex variables. There are also several strengths inherent to our microbiome assessment methods compared to previous studies in this area. We identified amplicon sequence variants as opposed to operational taxonomic units, allowing for more precise and reproducible identification of microbes [99]. Additionally, while

several prior studies measured differential abundance based on hand-selected taxa, we characterized all differentially abundant taxa associated with iron treatment. A key limitation of our study is that we did not perform longitudinal measurements of the microbiome, which will be necessary to confirm microbiome changes in adulthood that are contributable to iron supplementation in early life.

3.5. CONCLUSIONS

Our results support prior work demonstrating that postnatal iron supplementation alters gut microbiota development. Our study demonstrates that microbiome changes due to iron supplementation in pre-weanling rats depend on the form of supplemental iron, and shows that iron supplementation in early life results in long-term alterations in the microbiome of adult rats. The functional consequences of these gut microbiome changes remain to be elucidated.

3.6. REFERENCES

1. Burke, R.M.; Leon, J.S.; Suchdev, P.S. Identification, Prevention and Treatment of Iron Deficiency during the First 1000 Days. *Nutrients* **2014**, *6*, 4093–4114. [CrossRef] [PubMed]
2. Yang, Z.; Lönnerdal, B.; Adu-Afarwuah, S.; Brown, K.H.; Chaparro, C.M.; Cohen, R.J.; Domellöf, M.; Hernell, O.; Lartey, A.; Dewey, K.G. Prevalence and Predictors of Iron Deficiency in Fully Breastfed Infants at 6 mo of Age: Comparison of Data from 6 Studies. *Am. J. Clin. Nutr.* **2009**, *89*, 1433–1440. [CrossRef]
3. Black, M.M.; Quigg, A.M.; Hurley, K.M.; Pepper, M.R. Iron Deficiency and Iron-Deficiency Anemia in the First Two Years of Life: Strategies to Prevent Loss of Developmental Potential. *Nutr. Rev.* **2011**, *69*, S64–S70. [CrossRef] [PubMed]
4. East, P.; Doom, J.R.; Blanco, E.; Burrows, R.; Lozoff, B.; Gahagan, S. Iron Deficiency in Infancy and Neurocognitive and Educational Outcomes in Young Adulthood. *Dev. Psychol.* **2021**, *57*, 962–975. [CrossRef] [PubMed]
5. Shelov, S.P. *American Academy of Pediatrics Caring for Your Baby and Young Child: Birth to Age Five*; Bantam: New York, NY, USA, 2009; ISBN 978-0-553-38630-1.
6. World Health Organization. *Iron Deficiency Anaemia: Assessment, Prevention, and Control. A Guide for Programme Managers*; World Health Organization: Geneva, Switzerland, 2001.
7. Pasricha, S.-R.; Hayes, E.; Kalumba, K.; Biggs, B.-A. Effect of Daily Iron Supplementation on Health in Children aged 4–23 Months: A Systematic Review and Meta-Analysis of Randomised Controlled Trials. *Lancet Glob. Health* **2013**, *1*, e77–e86. [CrossRef]
8. Lönnerdal, B. Excess Iron Intake as a Factor in Growth, Infections, and Development of Infants and Young Children. *Am. J. Clin. Nutr.* **2017**, *106*, 1681S–1687S. [CrossRef]
9. Wessling-Resnick, M. Excess Iron: Considerations Related to Development and Early Growth. *Am. J. Clin. Nutr.* **2017**, *106*, 1600S–1605S. [CrossRef]

10. Jaeggi, T.; Kortman, G.A.M.; Moretti, D.; Chassard, C.; Holding, P.; Dostal, A.; Boekhorst, J.; Timmerman, H.M.; Swinkels, D.W.; Tjalsma, H.; et al. Iron Fortification Adversely Affects the Gut microbiome, Increases Pathogen Abundance and Induces Intestinal Inflammation in Kenyan Infants. *Gut* **2015**, *64*, 731–742. [CrossRef]
11. Dewey, K.G.; Domellof, M.; Cohen, R.J.; Rivera, L.L.; Hernell, O.; Lonnerdal, B. Iron Supplementation Affects Growth and Morbidity of Breast-Fed Infants: Results of a Randomized Trial in Sweden and Honduras. *J. Nutr.* **2002**, *132*, 3249–3255. [CrossRef]
12. Lind, T.; Seswandhana, R.; Persson, L.; Lönnerdal, B. Iron Supplementation of Iron-Replete Indonesian Infants is Associated with Reduced Weight-for-Age. *Acta Paediatr.* **2008**, *97*, 770–775. [CrossRef]
13. Majumdar, I.; Paul, P.; Talib, V.H.; Ranga, S. The Effect of Iron Therapy on the Growth of Iron-Replete and Iron-Deplete Children. *J. Trop. Pediatr.* **2003**, *49*, 84–88. [CrossRef] [PubMed]
14. Lozoff, B.; Castillo, M.; Clark, K.; Smith, J.B. Iron-Fortified vs. Low-Iron Infant Formula. *Arch. Pediatr. Adolesc. Med.* **2012**, *166*, 208–215. [CrossRef]
15. Gahagan, S.; Delker, E.; Blanco, E.; Burrows, R.; Lozoff, B. Randomized Controlled Trial of Iron-Fortified versus Low-Iron Infant Formula: Developmental Outcomes at 16 Years. *J. Pediatr.* **2019**, *212*, 124–130.e1. [CrossRef] [PubMed]
16. Agrawal, S.; Berggren, K.L.; Marks, E.; Fox, J.H. Impact of High Iron Intake on Cognition and Neurodegeneration in Humans and in Animal Models: A Systematic Review. *Nutr. Rev.* **2017**, *75*, 456–470. [CrossRef] [PubMed]
17. Sazawal, S.; Black, R.E.; Ramsan, M.; Chwaya, H.M.; Stoltzfus, R.J.; Dutta, A.; Dhingra, U.; Kabole, I.; Deb, S.; Othman, M.K.; et al. Effects of Routine Prophylactic Supplementation with Iron and Folic Acid on Admission to Hospital and Mortality in Preschool Children in a High Malaria Transmission Setting: Community-Based, Randomised, Placebo-Controlled Trial. *Lancet* **2006**, *367*, 133–143. [CrossRef]
18. Ghanchi, A.; James, P.T.; Cerami, C. Guts, Germs, and Iron: A Systematic Review on Iron Supplementation, Iron Fortification, and Diarrhea in Children Aged 4–59 Months. *Curr. Dev. Nutr.* **2019**, *3*, nzz005. [CrossRef]
19. Paganini, D.; Zimmermann, M.B. The Effects of Iron Fortification and Supplementation on the Gut Microbiome and Diarrhea in Infants and Children: A Review. *Am. J. Clin. Nutr.* **2017**, *106*, 1688S–1693S. [CrossRef] [PubMed]
20. Dietary Guidelines Advisory Committee. *Scientific Report of the 2020 Dietary Guidelines Advisory Committee: Advisory Report to the Secretary of Agriculture and the Secretary of Health and Human Services*; U.S. Department of Agriculture, Agricultural Research Service: Washington, DC, USA, 2020; p. 786.
21. Xu, J.; Gordon, J.I. Honor Thy Symbionts. *Proc. Natl. Acad. Sci. USA* **2003**, *100*, 10452–10459. [CrossRef]
22. Yatsunenko, T.; Rey, F.E.; Manary, M.J.; Trehan, I.; Dominguez-Bello, M.G.; Contreras, M.; Magris, M.; Hidalgo, G.; Baldassano, R.N.; Anokhin, A.P.; et al. Human Gut Microbiome Viewed Across Age and Geography. *Nature* **2012**, *486*, 222–227. [CrossRef]
23. Dominguez-Bello, M.G.; Godoy-Vitorino, F.; Knight, R.; Blaser, M.J. Role of the Microbiome in Human Development. *Gut* **2019**, *68*, 1108–1114. [CrossRef] [PubMed]
24. Koenig, J.E.; Spor, A.; Scalfone, N.; Fricker, A.D.; Stombaugh, J.; Knight, R.; Angenent, L.T.; Ley, R.E. Succession of Microbial Consortia in the Developing Infant Gut Microbiome. *Proc. Natl. Acad. Sci. USA* **2011**, *108*, 4578–4585. [CrossRef]
25. Adlerberth, I.; Wold, A.E. Establishment of the Gut Microbiota in Western Infants. *Acta Paediatr. Int. J. Paediatr.* **2009**, *98*, 229–238. [CrossRef]

26. Pacheco, A.R.; Barile, D.; Underwood, M.A.; Mills, D.A. The Impact of the Milk Glycobiome on the Neonate Gut Microbiota. *Annu. Rev. Anim. Biosci.* **2015**, *3*, 419–445. [CrossRef]
27. Zivkovic, A.M.; German, J.B.; Lebrilla, C.B.; Mills, D.A. Human Milk Glycobiome and its Impact on the Infant Gastrointestinal Microbiota. *Proc. Natl. Acad. Sci. USA* **2011**, *108*, 4653–4658. [CrossRef] [PubMed]
28. Domellöf, M.; Lönnerdal, B.; Abrams, S.; Hernell, O. Iron Absorption in Breast-fed Infants: Effects of Age, Iron Status, Iron Supplements, and Complementary Foods. *Am. J. Clin. Nutr.* **2002**, *76*, 198–204. [CrossRef]
29. Paganini, D.; Uyoga, M.A.; Kortman, G.A.M.; Cercamondi, C.I.; Moretti, D.; Barth-Jaeggi, T.; Schwab, C.; Boekhorst, J.; Timmerman, H.M.; Lacroix, C.; et al. Prebiotic Galacto-oligosaccharides Mitigate the Adverse Effects of Iron Fortification on the Gut Microbiome: A Randomised Controlled Study in Kenyan Infants. *Gut* **2017**, *66*, 1956–1967. [CrossRef] [PubMed]
30. Sjödin, K.S.; Domellöf, M.; Lagerqvist, C.; Hernell, O.; Lönnerdal, B.; Szymlek-Gay, E.A.; Sjödin, A.; West, C.E.; Lind, T. Administration of Ferrous Sulfate Drops has Significant Effects on the Gut Microbiota of Iron-Sufficient Infants: A Randomised Controlled Study. *Gut* **2018**, *68*, 2095–2097. [CrossRef]
31. Tang, M.; Frank, D.N.; Hendricks, A.E.; Ir, D.; Esamai, F.; Liechty, E.; Hambidge, K.M.; Krebs, N.F. Iron in Micronutrient Powder Promotes an Unfavorable Gut Microbiota in Kenyan Infants. *Nutrients* **2017**, *9*, 776. [CrossRef]
32. Kalipatnapu, S.; Kuppuswamy, S.; Venugopal, G.; Kaliaperumal, V.; Ramadass, B. Fecal Total Iron Concentration is Inversely Associated with Fecal Lactobacillus in Preschool Children. *J. Gastroenterol. Hepatol.* **2017**, *32*, 1475–1479. [CrossRef]
33. Das, N.K.; Schwartz, A.J.; Barthel, G.; Inohara, N.; Liu, Q.; Sankar, A.; Hill, D.R.; Ma, X.; Lamberg, O.; Schnizlein, M.K.; et al. Microbial Metabolite Signaling Is Required for Systemic Iron Homeostasis. *Cell Metab.* **2020**, *31*, 115–130.e6. [CrossRef]
34. Fukuda, S.; Toh, H.; Hase, K.; Oshima, K.; Nakanishi, Y.; Yoshimura, K.; Tobe, T.; Clarke, J.M.; Topping, D.L.; Suzuki, T.; et al. Bifidobacteria Can Protect from Enteropathogenic Infection through Production of Acetate. *Nature* **2011**, *469*, 543–547. [CrossRef]
35. Zelante, T.; Iannitti, R.G.; Cunha, C.; De Luca, A.; Giovannini, G.; Pieraccini, G.; Zecchi, R.; D'Angelo, C.; Massi-Benedetti, C.; Fallarino, F.; et al. Tryptophan Catabolites from Microbiota Engage Aryl Hydrocarbon Receptor and Balance Mucosal Reactivity via Interleukin-22. *Immunity* **2013**, *39*, 372–385. [CrossRef]
36. Satoh-Takayama, N.; Vosshenrich, C.; Lesjean-Pottier, S.; Sawa, S.; Lochner, M.; Rattis, F.; Mention, J.-J.; Thiam, K.; Cerf-Bensussan, N.; Mandelboim, O.; et al. Microbial Flora Drives Interleukin 22 Production in Intestinal NKp46+ Cells that Provide Innate Mucosal Immune Defense. *Immunity* **2008**, *29*, 958–970. [CrossRef] [PubMed]
37. Selkrig, J.; Wong, P.; Zhang, X.; Pettersson, S. Metabolic Rinkering by the Gut Microbiome. *Gut Microbes* **2014**, *5*, 369–380. [CrossRef]
38. Perry, R.J.; Peng, L.; Barry, N.A.; Cline, G.W.; Zhang, D.; Cardone, R.L.; Petersen, K.F.; Kibbey, R.G.; Goodman, A.L.; Shulman, G.I. Acetate Mediates a Microbiome–Brain–β-Cell Axis to Promote Metabolic Syndrome. *Nature* **2016**, *534*, 213–217. [CrossRef]
39. McMillen, S.; Lönnerdal, B. Postnatal Iron Supplementation with Ferrous Sulfate vs. Ferrous Bis-Glycinate Chelate: Effects on Iron Metabolism, Growth, and Central Nervous System Development in Sprague Dawley Rat Pups. *Nutrients* **2021**, *13*, 1406. [CrossRef]
40. Bagna, R.; Spada, E.; Mazzone, R.; Saracco, P.; Boetti, T.; Cester, E.A.; Bertino, E.; Coscia, A. Efficacy of Supplementation with Iron Sulfate Compared to Iron Bisglycinate Chelate in Preterm Infants. *Curr. Pediatr. Rev.* **2018**, *14*, 123–129. [CrossRef] [PubMed]
41. Rasband, W.S. *ImageJ*; Bethesda: Rockville, MD, USA, 1997.

42. Bolyen, E.; Rideout, J.R.; Dillon, M.R.; Bokulich, N.A.; Abnet, C.C.; Al-Ghalith, G.A.; Alexander, H.; Alm, E.J.; Arumugam, M.; Asnicar, F.; et al. Reproducible, Interactive, Scalable and Extensible Microbiome Data Science using QIIME 2. *Nat. Biotechnol.* **2019**, *37*, 852–857. [CrossRef] [PubMed]
43. Hamady, M.; Knight, R. Microbial Community Profiling for Human Microbiome Projects: Tools, Techniques, and Challenges. *Genome Res.* **2009**, *19*, 1141–1152. [CrossRef] [PubMed]
44. Hamady, M.; Walker, J.J.; Harris, J.; Gold, N.J.; Knight, R.T. Error-correcting Barcoded Primers for Pyrosequencing Hundreds of Samples in Multiplex. *Nat. Methods* **2008**, *5*, 235–237. [CrossRef] [PubMed]
45. Callahan, B.J.; Mcmurdie, P.J.; Rosen, M.J.; Han, A.W.; Johnson, A.J.A.; Holmes, S.P. DADA$_2$: High-Resolution Sample Inference from Illumina Amplicon Data. *Nat. Methods* **2016**, *13*, 581–583. [CrossRef] [PubMed]
46. Bokulich, N.A.; Kaehler, B.D.; Rideout, J.R.; Dillon, M.; Bolyen, E.; Knight, R.; Huttley, G.A.; Gregory Caporaso, J. Optimizing Taxonomic Classification of Marker-Gene Amplicon Sequences with QIIME 2′s q2-feature-classifier Plugin. *Microbiome* **2018**, *6*, 90. [CrossRef] [PubMed]
47. Bokulich, N.; Robeson, M.; Dillon, M. Bokulich-Lab/RESCRIPt: 2020.6.0.Dev0. Zenodo, 2020. Available online: https://zenodo. org/record/3891932#.YeViVf7MJPY (accessed on 17 June 2020).
48. Quast, C.; Pruesse, E.; Yilmaz, P.; Gerken, J.; Schweer, T.; Yarza, P.; Peplies, J.; Glöckner, F.O. The SILVA Ribosomal RNA Gene Database Project: Improved Data Processing and Web-based Tools. *Nucleic Acids Res.* **2013**, *41*, D590–D596. [CrossRef]
49. Yilmaz, P.; Parfrey, L.W.; Yarza, P.; Gerken, J.; Pruesse, E.; Quast, C.; Schweer, T.; Peplies, J.; Ludwig, W.; Glöckner, F.O. The SILVA and "All-species Living Tree Project (LTP)" Taxonomic Frameworks. *Nucleic Acids Res.* **2014**, *42*, D643–D648. [CrossRef]
50. Glöckner, F.O.; Yilmaz, P.; Quast, C.; Gerken, J.; Beccati, A.; Ciuprina, A.; Bruns, G.; Yarza, P.; Peplies, J.; Westram, R.; et al. 25 Years of Serving the Community with Ribosomal RNA Gene Reference Databases and Tools. *J. Biotechnol.* **2017**, *261*, 169–176. [CrossRef] [PubMed]
51. O'Sullivan, A.; He, X.; McNiven, E.M.S.; Haggarty, N.; Lönnerdal, B.; Slupsky, C.M. Early Diet Impacts Infant Rhesus Gut Microbiome, Immunity, and Metabolism. *J. Proteome Res.* **2013**, *12*, 2833–2845. [CrossRef]
52. Weljie, A.M.; Newton, J.; Mercier, P.; Carlson, E.; Slupsky, C.M. Targeted Profiling: Quantitative Analysis of 1H NMR Metabolomics Data. *Anal. Chem.* **2006**, *78*, 4430–4442. [CrossRef] [PubMed]
53. Love, M.I.; Huber, W.; Anders, S. Moderated Estimation of Fold Change and Dispersion for RNA-seq Data with DESeq2. *Genome Biol.* **2014**, *15*, 550. [CrossRef] [PubMed]
54. Thorsen, J.; Brejnrod, A.; Mortensen, M.; Rasmussen, M.A.; Stokholm, J.; Abu Al-Soud, W.; Sørensen, S.; Bisgaard, H.; Waage, J. Large-scale Benchmarking Reveals False Discoveries and Count Transformation Sensitivity in 16S rRNA Gene Amplicon Data Analysis Methods used in Microbiome Studies. *Microbiome* **2016**, *4*, 62. [CrossRef] [PubMed]
55. Stokar-Regenscheit, N.; Sydler, T.; Bürgi, E.; Lippuner, A.; Naegeli, H.; Sidler, X. Lethal Gastric Mucosal Necrosis due to Administration of Oral Ferrous Bisglycinate Chelate to Suckling Piglets. *J. Comp. Pathol.* **2017**, *157*, 39–45. [CrossRef] [PubMed]
56. Mullaney, T.P.; Brown, C.M. Iron Toxicity in Neonatal Foals. *Equine Veter. J.* **1988**, *20*, 119–124. [CrossRef] [PubMed]
57. Parks, O.B.; Pociask, D.A.; Hodzic, Z.; Kolls, J.K.; Good, M. Interleukin-22 Signaling in the Regulation of Intestinal Health and Disease. *Front. Cell Dev. Biol.* **2016**, *3*, 85. [CrossRef]
58. Bel, S.; Pendse, M.; Wang, Y.; Li, Y.; Ruhn, K.A.; Hassell, B.; Leal, T.; Winter, S.E.; Xavier, R.J.; Hooper, L.V. Paneth Cells Secrete Lysozyme via Secretory Autophagy during Bacterial Infection of the Intestine. *Science* **2017**, *357*, 1047–1052. [CrossRef]

59. Coorens, M.; Rao, A.; Gräfe, S.K.; Unelius, D.; Lindforss, U.; Agerberth, B.; Mjösberg, J.; Bergman, P. Innate Lymphoid Cell Type 3–derived Interleukin-22 Boosts Lipocalin-2 Production in Intestinal Epithelial Cells via Synergy between STAT3 and NF-κB. *J. Biol. Chem.* **2019**, *294*, 6027–6041. [CrossRef] [PubMed]
60. Zheng, Y.; Valdez, P.A.; Danilenko, D.M.; Hu, Y.; Sa, S.M.; Gong, Q.; Abbas, A.R.; Modrusan, Z.; Ghilardi, N.; De Sauvage, F.J.; et al. Interleukin-22 Mediates Early Host Defense Against Attaching and Effacing Bacterial Pathogens. *Nat. Med.* **2008**, *14*, 282–289. [CrossRef] [PubMed]
61. Hendrikx, T.; Duan, Y.; Wang, Y.; Oh, J.-H.; Alexander, L.M.; Huang, W.; Stärkel, P.; Ho, S.B.; Gao, B.; Fiehn, O.; et al. Bacteria Engineered to Produce IL-22 in Intestine Induce Expression of REG3G to Reduce Ethanol-Induced Liver Disease in Mice. *Gut* **2018**, *68*, 1504–1515. [CrossRef] [PubMed]
62. Li, J.; Cao, F.; Yin, H.; Huang, Z.; Lin, Z.; Mao, N.; Sun, B.; Wang, G. Ferroptosis: Past, Present and Future. *Cell Death Dis.* **2020**, *11*, 88. [CrossRef] [PubMed]
63. Chen, X.; Yu, C.; Kang, R.; Tang, D. Iron Metabolism in Ferroptosis. *Front. Cell Dev. Biol.* **2020**, *8*, 590226. [CrossRef]
64. Forcina, G.C.; Dixon, S.J. GPX4 at the Crossroads of Lipid Homeostasis and Ferroptosis. *Proteomics* **2019**, *19*, e1800311. [CrossRef]
65. Park, M.W.; Cha, H.W.; Kim, J.; Kim, J.H.; Yang, H.; Yoon, S.; Boonpraman, N.; Yi, S.S.; Yoo, I.D.; Moon, J.-S. NOX4 Promotes Ferroptosis of Astrocytes by Oxidative Stress-Induced Lipid Peroxidation via the Impairment of Mitochondrial Metabolism in Alzheimer's Diseases. *Redox Biol.* **2021**, *41*, 101947. [CrossRef]
66. Bhinder, G.; Allaire, J.M.; Garcia, C.; Lau, J.T.; Chan, J.M.; Ryz, N.R.; Bosman, E.S.; Graef, F.A.; Crowley, S.M.; Celiberto, L.S.; et al. Milk Fat Globule Membrane Supplementation in Formula Modulates the Neonatal Gut Microbiome and Normalizes Intestinal Development. *Sci. Rep.* **2017**, *7*, 45274. [CrossRef]
67. Zmora, N.; Suez, J.; Elinav, E. You Are What You Eat: Diet, hHalth and the Gut Microbiota. *Nat. Rev. Gastroenterol. Hepatol.* **2019**, *16*, 35–56. [CrossRef]
68. Shin, N.-R.; Whon, T.W.; Bae, J.-W. Proteobacteria: Microbial Signature of Dysbiosis in Gut Microbiota. *Trends Biotechnol.* **2015**, *33*, 496–503. [CrossRef]
69. Moya-Alvarez, V.; Ouédraogo, S.; Accrombessi, M.; Massougbodgi, A.; Cot, M.; Cottrell, G. High Iron Levels Are Associated with Increased Malaria Risk in Infants during the First Year of Life in Benin. *Am. J. Trop. Med. Hyg.* **2017**, *97*, 497–503. [CrossRef]
70. Ji, P.; Lönnerdal, B.; Kim, K.; Jinno, C.N. Iron Oversupplementation Causes Hippocampal Iron Overloading and Impairs Social Novelty Recognition in Nursing Piglets. *J. Nutr.* **2019**, *149*, 398–405. [CrossRef]
71. Fredriksson, A.; Schröder, N.; Eriksson, P.; Izquierdo, I.; Archer, T. Maze Learning and Motor Activity Deficits in Adult Mice Induced by Iron Exposure during a Critical Postnatal Period. *Dev. Brain Res.* **2000**, *119*, 65–74. [CrossRef]
72. De Lima, M.N.; Presti-Torres, J.; Caldana, F.; Grazziotin, M.M.; Scalco, F.S.; Guimarães, M.R.; Bromberg, E.; Franke, S.I.; Henriques, J.A.; Schröder, N. Desferoxamine Reverses Neonatal Iron-Induced Recognition Memory Impairment in Rats. *Eur. J. Pharmacol.* **2007**, *570*, 111–114. [CrossRef]
73. Paganini, D.; Uyoga, M.A.; Kortman, G.A.M.; Cercamondi, C.I.; Winkler, H.; Boekhorst, J.; Moretti, D.; Lacroix, C.; Karanja, S.; Zimmermann, M.B. Iron-containing Micronutrient Powders Modify the Effect of Oral Antibiotics on the Infant Gut Microbiome and Increase Post-Antibiotic Diarrhoea Risk: A Controlled Study in Kenya. *Gut* **2018**, *68*, 645–653. [CrossRef]
74. Zimmermann, M.B.; Chassard, C.; Rohner, F.; N'Goran, E.K.; Nindjin, C.; Dostal, A.; Utzinger, J.; Ghattas, H.; Lacroix, C.; Hurrell, R.F. The Effects of Iron Fortification on the Gut Microbiota in African Children: A Randomized Controlled Trial in Côte d'Ivoire. *Am. J. Clin. Nutr.* **2010**, *92*, 1406–1415. [CrossRef]

75. Zakrzewski, M.; Wilkins, S.J.; Helman, S.L.; Brilli, E.; Tarantino, G.; Anderson, G.J.; Frazer, D.M. Supplementation with Sucrosomial® Iron leads to Favourable Changes in the Intestinal Microbiome when Compared to Ferrous Sulfate in Mice. *BioMetals* **2021**, 1–12. [CrossRef]
76. Constante, M.; Fragoso, G.; Lupien-Meilleur, J.; Calvé, A.; Santos, M.M. Iron Supplements Modulate Colon Microbiota Composi- tion and Potentiate the Protective Effects of Probiotics in Dextran Sodium Sulfate-induced Colitis. *Inflamm. Bowel Dis.* **2017**, *23*, 753–766. [CrossRef]
77. Moore, R.E.; Townsend, S.D. Temporal Development of the Infant Gut Microbiome. *Open Biol.* **2019**, *9*, 190128. [CrossRef]
78. Mueller, N.; Bakacs, E.; Combellick, J.; Grigoryan, Z.; Dominguez-Bello, M.G. The Infant Microbiome Development: Mom Matters. *Trends Mol. Med.* **2015**, *21*, 109–117. [CrossRef]
79. Guaraldi, F.; Salvatori, G. Effect of Breast and Formula Feeding on Gut Microbiota Shaping in Newborns. *Front. Cell. Infect. Microbiol.* **2012**, *2*, 94. [CrossRef]
80. Lönnerdal, B.; Keen, C.L.; Ohtake, M.; Tamura, T. Iron, Zinc, Copper, and Manganese in Infant Formulas. *Arch. Pediatr. Adolesc. Med.* **1983**, *137*, 433–437. [CrossRef]
81. Bode, L. Human Milk oligosaccharides: Every Baby Needs a Sugar Mama. *Glycobiology.* **2012**, *22*, 1147–1162. [CrossRef]
82. Walter, J.; Britton, R.A.; Roos, S. Host-Microbial Symbiosis in the Vertebrate Gastrointestinal Tract and the Lactobacillus reuteri Paradigm. *Proc. Natl. Acad. Sci. USA* **2011**, *108*, 4645–4652. [CrossRef]
83. Martin, F.-P.; Wang, Y.; Sprenger, N.; Yap, I.K.S.; Lundstedt, T.; Lek, P.; Rezzi, S.; Ramadan, Z.; Van Bladeren, P.; Fay, L.B.; et al. Probiotic Modulation of Symbiotic Gut Microbial–Host Metabolic Interactions in a Humanized Microbiome Mouse Model. *Mol. Syst. Biol.* **2008**, *4*, 157. [CrossRef]
84. Flemer, B.; Gaci, N.; Borrel, G.; Sanderson, I.; Chaudhary, P.P.; Tottey, W.; O'Toole, P.W.; Brugère, J.-F. Fecal Microbiota Variation Across the Lifespan of the Healthy Laboratory Rat. *Gut Microbes* **2017**, *8*, 428–439. [CrossRef]
85. Frese, S.A.; Benson, A.K.; Tannock, G.W.; Loach, D.M.; Kim, J.; Zhang, M.; Oh, P.L.; Heng, N.C.K.; Patil, P.B.; Juge, N.; et al. The Evolution of Host Specialization in the Vertebrate Gut Symbiont Lactobacillus reuteri. *PLoS Genet.* **2011**, *7*, e1001314. [CrossRef]
86. Domellöf, M.; Lönnerdal, B.; Dewey, K.G.; Cohen, R.J.; Hernell, O. Iron, Zinc, and Copper Concentrations in Breast Milk are Independent of Maternal Mineral Status. *Am. J. Clin. Nutr.* **2004**, *79*, 111–115. [CrossRef]
87. Keen, C.L.; Lönnerdal, B.; Clegg, M.; Hurley, L.S. Developmental Changes in Composition of Rat Milk: Trace Elements, Minerals, Protein, Carbohydrate and Fat. *J. Nutr.* **1981**, *111*, 226–236. [CrossRef] [PubMed]
88. Furusawa, Y.; Obata, Y.; Fukuda, S.; Endo, T.A.; Nakato, G.; Takahashi, D.; Nakanishi, Y.; Uetake, C.; Kato, K.; Kato, T.; et al. Commensal Microbe-Derived Butyrate Induces the Differentiation of Colonic Regulatory T Cells. *Nature* **2013**, *504*, 446–450. [CrossRef]
89. De Vadder, F.; Kovatcheva-Datchary, P.; Goncalves, D.; Vinera, J.; Zitoun, C.; Duchampt, A.; Bäckhed, F.; Mithieux, G. Microbiota-Generated Metabolites Promote Metabolic Benefits via Gut-Brain Neural Circuits. *Cell* **2014**, *156*, 84–96. [CrossRef]
90. Kortman, G.A.M.; Dutilh, B.E.; Maathuis, A.J.H.; Engelke, U.F.; Boekhorst, J.; Keegan, K.P.; Nielsen, F.G.G.; Betley, J.; Weir, J.C.; Kingsbury, Z.; et al. Microbial Metabolism Shifts Towards an Adverse Profile with Supplementary Iron in the TIM-2 In vitro Model of the Human Colon. *Front. Microbiol.* **2016**, *6*, 1481. [CrossRef]
91. Rath, S.; Rud, T.; Pieper, D.H.; Vital, M. Potential TMA-Producing Bacteria Are Ubiquitously Found in Mammalia. *Front. Microbiol.* **2020**, *10*, 2966. [CrossRef]
92. Rath, S.; Heidrich, B.; Pieper, D.H.; Vital, M. Uncovering the Trimethylamine-Producing Bacteria of the Human Gut Microbiota. *Microbiome* **2017**, *5*, 54. [CrossRef]

93. Andrews, S.C.; Robinson, A.K.; Rodríguez-Quiñones, F. Bacterial Iron Homeostasis. *FEMS Microbiol. Rev.* **2003**, *27*, 215–237. [CrossRef]
94. Weinberg, E.D. The Lactobacillus Anomaly: Total Iron Abstinence. *Perspect. Biol. Med.* **1997**, *40*, 578–583. [CrossRef] [PubMed]
95. Qi, H.; Li, Y.; Yun, H.; Zhang, T.; Huang, Y.; Zhou, J.; Yan, H.; Wei, J.; Liu, Y.; Zhang, Z.; et al. Lactobacillus Maintains Healthy Gut Mucosa by Producing L-Ornithine. *Commun. Biol.* **2019**, *2*, 179. [CrossRef] [PubMed]
96. Mihi, B.; Gong, Q.; Nolan, L.S.; Gale, S.E.; Goree, M.; Hu, E.; Lanik, W.E.; Rimer, J.M.; Liu, V.; Parks, O.B.; et al. Interleukin-22 Signaling Attenuates Necrotizing Enterocolitis by Promoting Epithelial Cell Regeneration. *Cell Rep. Med.* **2021**, *2*, 100320. [CrossRef] [PubMed]
97. Leong, W.-I.; Bowlus, C.; Tallkvist, J.; Lönnerdal, B. Iron Supplementation during Infancy—Effects on Expression of Iron Transporters, Iron Absorption, and Iron Utilization in Rat Pups. *Am. J. Clin. Nutr.* **2003**, *78*, 1203–1211. [CrossRef] [PubMed]
98. Leong, W.-I.; Bowlus, C.; Tallkvist, J.; Lönnerdal, B. DMT1 and FPN1 Expression during Infancy: Developmental Regulation of Iron Absorption. *Am. J. Physiol. Liver Physiol.* **2003**, *285*, G1153–G1161. [CrossRef] [PubMed]
99. Callahan, B.J.; McMurdie, P.J.; Holmes, S.P. Exact Sequence Variants Should Replace Operational Taxonomic Units in Marker-Gene Data Analysis. *ISME J.* **2017**, *11*, 2639–2643. [CrossRef] [PubMed]

FIGURES

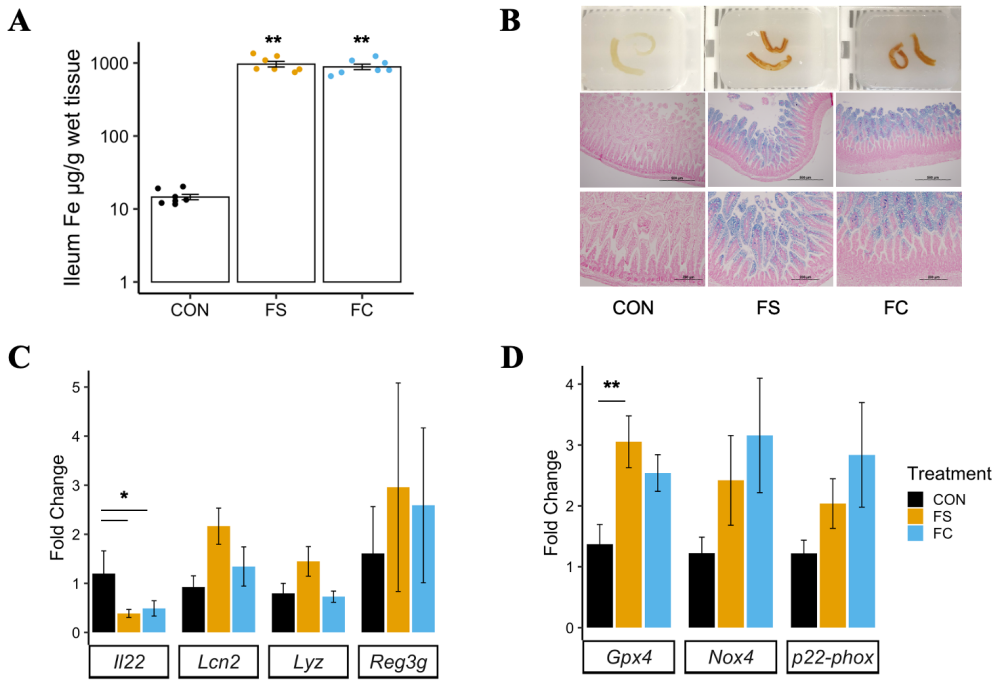

Figure 1. Postnatal iron supplementation with ferrous sulfate (FS) or ferrous bis-glycinate (Ferrochel ®; FC) leads to iron loading in the distal intestine and altered intestinal gene expression in pre-weanling rats. (**A**) Iron concentration in distal small intestine tissue (n = 7/group, 2 litters/group) collected from rat pups at PD 15 following 13 days of daily iron supplementation with FS or FC, or vehicle control (CON), assessed by atomic absorption spectrometry. Biological replicates are shown as individual data points with mean ±

SEM. Differences in iron concentration among groups were detected with a Kruskal–Wallis test and Wilcox pairwise test. (**B**) Top row: distal small intestine samples exhibiting darkening effect of iron supplementation. Middle and bottom row: 10× (scale = 500 µm) and 20× (scale = 200 µm) objective microscope images of distal small intestine sections stained for iron with Perls' Prussian blue staining (representative samples; n = 6/group, 3 litters/group). (**C**) mRNA expression of genes involved in regulation of mucosal immunity, quantified by real-time PCR (n = 5–8/group, 2 litters/group). (**D**) mRNA expression of genes involved in regulation of ferroptosis, an iron overload-dependent form of cell death. Gene expression values are shown as mean fold-change ± SEM. mRNA expression was normalized to *Actb*, and differences were detected among groups by one-way ANOVA and Tukey's multiple comparisons. *p*-value summary: *, $p < 0.05$; **, $p < 0.01$.

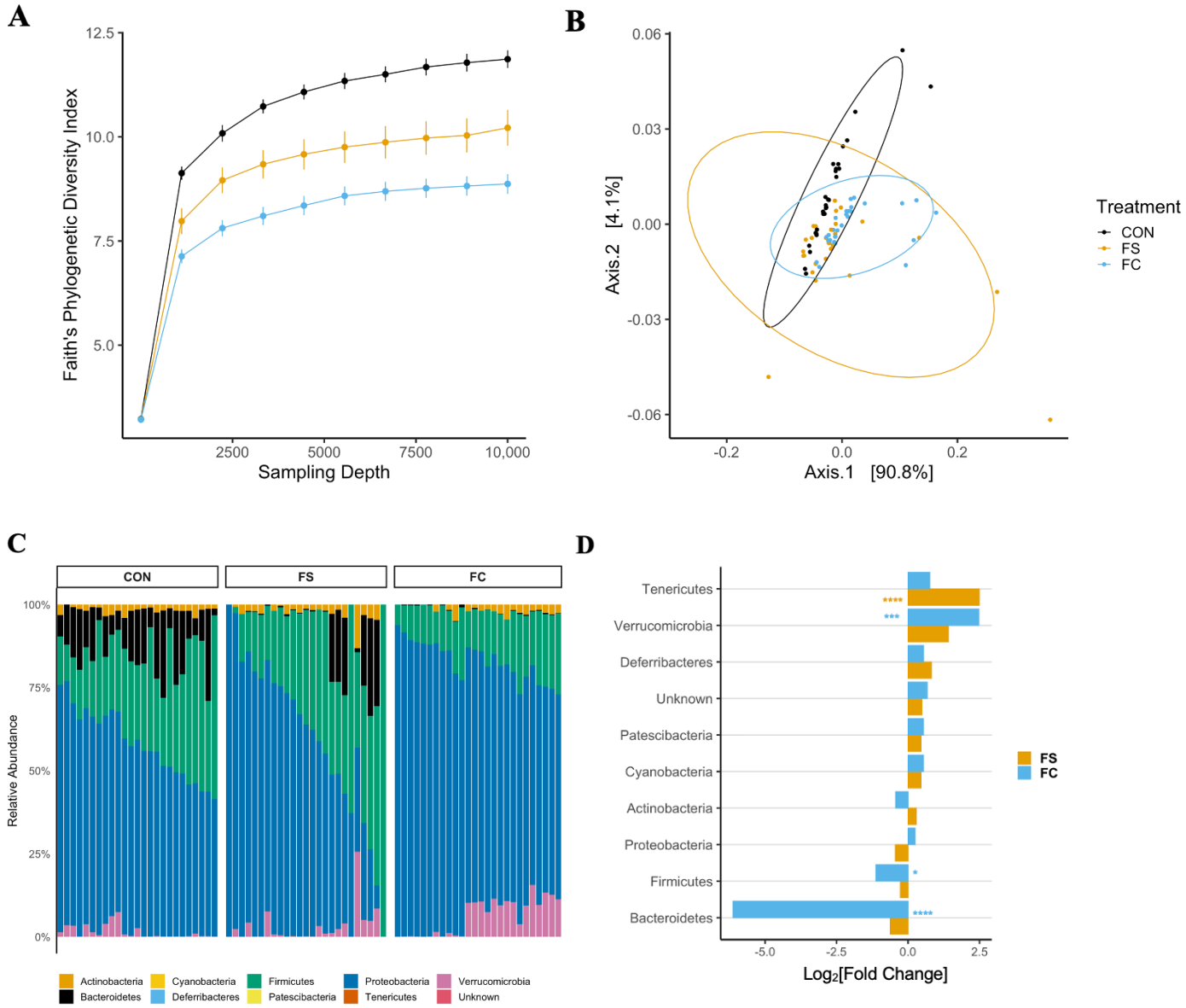

Figure 2. Alterations in the cecal microbiome depend on iron form. (**A**) Alpha-diversity rarefaction plot depicting Faith's Phylogenetic Diversity (FPD) Index by treatment group and sampling depth, shown as mean ± SEM (n = 20–29/(group × sampling depth), 3 litters/group). Iron treatments decreased FPD; this was true for all sampling depths >1, with the largest effect upon FC treatment ($p < 0.05$). (**B**) Principal coordinate axes 1 and 2 from Principal Coordinate Analysis (PCoA) of Weighted UniFrac distances in pups (n = 27–29/group, 3 litters/group) following FS or FC supplementation; no separation due to treatment group detected ($p = 0.08$). (**C**) Relative abundance of phyla (%) by treatment group; each column represents an individual pup (n = 25–26/group, 3 litters/group). (**D**) Differential phyla abundance, represented as $\log_2$[Fold Change] from CON for each iron treatment group (n = 27–29/group, 3 litters/group); phyla are ordered by magnitude of change and bars are labeled with color according to iron treatment group. Repeated Kruskal–Wallis tests with Dunn's multiple comparisons were used to test for differences in FPD among groups at each sampling depth. A PERMANOVA test was applied to detect microbiome compositional dissimilarity among treatment groups, using a nested model; litter was nested within treatment. Additional alpha- and beta-diversity metrics from this age group are included in Figure S2, and *p*-values for diversity analyses in pups are listed in Table S2. Differential abundance of phyla was assessed with DESeq2, and FDR-adjusted *p*-values <0.05 from pairwise comparisons were considered significant. *p*-values from the pairwise phyla differential abundance results are provided in Table S3. *p*-value summary: *, $p < 0.05$; **, $p < 0.01$; ***, $p < 0.001$; ****, $p < 0.0001$.

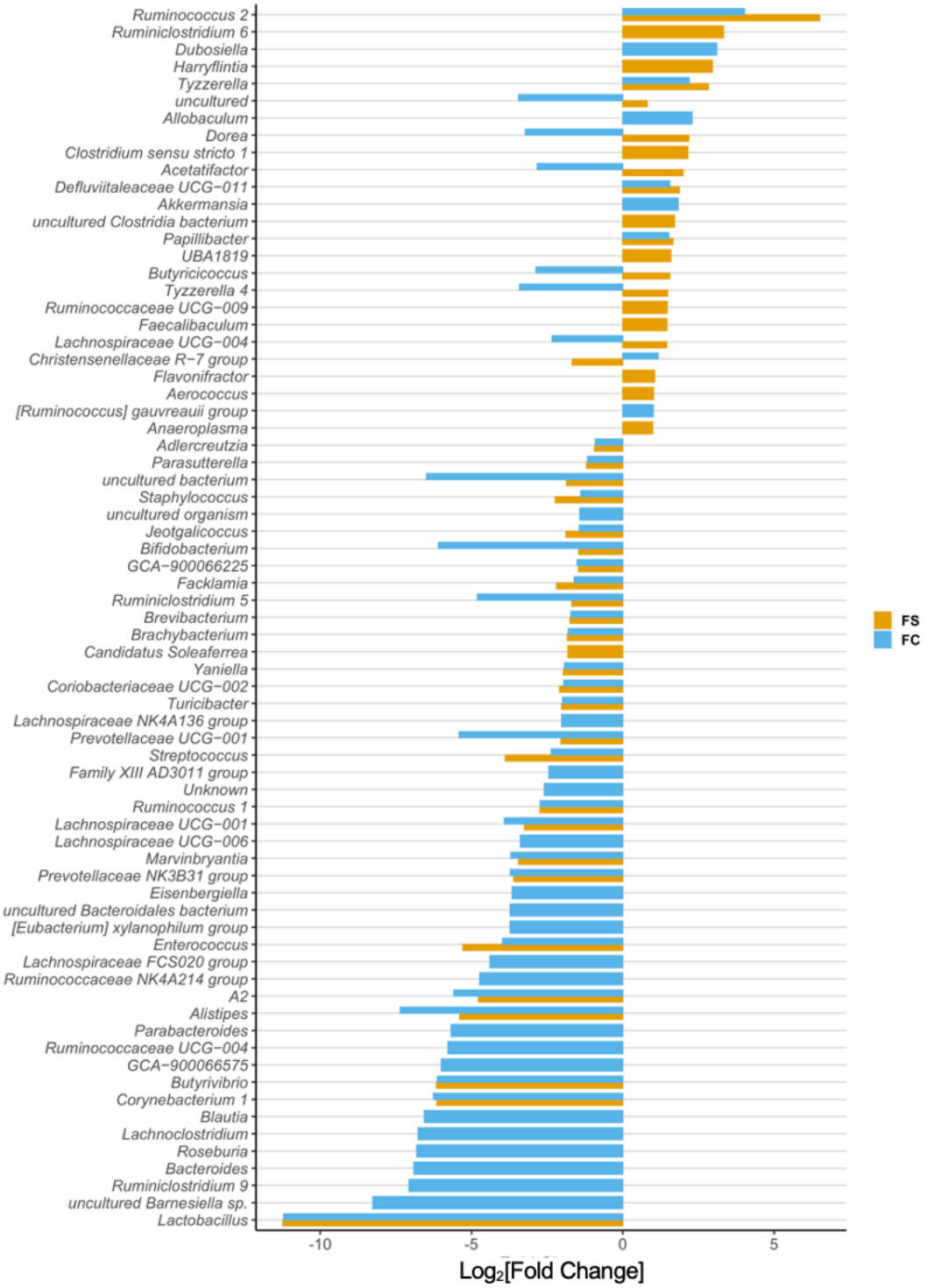

Figure 3. Differentially abundant genera due to iron form (n = 27–29/group, 3 litters/group). Differentially abundant genera are represented as $\log_2$[Fold Change] from CON for each iron group. Genera are ordered by magnitude of change. Differential abundance was assessed with DESeq2, and FDR-adjusted *p*-values < 0.05 were considered significant. All significant results are shown in the plot, and their adjusted *p*-values are listed in Table S4.

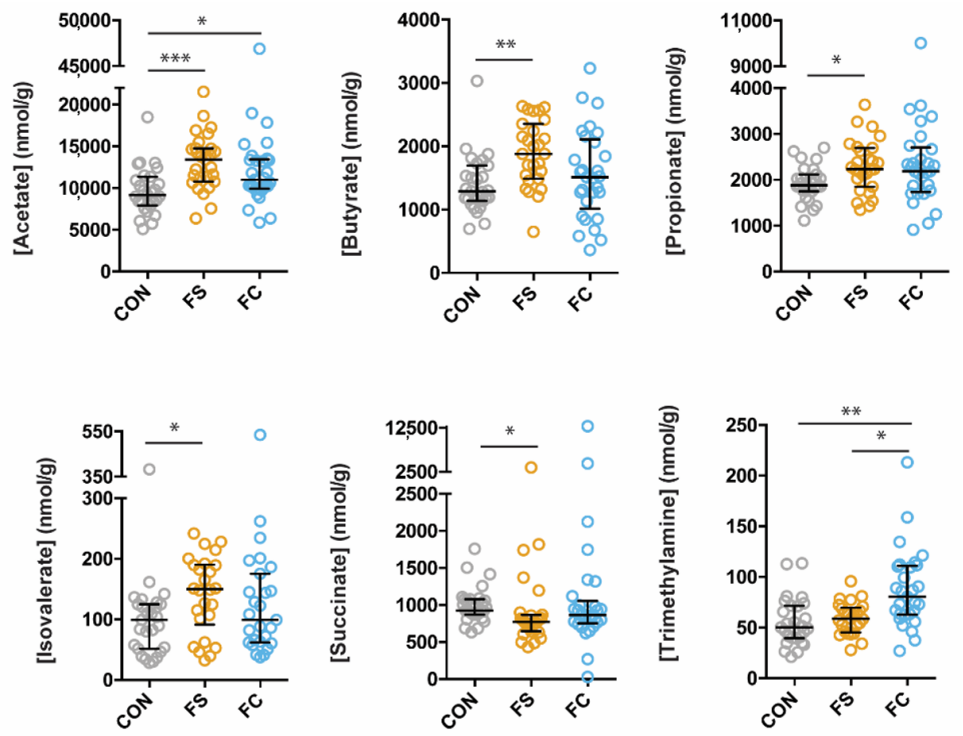

Figure 4. Cecal metabolite differences due to iron form. Metabolites were analyzed by Kruskal–Wallis with Dunn's multiple comparisons. All metabolites shown are significant by Kruskal–Wallis. Median, and interquartile range of concentrations are indicated (n = 27–29/group, 3 litters/group). *p*-value summary: *, $p < 0.05$; **, $p < 0.01$; ***, $p < 0.001$.

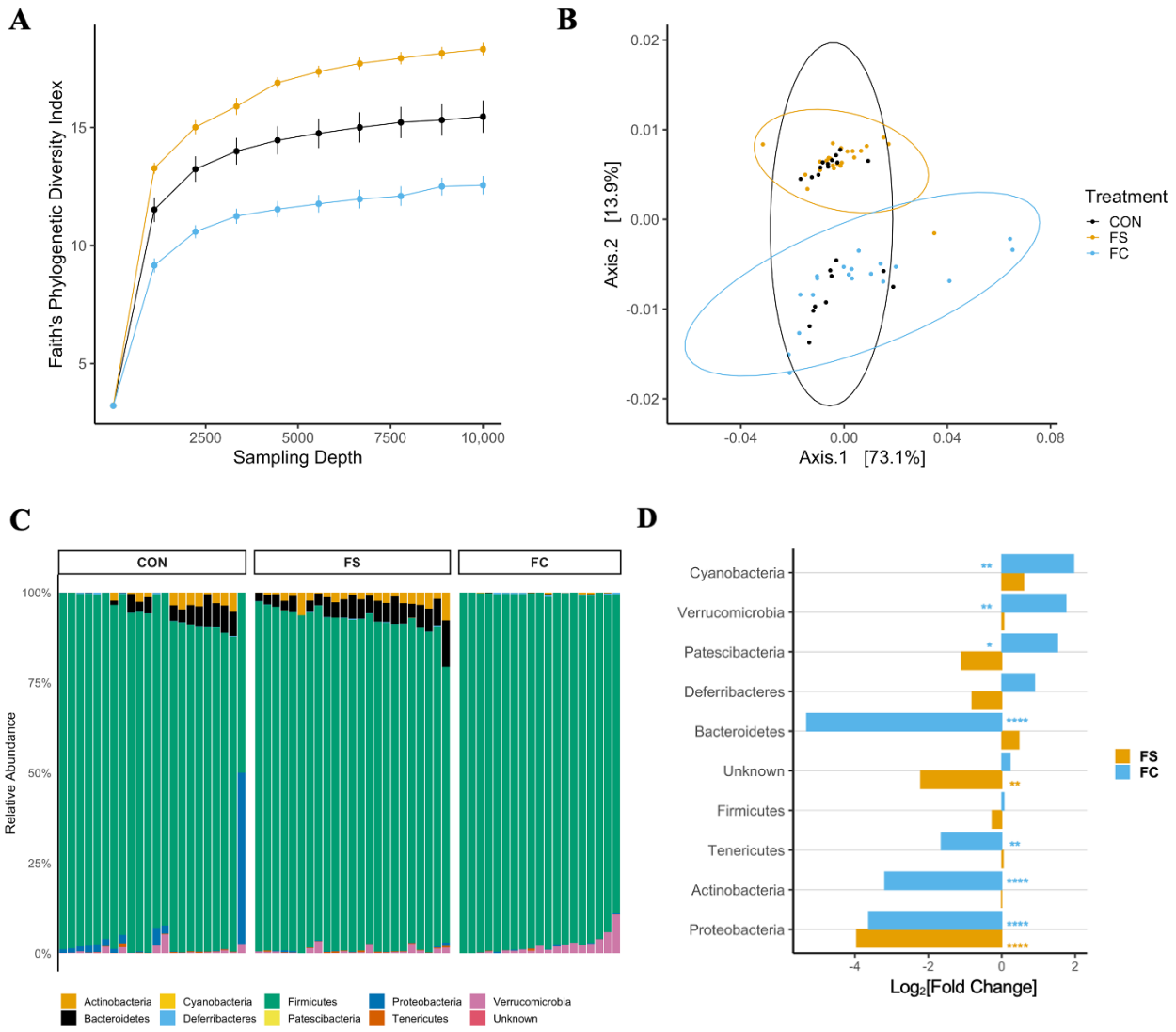

Figure 5. Cecal microbiome effects in young adult (YA) rats supplemented with FS or FC during the pre-weaning period. (**A**) Alpha-diversity rarefaction plot depicting Faith's Phylogenetic Diversity (FPD) Index by treatment group and sampling depth, shown as mean ± SEM (n = 12–23/(group × sampling depth), 4 litters/group). Postnatal FS treatment increased YA rat cecal microbiome FPD, while FC decreased FPD compared to CON across all sampling depths >1 ($p < 0.05$). (**B**) Principal Coordinate Analysis (PCoA) of Weighted UniFrac distances in YA rats (n = 19–23/group, 4 litters/group), depicting separation due to treatment group ($p < 0.01$) (**C**) Relative abundance of phyla (%) by treatment group; each column represents an individual animal (n = 19–23/group, 4 litters/group). (**D**) Differential phyla abundance, represented as $\log_2$[Fold Change] from CON for each iron group (n = 19–23/group, 4 litters/group); phyla are ordered by magnitude of change and bars are labeled with color according to iron group. Repeated Kruskal–Wallis tests with Dunn's multiple comparisons were used to test for differences in FPD among groups at each sampling depth. Weighted UniFrac PCoA results were applied to a PERMANOVA test. Additional alpha- and beta-diversity metrics for YA rats are included in Figure S2. *p*-values for YA diversity analyses are listed in Table S6. Differential abundance of phyla was assessed with DESeq2, and FDR-adjusted *p*-values <0.05 from pairwise comparisons were considered significant. *p*-values from the pairwise phyla differential abundance results are provided in Table S6. *p*-value summary: *, $p < 0.05$; **, $p < 0.01$; ***, $p < 0.001$; ****, $p < 0.0001$.

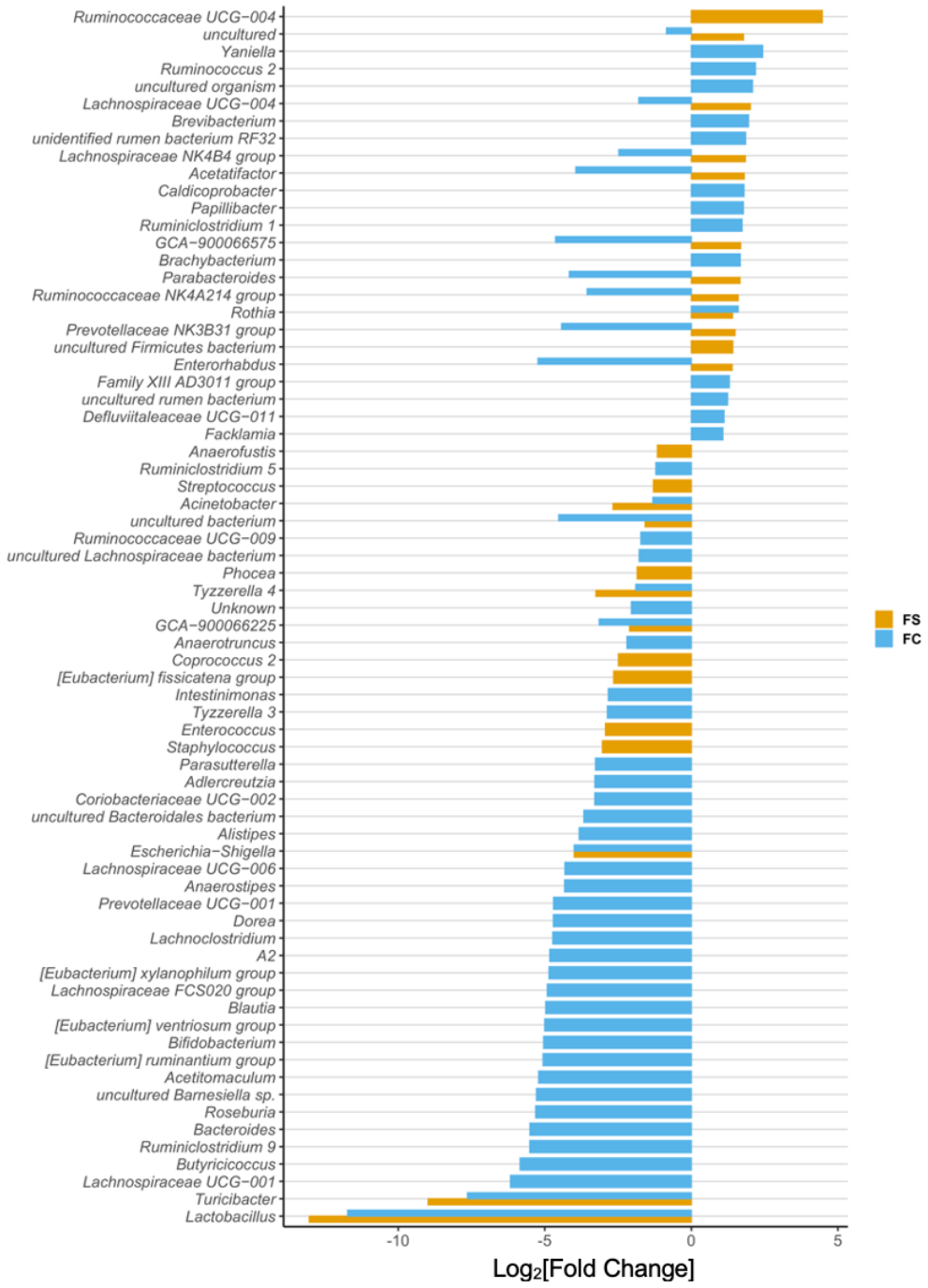

Figure 6. Differentially abundant genera in young adult (YA) rats due to iron form (n = 19–23/group, 4 litters/group). Differentially abundant genera are represented as $\log_2$[Fold Change] from CON for each iron group. Genera are ordered by magnitude of change. Differential abundance was assessed with DESeq2, and FDR-adjusted p-values < 0.05 were considered significant. All significant comparison results are shown in the plot, and their adjusted p-values are listed in Table S8.

SUPPLEMENTARY FIGURES & TABLES

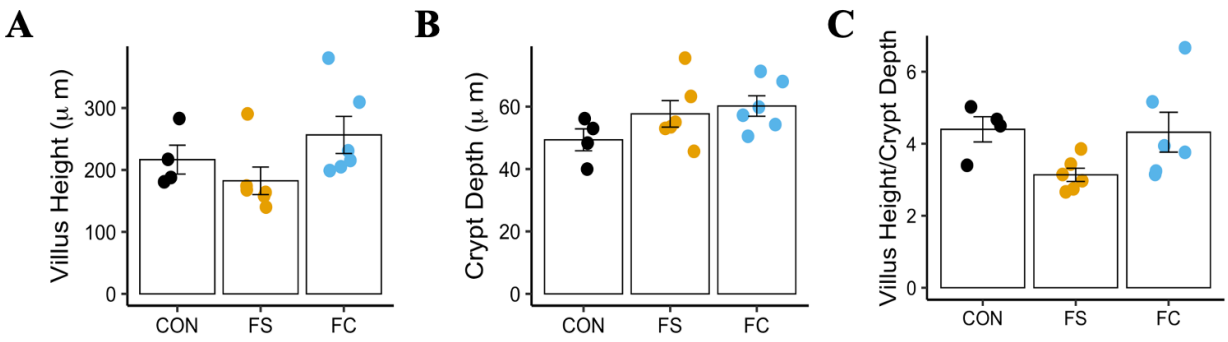

Supplementary Figure 1. Ileal morphology following FS or FC supplementation at PD 15. Ileal morphology was assessed in fixed, H&E-stained sections (n = 6/group, 3 litters/group). Mean A) villus height and B) crypt depth were calculated from 10 technical replicate measurements per sample/biological replicate. C) A ratio of villus height/crypt depth is also included.

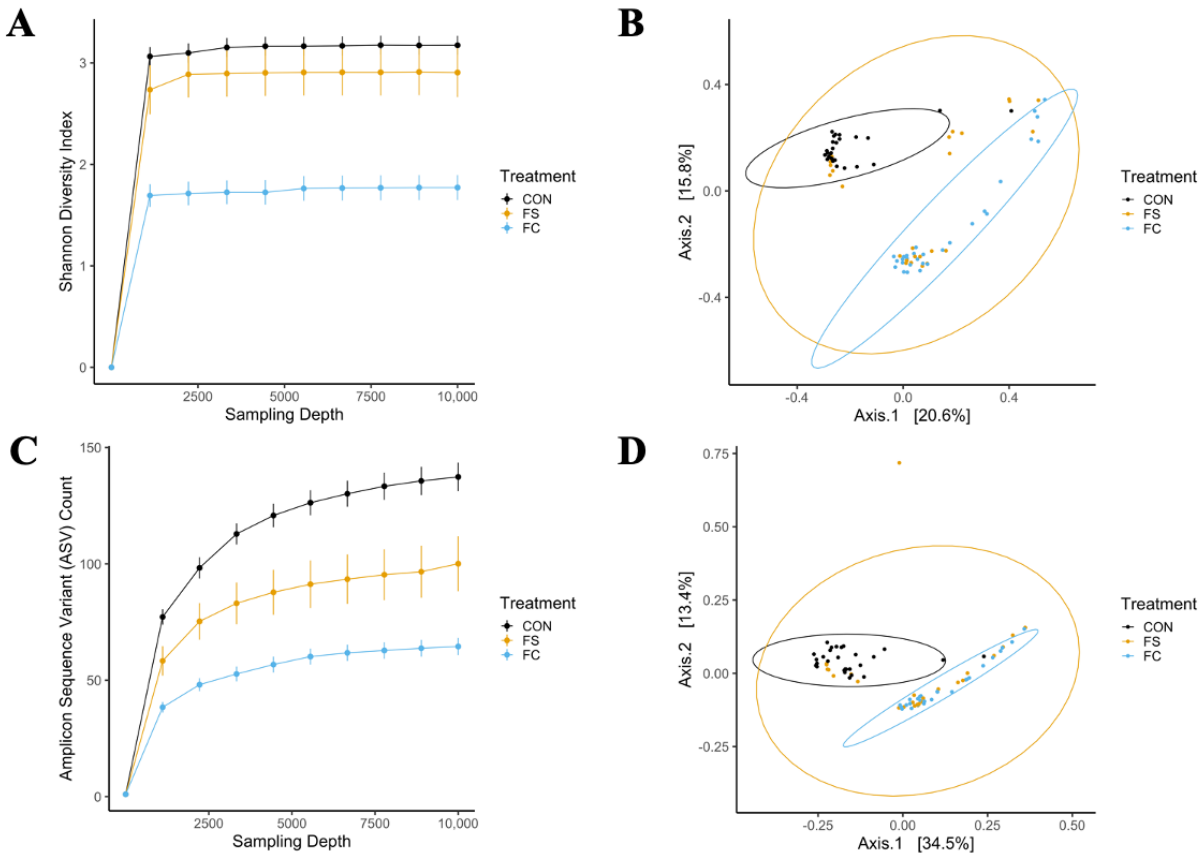

Supplementary Figure 2. Additional alpha-diversity & beta-diversity measures at PD 15. A) Alpha-diversity rarefaction plot depicting Shannon diversity by treatment group and sampling depth (n = 20-29/(group x sampling depth), n = 3 litters/group). Shannon index was decreased in both FS and FC groups compared to the CON at all sampling depths > 1. B) Principal coordinate analysis of Bray-Curtis distances, labeled by treatment group: all groups were dissimilar from each other by PERMANOVA (n = 27-29/group, 3 litters/group). C) Alpha-diversity rarefaction plot depicting Amplicon Sequence Variant (ASV) count (i.e., richness) by treatment group and sampling depth (n = 20-29/(group x sampling depth), n = 3 litters/group). ASV count decreased in both iron groups compared to the CON at all sampling depths > 1. D) Principal coordinate analysis of unweighted UniFrac distances, labeled by treatment group: all groups were dissimilar from each other by PERMANOVA (n = 27-29/group, 3 litters/group). Repeated Kruskal-Wallis tests with Dunn's multiple comparisons were used to test for differences in Shannon and ASV count among groups at each sampling depth. A PERMANOVA test was applied to detect microbiome compositional dissimilarity among treatment groups, using a nested model, with litter nested within treatment factor to account for litter effects.

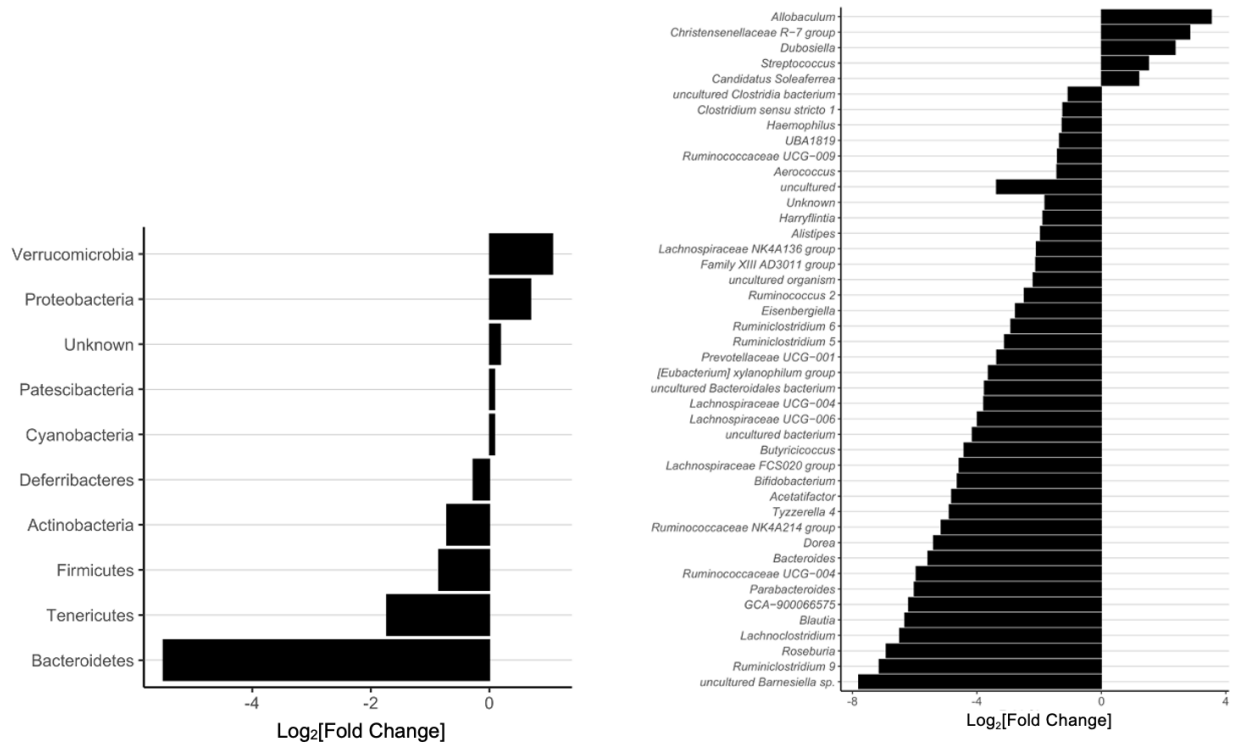

Supplementary Figure 3. Differential abundance of cecal bacteria at the phylum (left) and genus level (right) in FC vs. FS treated pups at PD 15. All genera plotted are significantly different between iron groups. Differential abundance was determined using DESeq2 and FDR-adjusted p-values < 0.05 from pairwise group comparisons were considered significant. P-values are listed in Tables S3-4.

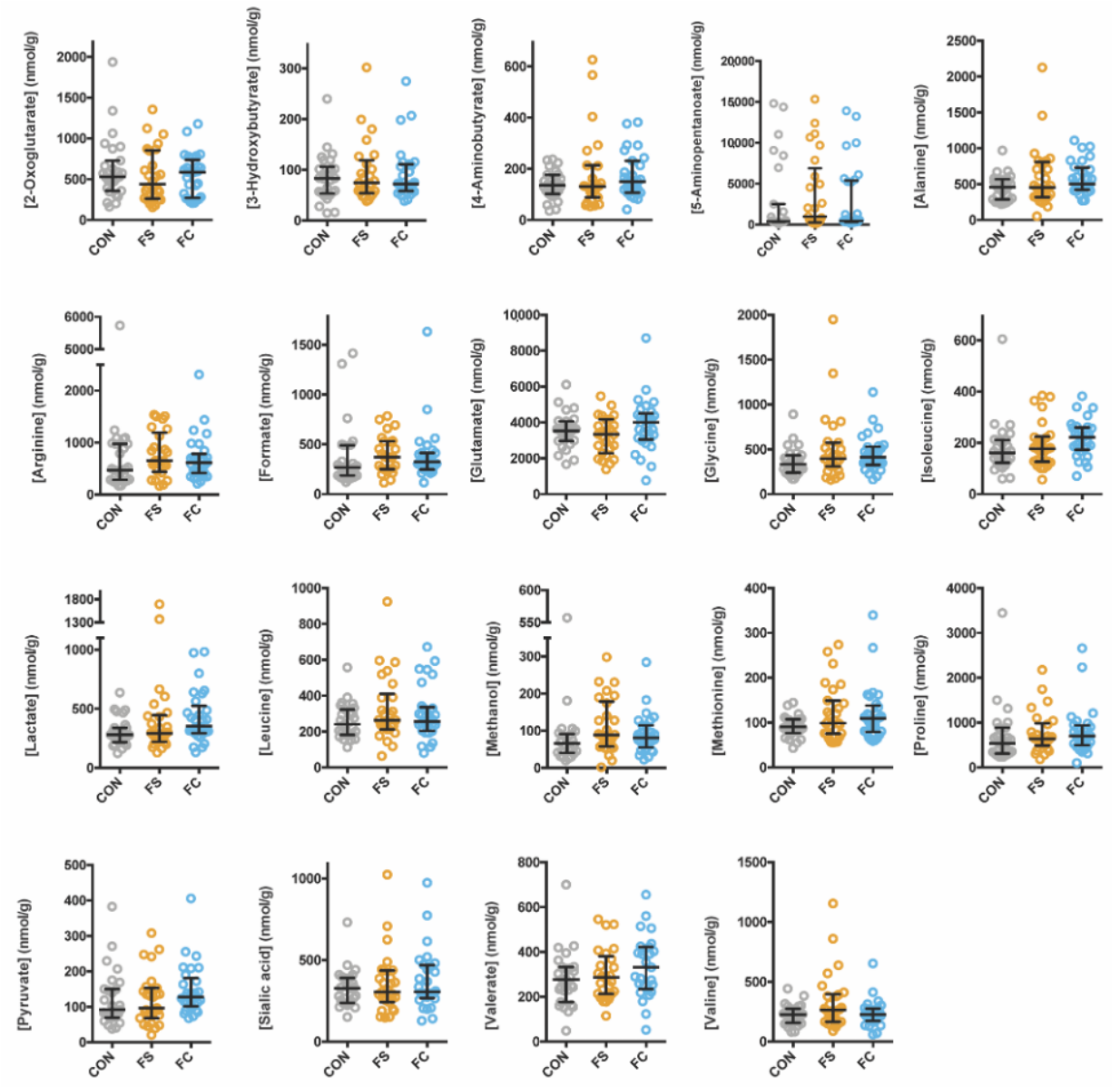

Supplementary Figure 4. Cecal metabolites detected in pups that were not affected by iron treatment or iron form. Metabolites were analyzed by Kruskal-Wallis followed by Dunn's multiple comparison testing. All metabolites shown are significant by Kruskal-Wallis. Median and interquartile range of concentrations are indicated (n = 27-29/group, 3 litters/group).

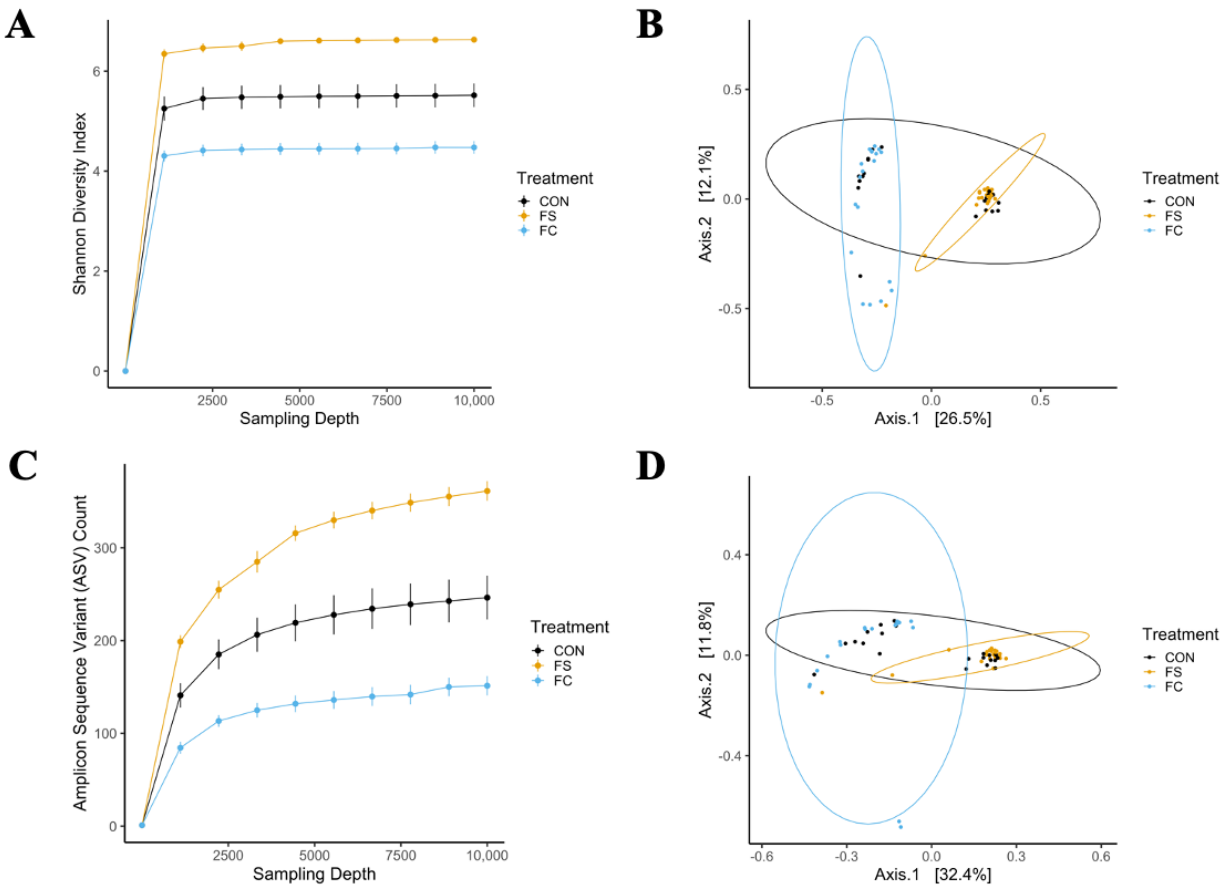

Supplementary Figure 5. Additional alpha-diversity & beta-diversity measures in YA rats. A) Alpha-diversity rarefaction plot depicting Shannon diversity by treatment group and sampling depth (n = 12-23/(group x sampling depth), 4 litters/group). Shannon index was increased in the FS group and decreased in the FC group compared to the CON at all sampling depths > 1. B) Principal coordinate analysis of Bray-Curtis distances, labeled by treatment group: all groups were dissimilar from each other by PERMANOVA (n = 19-23/group, 4 litters/group). C) Alpha-diversity rarefaction plot depicting Amplicon Sequence Variant (ASV) count (i.e., richness) by treatment group and sampling depth (n = 12-23/(group x sampling depth), 4 litters/group). ASV count was increased in the FS group and decreased in the FC group compared to the CON at all sampling depths > 1. D) Principal coordinate analysis of unweighted UniFrac distances, labeled by treatment group: all groups were dissimilar from each other by PERMANOVA (n = 19-23/group, 4 litters/group). Repeated Kruskal-Wallis tests with Dunn's multiple comparisons were used to test for differences in Shannon and ASV count among groups at each sampling depth. A PERMANOVA test was applied to detect microbiome compositional dissimilarity among treatment groups, using a nested model, with litter nested within treatment factor to account for litter effects.

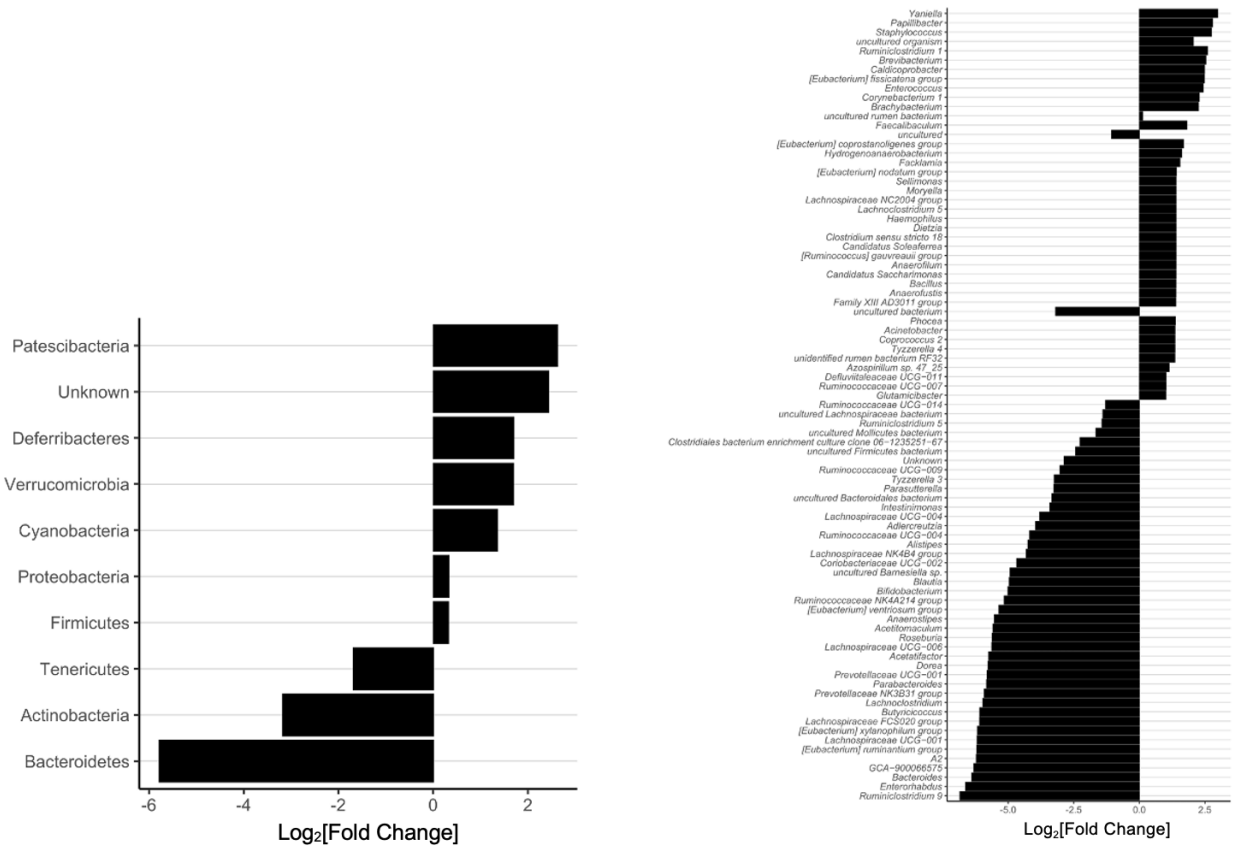

Supplementary Figure 6. Differential abundance of cecal bacteria at the phylum (left) and genus level (right) in YA rats postnatally supplemented with FC vs. FS. All genera plotted are significantly different between iron groups. Differential abundance was determined using DESeq2 and FDR-adjusted p-values < 0.05 from pairwise group comparisons were considered significant. P-values are listed in Tables S7-8.

Supplementary Table 1. Primer sequences for real-time PCR and 16s rRNA library construction.

Gene	Primer Sequence
Actb Forward[1]	5'-GAAATCGTGCGTGACATTAAAGAG -3
Actb Reverse[1]	5'-GCGGCAGTGGCCATCTC-3'
Il-22 Forward	5'- ATGCTCTGCCCATCAACTC -3'
Il-22 Reverse	5'- GCAGAACATCTTCAAGGGTG - 3'
Lcn2 Forward	5'-CAGAAAGAAAGACAAAGCCG-3'
Lcn2 Reverse	5'-TGGCAAACTGGTCGTAGTC-3'
Lyz Forward	5'-AGGAATGGGATGTCTGGCTAC-3'
Lyz Reverse	5'-GGTATCCCACAGGCGTTCTT-3'
Reg3g Forward	5'-ATGCCAAGGAAGATGTGCCCAC-3'
Reg3g Reverse	5'-AATCAAGGAGGACACAAAGG-3'
Gpx4 Forward[2]	5`-CAGCAAGATCTGTGTAAATGGGG- 3`
Gpx4 Reverse[2]	5`-CTTGGTGAAGTTCCATTTGATGG- 3`
Nox4 Forward[3]	5'-GTGAACGCCCTGAACTTCTC-3'
Nox4 Reverse[3]	5'-TTCTGGGATCCTCATTCTGG-3'
p22^{phox} Forward[3]	5'-TGTTGCAGGAGTGCTCATCTGTCT-3'
p22^{phox} Reverse[3]	5'-AGGACAGCCCGGACGTAGTAATTT-3'
16s rRNA V4 Forward[#]	5'-AATGATACGGCGACCACCGAGATCTACACTCTTTCCCTACACGACGCTCTTCCGATCTNNNNNNNN*GTGTGCCAGCMGCCGCGGTAA-3'
16s rRNA V4 Reverse[#]	5'-CAAGCAGAAGACGGCATACGAGATCGGTCTCGGCATTCCTGCTGAACCGCTCTTCCGATCTCCGGACTACHVGGGTWTCTAAT-3'

[#]Full primer sequence with Illumina adaptor sequencing primer, barcode (forward only), linker, and PCR primer; *8-Nucleotide Barcode

[1] Li, Y.; Yu, P.; Chang, S.-Y.; Wu, Q.; Yu, P.; Xie, C.; Wu, W.; Zhao, B.; Gao, G.; Chang, Y.-Z. Hypobaric Hypoxia Regulates Brain Iron Homeostasis in Rats. *J. Cell. Biochem*. **2017**, 118, 1596–1605. https://doi.org/10.1002/jcb.25822.

[2] Sukhanova, I.A.; Sebentsova, E.A.; Khukhareva, D.D.; Manchenko, D.M.; Glazova, N.Y.; Vishnyakova, P.A.; Inozemtzeva, L.S.; Dolotov, O.V.; Vyokikh, M.Y.; Levitskaya, N.G. Gender-Dependent Changes in Physical Development, BDNF Content and GSH Redox System in a Model of Acute Neonatal Hypoxia in Rats*, Behavioural Brain Research*, **2018**, 350, 87-98. https://doi.org/10.1016/j.bbr.2018.05.008.

[3] Cavdar, Z.; Oktan, M.A.; Ural, C.; Calisir, M.; Kocak, A.; Heybeli, C.; Yildiz, S.; Arici A.; Ellidokuz, H.; Celik, A.; Yilmaz, O.; Sarioglu, S.; Cavdar, C. Renoprotective Effects of Alpha Lipoic Acid on Iron Overload-Induced Kidney Injury in Rats by Suppressing NADPH Oxidase 4 and p38 MAPK Signaling. *Biol Trace Elem Res* **193,** 483–493 (2020). https://doi.org/10.1007/s12011-019-01733-3.

Supplementary Table 2. P-values from diversity statistical analyses at PD 15.

Alpha-Diversity Metric (Sampling Depth)	**P-Value**			
Faith's PD[1]	Treatment[2]	FS vs. CON[3]	FC vs. CON[3]	FC vs. FS[3]
(1)	0.1108	0.0347	0.0346	0.4871
(1112)	<0.0001	0.0013	<0.0001	0.0075
(2223)	<0.0001	0.0028	<0.0001	0.0058
(3334)	<0.0001	0.0011	<0.0001	0.0059
(4445)	<0.0001	<0.0001	<0.0001	0.0078
(5556)	<0.0001	0.0006	<0.0001	0.0126
(6667)	<0.0001	0.0007	<0.0001	0.0123
(7778)	<0.0001	0.0006	<0.0001	0.0144
(8889)	<0.0001	0.0005	<0.0001	0.0169
(10,000)	<0.0001	0.0011	<0.0001	0.0104
Shannon[4]	Treatment[2]	FS vs. CON[3]	FC vs. CON[3]	FC vs. FS[3]
(1)	NA			
(1112)	<0.0001	0.0507	<0.0001	0.0001
(2223)	<0.0001	0.0966	<0.0001	<0.0001
(3334)	<0.0001	0.0741	<0.0001	0.0001
(4445)	<0.0001	0.0782	<0.0001	0.0001
(5556)	<0.0001	0.0762	<0.0001	0.0001
(6667)	<0.0001	0.0741	<0.0001	0.0001
(7778)	<0.0001	0.0670	<0.0001	0.0001
(8889)	<0.0001	0.0672	<0.0001	0.0001
(10,000)	<0.0001	0.0702	<0.0001	0.0001
ASVs[5]	Treatment[2]	FS vs. CON[3]	FC vs. CON[3]	FC vs. FS[3]
(1)	NA			
(1112)	<0.0001	0.0036	<0.0001	0.0041
(2223)	<0.0001	0.0049	<0.0001	0.0038
(3334)	<0.0001	0.0013	<0.0001	0.0056
(4445)	<0.0001	0.0012	<0.0001	0.0084
(5556)	<0.0001	0.0012	<0.0001	0.0118
(6667)	<0.0001	0.0012	<0.0001	0.0133
(7778)	<0.0001	0.0013	<0.0001	0.0128
(8889)	<0.0001	0.0010	<0.0001	0.0150
(10,000)	<0.0001	0.0021	<0.0001	0.0109

	P-Value[6]				
Beta-Diversity Metric	Treatment	Sex	Treatment: Litter	Treatment: Sex	Treatment: Sex:Litter
Weighted UniFrac	0.0806	0.9027	0.4188	0.4792	0.1542
Unweighted UniFrac	<0.0001	0.1910	<0.0001	0.0094	<0.0001
Bray-Curtis	<0.0001	0.1643	<0.0001	0.0631	0.0762

[1]Faith's Phylogenetic Diversity. [2]Kruskal-Wallis test for treatment effect. [3]Dunn's pairwise group comparisons. [4]Shannon's Diversity. [5]Amplicon Sequence Variant count (richness). [6]Permutational analysis of variance (PERMANOVA)

Supplementary Table 3. Phylum differential abundance group comparisons at PD15.

Phylum	Comparison	baseMean	log2FoldChange	padj
Actinobacteria	FS_vs_CON	703.827659	0.28597037	0.58918018
Bacteroidetes	FS_vs_CON	2635.15429	-0.6223581	0.34548905
Cyanobacteria	FS_vs_CON	1.71118619	0.45257065	0.33812189
Deferribacteres	FS_vs_CON	1.79451952	0.81560873	0.13738362
Firmicutes	FS_vs_CON	8568.86702	-0.2698228	0.5888096
Patescibacteria	FS_vs_CON	1.71118619	0.45257065	0.33812189
Proteobacteria	FS_vs_CON	20396.4905	-0.4459152	0.33812189
Tenericutes	FS_vs_CON	2.81411863	2.49124336	2.44E-06
Verrucomicrobia	FS_vs_CON	1195.09706	1.41225889	0.11346409
Unknown	FS_vs_CON	1.73555216	0.48361737	0.33812189
Actinobacteria	FC_vs_CON	703.827659	-0.4331528	0.45001362
Bacteroidetes	FC_vs_CON	2635.15429	-6.1216826	1.58E-26
Cyanobacteria	FC_vs_CON	1.71118619	0.53769121	0.22095926
Deferribacteres	FC_vs_CON	1.79451952	0.54169409	0.23724916
Firmicutes	FC_vs_CON	8568.86702	-1.123884	0.02578339
Patescibacteria	FC_vs_CON	1.71118619	0.53769121	0.22095926
Proteobacteria	FC_vs_CON	20396.4905	0.24616001	0.5060345
Tenericutes	FC_vs_CON	2.81411863	0.76021629	0.22095926
Verrucomicrobia	FC_vs_CON	1195.09706	2.47551078	0.00023836
Unknown	FC_vs_CON	1.73555216	0.66777386	0.22095926
Actinobacteria	FC_vs_FS	703.827659	-0.7191231	0.28484582
Bacteroidetes	FC_vs_FS	2635.15429	-5.4993245	3.85E-21
Cyanobacteria	FC_vs_FS	1.71118619	0.08512055	0.81817107
Deferribacteres	FC_vs_FS	1.79451952	-0.2739146	0.69203079
Firmicutes	FC_vs_FS	8568.86702	-0.8540612	0.14984137
Patescibacteria	FC_vs_FS	1.71118619	0.08512055	0.81817107
Proteobacteria	FC_vs_FS	20396.4905	0.69207522	0.15996684
Tenericutes	FC_vs_FS	2.81411863	-1.7310271	0.00105402
Verrucomicrobia	FC_vs_FS	1195.09706	1.06325189	0.16710452
Unknown	FC_vs_FS	1.73555216	0.18415649	0.79143125

Supplementary Table 4. Genus differential abundance group comparisons at PD15.

Genus	Comparison	baseMean	log2FoldChange	padj
Lactobacillus	FC_vs_CON	943.343916	-11.2054027	5.91E-53
Lactobacillus	FS_vs_CON	943.343916	-11.23517868	4.23E-51
Corynebacterium 1	FC_vs_CON	31.0486927	-6.257605456	4.13E-36
Corynebacterium 1	FS_vs_CON	31.0486927	-6.147020256	3.04E-34
Alistipes	FC_vs_CON	87.7495671	-7.351784331	3.77E-29
Roseburia	FC_vs_CON	843.041103	-6.810033651	3.77E-29
Ruminiclostridium 9	FC_vs_CON	137.932944	-7.068756355	4.41E-29
Roseburia	FC_vs_FS	843.041103	-6.918374768	4.81E-29
Ruminiclostridium 9	FC_vs_FS	137.932944	-7.145837222	7.57E-29
Lachnoclostridium	FC_vs_CON	129.069791	-6.763864109	5.03E-28
uncultured Barnesiella sp.	FC_vs_CON	209.180772	-8.26164139	8.59E-28
Bacteroides	FC_vs_CON	691.280665	-6.90262688	2.49E-27
uncultured bacterium	FC_vs_CON	194.772508	-6.487304064	2.92E-26
Butyrivibrio	FC_vs_CON	28.5753277	-6.129347333	4.94E-26
Lachnoclostridium	FC_vs_FS	129.069791	-6.489045554	4.26E-25
Prevotellaceae UCG−001	FC_vs_CON	21.1685806	-5.41264579	4.84E-25
GCA−900066575	FC_vs_FS	53.9507492	-6.202951435	7.53E-25
Butyrivibrio	FS_vs_CON	28.5753277	-6.160081634	1.15E-24
uncultured Barnesiella sp.	FC_vs_FS	209.180772	-7.806397155	2.58E-24
GCA-900066575	FC_vs_CON	53.9507492	-5.997231736	4.64E-24
A2	FC_vs_CON	20.1290152	-5.585794341	1.14E-22
Parabacteroides	FC_vs_FS	2137.90368	-6.018782706	3.01E-21
Blautia	FC_vs_CON	1069.40878	-6.560698938	3.17E-21
Enterococcus	FS_vs_CON	16.4559886	-5.283282694	2.00E-20
Parabacteroides	FC_vs_CON	2137.90368	-5.676176076	1.07E-19
uncultured	FC_vs_CON	394.333165	-5.389424988	1.07E-19
Blautia	FC_vs_FS	1069.40878	-6.32235754	4.15E-19
Bifidobacterium	FC_vs_CON	37.1723205	-6.093653026	1.18E-18
Ruminococcaceae UCG−004	FC_vs_FS	74.2474539	-5.956391187	1.52E-18
Dorea	FC_vs_FS	20.2595329	-5.400013303	2.36E-18
Ruminococcaceae UCG−004	FC_vs_CON	74.2474539	-5.779379862	4.00E-18
Ruminiclostridium 5	FC_vs_CON	88.7515121	-4.804650556	4.94E-18
Bacteroides	FC_vs_FS	691.280665	-5.575954943	9.17E-18
Ruminococcus 2	FS_vs_CON	321.495762	6.504726938	9.99E-18
A2	FS_vs_CON	20.1290152	-4.769059001	1.82E-17
Alistipes	FS_vs_CON	87.7495671	-5.391805283	4.24E-17
uncultured	FC_vs_FS	394.333165	-5.047944312	6.71E-17
Ruminococcaceae NK4A214 group	FC_vs_FS	27.6491415	-5.153268129	5.71E-16
Lachnospiraceae FCS020 group	FC_vs_FS	21.8107195	-4.577687561	6.76E-16
Prevotellaceae NK3B31 group	FC_vs_CON	5.99282075	-3.713898082	7.36E-16
Lachnospiraceae FCS020 group	FC_vs_CON	21.8107195	-4.388253466	4.44E-15
Enterococcus	FC_vs_CON	16.4559886	-3.976861459	6.37E-15

Lachnospiraceae UCG−001	FC_vs_CON	6.94437535	-3.909293473	2.04E-14
Prevotellaceae NK3B31 group	FS_vs_CON	5.99282075	-3.602050531	2.20E-14
Acetatifactor	FC_vs_FS	14.0277087	-4.818296549	2.77E-14
Butyricicoccus	FC_vs_FS	11.4562801	-4.418002071	5.03E-14
Ruminococcaceae NK4A214 group	FC_vs_CON	27.6491415	-4.726550258	5.15E-14
Tyzzerella 4	FC_vs_FS	16.0396134	-4.892159519	1.02E-12
Lachnospiraceae UCG−006	FC_vs_FS	10.5895424	-3.990325886	1.78E-12
[Eubacterium] xylanophilum group	FC_vs_CON	10.361042	-3.72527298	4.28E-12
[Eubacterium] xylanophilum group	FC_vs_FS	10.361042	-3.638566341	3.06E-11
uncultured bacterium	FC_vs_FS	194.772508	-4.152684958	3.93E-11
Lachnospiraceae UCG−004	FC_vs_FS	7.67180536	-3.789248869	4.70E-11
Bifidobacterium	FC_vs_FS	37.1723205	-4.636273134	5.75E-11
Lachnospiraceae UCG−001	FS_vs_CON	6.94437535	-3.253299492	1.57E-10
Ruminiclostridium 6	FS_vs_CON	4.11142561	3.329217364	1.98E-10
Eisenbergiella	FC_vs_CON	7.9919944	-3.657999786	3.22E-10
Prevotellaceae UCG−001	FC_vs_FS	21.1685806	-3.369521952	5.56E-10
Marvinbryantia	FC_vs_CON	20.4290374	-3.698506609	5.58E-10
uncultured	FC_vs_CON	228.601474	-3.684153644	8.09E-10
Streptococcus	FS_vs_CON	91.7217949	-3.881505602	1.14E-09
Lachnospiraceae UCG−006	FC_vs_CON	10.5895424	-3.38531779	1.82E-09
Dubosiella	FC_vs_CON	22.0619511	3.102949782	2.06E-09
Ruminiclostridium 6	FC_vs_FS	4.11142561	-2.912986946	6.11E-09
uncultured Bacteroidales bacterium	FC_vs_CON	10.861042	-3.723859161	8.01E-09
uncultured Bacteroidales bacterium	FC_vs_FS	10.861042	-3.765574934	9.37E-09
uncultured	FC_vs_FS	228.601474	-3.498998978	9.80E-09
Harryflintia	FS_vs_CON	7.34161842	2.959963163	1.06E-08
Marvinbryantia	FS_vs_CON	20.4290374	-3.439243111	3.24E-08
Ruminiclostridium 5	FC_vs_FS	88.7515121	-3.119114705	5.66E-08
Ruminococcus 2	FC_vs_CON	321.495762	4.021804891	7.05E-08
Dorea	FC_vs_CON	20.2595329	-3.218620782	2.62E-07
Christensenellaceae R−7 group	FC_vs_FS	18.8476462	2.841349044	4.49E-07
Tyzzerella 4	FC_vs_CON	16.0396134	-3.413027173	7.57E-07
Allobaculum	FC_vs_FS	54.1839724	3.531318175	1.27E-06
Butyricicoccus	FC_vs_CON	11.4562801	-2.869376308	1.41E-06
Unknown	FC_vs_CON	647.718827	-2.593479496	2.52E-06
Turicibacter	FC_vs_CON	2.3501702	-1.991442032	2.99E-06
Coriobacteriaceae UCG−002	FC_vs_CON	2.87419557	-1.952481966	4.57E-06
Eisenbergiella	FC_vs_FS	7.9919944	-2.764685863	5.08E-06
Coriobacteriaceae UCG−002	FS_vs_CON	2.87419557	-2.089148552	5.62E-06
Dubosiella	FC_vs_FS	22.0619511	2.37203578	8.21E-06
Turicibacter	FS_vs_CON	2.3501702	-2.023357946	9.02E-06

Acetatifactor	FC_vs_CON	14.0277087	-2.82985385	1.13E-05
Yaniella	FC_vs_CON	2.28961344	-1.931604844	1.29E-05
uncultured	FS_vs_CON	136.226542	2.689102713	2.86E-05
Clostridium sensu stricto 1	FS_vs_CON	18.4608341	2.151358294	3.20E-05
Yaniella	FS_vs_CON	2.28961344	-1.963424876	3.35E-05
Brachybacterium	FC_vs_CON	2.15866106	-1.800938653	3.41E-05
Prevotellaceae UCG−001	FS_vs_CON	21.1685806	-2.043123838	3.75E-05
Facklamia	FS_vs_CON	5.7376221	-2.182870448	3.75E-05
Brevibacterium	FC_vs_CON	2.07664137	-1.713778527	4.29E-05
Ruminococcus 1	FC_vs_CON	152.19556	-2.72874267	4.34E-05
Tyzzerella	FS_vs_CON	39.6871385	2.827082801	5.00E-05
Family XIII AD3011 group	FC_vs_CON	16.92786	-2.443606159	6.16E-05
Staphylococcus	FS_vs_CON	46.7319341	-2.231779102	6.81E-05
Lachnospiraceae UCG−004	FC_vs_CON	7.67180536	-2.3397509	6.81E-05
Brachybacterium	FS_vs_CON	2.15866106	-1.832838099	6.86E-05
Brevibacterium	FS_vs_CON	2.07664137	-1.745791046	8.33E-05
Ruminococcus 1	FS_vs_CON	152.19556	-2.735077752	0.00010062
Streptococcus	FC_vs_CON	91.7217949	-2.368257518	0.00013857
Harryflintia	FC_vs_FS	7.34161842	-1.883044116	0.00018459
Lachnospiraceae NK4A136 group	FC_vs_FS	621.161071	-2.092981218	0.00018814
Lachnospiraceae NK4A136 group	FC_vs_CON	621.161071	-2.022065327	0.00019567
Dorea	FS_vs_CON	20.2595329	2.181392521	0.00028742
uncultured bacterium	FS_vs_CON	194.772508	-2.334619105	0.00037237
Candidatus Soleaferrea	FS_vs_CON	2.6256069	-1.812704475	0.00037237
uncultured Clostridia bacterium	FS_vs_CON	3.66684088	1.709144878	0.00079489
Family XIII AD3011 group	FC_vs_FS	16.92786	-2.11119267	0.00105365
Tyzzerella	FC_vs_CON	39.6871385	2.19266492	0.00111933
uncultured organism	FC_vs_FS	10.6022059	-2.199746717	0.00117072
Papillibacter	FS_vs_CON	4.69457407	1.655723721	0.00125534
Facklamia	FC_vs_CON	5.7376221	-1.602317825	0.0012586
Jeotgalicoccus	FS_vs_CON	76.1024512	-1.875900782	0.0013859
Acetatifactor	FS_vs_CON	14.0277087	1.988442699	0.00147479
Ruminococcus 2	FC_vs_FS	321.495762	-2.482922047	0.00175737
Allobaculum	FC_vs_CON	54.1839724	2.28574523	0.00176994
Unknown	FC_vs_FS	647.718827	-1.818557436	0.001928
Papillibacter	FC_vs_CON	4.69457407	1.515567825	0.00197424
Defluviitaleaceae UCG−011	FS_vs_CON	86.9538377	1.868385301	0.00210218
GCA−900066225	FC_vs_CON	7.71173761	-1.508080678	0.00271297
Aerococcus	FC_vs_FS	7.04821059	-1.432843032	0.0038711
Parasutterella	FC_vs_CON	1.67056582	-1.164849302	0.00528682
UBA1819	FS_vs_CON	8.90396681	1.588243399	0.0057122
Ruminiclostridium 5	FS_vs_CON	88.7515121	-1.685535851	0.00615359
Christensenellaceae R−7 group	FS_vs_CON	18.8476462	-1.673736317	0.00623561
GCA-900066225	FS_vs_CON	7.71173761	-1.465727826	0.00623561

Parasutterella	FS_vs_CON	1.67056582	-1.197023886	0.00708011
Butyricicoccus	FS_vs_CON	11.4562801	1.548625762	0.00742389
Defluviitaleaceae UCG−011	FC_vs_CON	86.9538377	1.553513294	0.00788842
Alistipes	FC_vs_FS	87.7495671	-1.959979049	0.00847069
Akkermansia	FC_vs_CON	1419.64758	1.829097439	0.01062134
Jeotgalicoccus	FC_vs_CON	76.1024512	-1.438837176	0.01091676
uncultured	FC_vs_CON	150.057441	-1.260348868	0.01091676
Staphylococcus	FC_vs_CON	46.7319341	-1.388924621	0.01098959
Lachnospiraceae UCG−004	FS_vs_CON	7.67180536	1.449497969	0.01122382
uncultured	FC_vs_FS	136.226542	-1.583467282	0.01796532
Clostridium sensu stricto 1	FC_vs_FS	18.4608341	-1.24537557	0.01976096
UBA1819	FC_vs_FS	8.90396681	-1.350481228	0.01976096
Ruminococcaceae UCG−009	FS_vs_CON	8.99034759	1.466312698	0.0198437
[Ruminococcus] gauvreauii group	FC_vs_CON	1.42236223	1.003701849	0.02096697
uncultured	FS_vs_CON	150.057441	-1.212349475	0.02299362
Flavonifractor	FS_vs_CON	1.43247059	1.047356077	0.02299362
Ruminococcaceae UCG−009	FC_vs_FS	8.99034759	-1.416327663	0.02428004
Streptococcus	FC_vs_FS	91.7217949	1.513248084	0.02970451
Candidatus Soleaferrea	FC_vs_FS	2.6256069	1.204416941	0.02970451
uncultured bacterium	FS_vs_CON	10.2376826	-1.382450735	0.0319048
Haemophilus	FC_vs_FS	5.0336956	-1.267429579	0.03330842
uncultured	FS_vs_CON	1.48303661	0.939428653	0.03348201
Adlercreutzia	FC_vs_CON	1.52770868	-0.905571756	0.03473611
Anaeroplasma	FS_vs_CON	1.56786663	0.985016645	0.03713742
uncultured organism	FC_vs_CON	10.6022059	-1.420277571	0.03801911
Faecalibaculum	FS_vs_CON	43.5243414	1.457861125	0.03859935
Tyzzerella 4	FS_vs_CON	16.0396134	1.479132346	0.0387226
Adlercreutzia	FS_vs_CON	1.52770868	-0.937801356	0.03926375
uncultured Clostridia bacterium	FC_vs_FS	3.66684088	-1.071782397	0.03968369
Christensenellaceae R−7 group	FC_vs_CON	18.8476462	1.167612727	0.04421831
Bifidobacterium	FS_vs_CON	37.1723205	-1.457379892	0.0481069
Aerococcus	FS_vs_CON	7.04821059	1.013597058	0.0481069

Supplementary Table 5. Iron status and weight of YA rats following daily postnatal iron supplementation with FS or FC.

Males				
	CON	**FS**	**FC**	**P-Value**
Hb (mg/L)	17.7 ± 1.4	17.4 ± 2.7	17.9 ± 0.8	0.8635
Fe (ppm)				
Liver	75.5 ± 14.7	76.9 ± 14.9	92.0 ± 14.7	0.1005
Spleen	166.7 ± 32.8	186.5 ± 50.8	171.6 ± 23.6	0.5303
Weight (g)				
Body	297.8 ± 29.46	303.3 ± 15.8	310.9 ± 15.0	0.3342
Liver	11.70 ± 0.95	12.47 ± 0.62	11.59 ± 1.4	0.1139
Brain	1.87 ± 0.11	1.89 ± 0.11	1.94 ± 0.09	0.1823
Females				
	CON	**FS**	**FC**	**P-Value**
Hb (mg/L)	18.1 ± 1.9	17.1 ± 4.3	17.0 ± 1.5	0.6475
Fe (ppm)				
Liver	172.8 ± 36.1	144.2 ± 29.9	169.5 ± 25.9	0.1536
Spleen	284.4 ± 74.7	251.6 ± 105.5	258.9 ± 38.03	0.9567
Weight (g)				
Body	188.8 ± 15.0	194.2 ± 13.0	200.9 ± 12.3	0.0939
Liver	6.91 ± 0.47	7.44 ± 0.92	7.32 ± 0.83	0.1951
Brain	1.80 ± 0.06	1.78 ± 0.07	1.79 ± 0.06	0.5674

Supplementary Table 6. P-values from diversity statistical analyses in YA rats.

Alpha-Diversity Metric (Sampling Depth)	**P-Value**			
Faith's PD[1]	Treatment[2]	FS vs. CON[3]	FC vs. CON[3]	FC vs. FS[3]
(1)	0.6783	0.1953	0.4034	0.2814
(1112)	<0.0001	0.0129	0.0022	<0.0001
(2223)	<0.0001	0.0103	0.0039	<0.0001
(3334)	<0.0001	0.0078	0.0047	<0.0001
(4445)	<0.0001	0.0016	0.0052	<0.0001
(5556)	<0.0001	0.0019	0.0052	<0.0001
(6667)	<0.0001	0.0018	0.0053	<0.0001
(7778)	<0.0001	0.0006	<0.0001	0.0144
(8889)	<0.0001	0.0011	0.0090	<0.0001
(10,000)	<0.0001	0.0015	0.0086	<0.0001
Shannon[4]	Treatment[2]	FS vs. CON[3]	FC vs. CON[3]	FC vs. FS[3]
(1)	NA			
(1112)	<0.0001	0.0005	0.0115	<0.0001
(2223)	<0.0001	0.0007	0.0143	<0.0001
(3334)	<0.0001	0.0009	0.0117	<0.0001
(4445)	<0.0001	0.0004	0.0150	<0.0001
(5556)	<0.0001	0.0004	0.0152	<0.0001
(6667)	<0.0001	0.0004	0.0150	<0.0001
(7778)	<0.0001	0.0004	0.0168	<0.0001
(8889)	<0.0001	0.0004	0.0184	<0.0001
(10,000)	<0.0001	0.0005	0.0176	<0.0001
ASVs[5]	Treatment[2]	FS vs. CON[3]	FC vs. CON[3]	FC vs. FS[3]
(1)	NA			
(1112)	<0.0001	0.0009	0.0139	<0.0001
(2223)	<0.0001	0.0006	0.0236	<0.0001
(3334)	<0.0001	0.0010	0.0189	<0.0001
(4445)	<0.0001	0.0003	0.0180	<0.0001
(5556)	<0.0001	0.0003	0.0173	0.0001
(6667)	<0.0001	0.0003	0.0166	<0.0001
(7778)	<0.0001	0.0003	0.0169	<0.0001
(8889)	<0.0001	0.0002	0.0278	<0.0001
(10,000)	<0.0001	0.0002	0.0267	<0.0001

	P-Value[6]				
Beta-Diversity Metric	Treatment	Sex	Treatment: Litter	Treatment: Sex	Treatment: Sex:Litter
Weighted UniFrac	0.0034	0.9558	0.4016	0.6150	0.8102
Unweighted UniFrac	<0.0001	0.1021	<0.0001	0.2973	0.2322
Bray-Curtis	<0.0001	0.0644	<0.0001	0.2727	0.0244

[1]Faith's Phylogenetic Diversity. [2]Kruskal-Wallis test for treatment effect. [3]Dunn's pairwise group comparisons. [4]Shannon's Diversity. [5]Amplicon Sequence Variant count (richness). [6]Permutational analysis of variance (PERMANOVA).

Supplementary Table 7. Young adult rat Phylum differential abundance supplementation group comparisons.

Phylum	Comparison	baseMean	log2FoldChange	padj
Actinobacteria	FS_vs_CON	521.634916	-0.0076584	0.98918101
Bacteroidetes	FS_vs_CON	1092.95573	0.46734273	0.56773788
Cyanobacteria	FS_vs_CON	4.77673283	0.6021831	0.4807081
Deferribacteres	FS_vs_CON	52.9791407	-0.8085905	0.21032867
Firmicutes	FS_vs_CON	37104.3337	-0.2605321	0.52908704
Patescibacteria	FS_vs_CON	3.82646994	-1.1051869	0.21032867
Proteobacteria	FS_vs_CON	262.734388	-3.9526979	3.10E-14
Tenericutes	FS_vs_CON	52.8866125	0.04124699	0.98918101
Verrucomicrobia	FS_vs_CON	394.528763	0.05637982	0.98918101
Unknown	FS_vs_CON	4.39389495	-2.2072996	0.00199727
Actinobacteria	FC_vs_CON	521.634916	-3.185122	4.10E-07
Bacteroidetes	FC_vs_CON	1092.95573	-5.3154188	7.81E-18
Cyanobacteria	FC_vs_CON	4.77673283	1.95798226	0.00101018
Deferribacteres	FC_vs_CON	52.9791407	0.8934887	0.08971613
Firmicutes	FC_vs_CON	37104.3337	0.06089323	0.82395484
Patescibacteria	FC_vs_CON	3.82646994	1.51685881	0.02208081
Proteobacteria	FC_vs_CON	262.734388	-3.6236625	7.58E-11
Tenericutes	FC_vs_CON	52.8866125	-1.6483561	0.00101018
Verrucomicrobia	FC_vs_CON	394.528763	1.74684294	0.00126733
Unknown	FC_vs_CON	4.39389495	0.22675945	0.81159844
Actinobacteria	FC_vs_FS	521.634916	-3.1774636	4.97E-07
Bacteroidetes	FC_vs_FS	1092.95573	-5.7827616	2.16E-21
Cyanobacteria	FC_vs_FS	4.77673283	1.35579916	0.01203638
Deferribacteres	FC_vs_FS	52.9791407	1.70207924	0.00092951
Firmicutes	FC_vs_FS	37104.3337	0.32142529	0.26169019
Patescibacteria	FC_vs_FS	3.82646994	2.6220457	8.07E-05
Proteobacteria	FC_vs_FS	262.734388	0.32903538	0.53824442
Tenericutes	FC_vs_FS	52.8866125	-1.6896031	0.00064748
Verrucomicrobia	FC_vs_FS	394.528763	1.69046312	0.00142814
Unknown	FC_vs_FS	4.39389495	2.43405904	0.00064748

Supplementary Table 8. Young adult rat Genus differential abundance supplementation group comparisons.

Genus	Comparison	baseMean	log2FoldChange	padj
Lactobacillus	FS_vs_CON	2483.7457	-13.03162978	1.91E-55
Lactobacillus	FC_vs_CON	2483.7457	-11.9770344	1.54E-41
Turicibacter	FS_vs_CON	148.167448	-8.983425394	8.14E-35
Turicibacter	FC_vs_CON	148.167448	-7.923251714	4.69E-24
uncultured bacterium	FC_vs_FS	818.083013	-7.521156478	3.29E-30
Ruminiclostridium 9	FC_vs_FS	218.961501	-6.922327075	8.82E-28
uncultured bacterium	FC_vs_CON	818.083013	-6.905999698	3.38E-25
Enterorhabdus	FC_vs_FS	99.8269249	-6.887098457	2.36E-26
[Eubacterium] ruminantium group	FC_vs_FS	89.6268716	-6.603413348	2.39E-11
Bacteroides	FC_vs_FS	229.64174	-6.44506143	2.32E-23
A2	FC_vs_FS	101.391184	-6.333072906	1.13E-21
GCA−900066575	FC_vs_FS	255.51557	-6.327545592	2.63E-22
Butyricicoccus	FC_vs_FS	89.1224262	-6.318895306	1.13E-21
Lachnospiraceae UCG−001	FC_vs_FS	1380.3985	-6.134109613	9.48E-17
Lachnospiraceae FCS020 group	FC_vs_FS	175.855168	-6.111987018	3.26E-22
Prevotellaceae NK3B31 group	FC_vs_FS	88.9237736	-6.074822995	1.13E-21
Dorea	FC_vs_FS	59.3152826	-6.06387171	1.16E-22
[Eubacterium] xylanophilum group	FC_vs_FS	1503.59081	-6.043506036	5.61E-23
Butyricicoccus	FC_vs_CON	89.1224262	-6.033874434	4.99E-19
Lachnospiraceae UCG−001	FC_vs_CON	1380.3985	-6.005018324	1.88E-15
Lachnoclostridium	FC_vs_FS	941.055958	-5.825335273	2.94E-20
Parabacteroides	FC_vs_FS	136.702842	-5.817975789	2.47E-24
Acetatifactor	FC_vs_FS	105.120581	-5.8052612	2.07E-19
Prevotellaceae UCG−001	FC_vs_FS	249.412684	-5.799364282	2.91E-20
Acetitomaculum	FC_vs_FS	144.340698	-5.62015411	7.83E-21
[Eubacterium] ventriosum group	FC_vs_FS	52.2457487	-5.585730775	5.07E-17
Ruminiclostridium 9	FC_vs_CON	218.961501	-5.533820778	1.01E-17
Roseburia	FC_vs_FS	2396.83108	-5.499657081	1.04E-18
Bacteroides	FC_vs_CON	229.64174	-5.493030086	7.97E-17
Lachnospiraceae UCG−006	FC_vs_FS	412.586107	-5.489149124	3.55E-18
Anaerostipes	FC_vs_FS	294.274519	-5.474644475	2.28E-10
Ruminococcaceae NK4A214 group	FC_vs_FS	35.1980214	-5.459692383	3.63E-21
Enterorhabdus	FC_vs_CON	99.8269249	-5.454920188	1.24E-16
[Eubacterium] ruminantium group	FC_vs_CON	89.6268716	-5.378929193	1.15E-07
uncultured Barnesiella sp.	FC_vs_CON	226.242545	-5.227605556	1.17E-07
[Eubacterium] ventriosum group	FC_vs_CON	52.2457487	-5.197475841	2.29E-14

Acetitomaculum	FC_vs_CON	144.340698	-5.176374216	4.56E-17
Roseburia	FC_vs_CON	2396.83108	-5.143050954	8.04E-16
uncultured bacterium	FC_vs_FS	29.5323043	-5.075861289	9.21E-16
A2	FC_vs_CON	101.391184	-4.982591621	1.92E-13
uncultured Barnesiella sp.	FC_vs_FS	226.242545	-4.918731916	4.09E-07
Dorea	FC_vs_CON	59.3152826	-4.90685174	7.49E-15
Bifidobacterium	FC_vs_CON	654.431753	-4.904175571	6.06E-11
Blautia	FC_vs_FS	390.195135	-4.898503227	4.64E-14
Bifidobacterium	FC_vs_FS	654.431753	-4.880602147	3.71E-11
Lachnospiraceae FCS020 group	FC_vs_CON	175.855168	-4.856665745	4.62E-14
Blautia	FC_vs_CON	390.195135	-4.797562981	4.20E-13
[Eubacterium] xylanophilum group	FC_vs_CON	1503.59081	-4.702148123	4.62E-14
Prevotellaceae UCG−001	FC_vs_CON	249.412684	-4.61914502	7.45E-13
Lachnospiraceae NK4B4 group	FC_vs_FS	19.9719551	-4.618470482	2.00E-09
Coriobacteriaceae UCG−002	FC_vs_FS	102.389941	-4.615111992	1.02E-10
GCA−900066575	FC_vs_CON	255.51557	-4.573171101	5.80E-12
Prevotellaceae NK3B31 group	FC_vs_CON	88.9237736	-4.552936459	2.50E-12
Alistipes	FC_vs_FS	24.4990952	-4.544697067	5.36E-12
Lachnoclostridium	FC_vs_CON	941.055958	-4.530249463	2.51E-12
uncultured	FC_vs_FS	228.108237	-4.498742077	2.82E-13
Ruminococcaceae UCG−004	FC_vs_FS	15.0495545	-4.487837851	2.05E-11
Adlercreutzia	FC_vs_FS	18.9445377	-4.220372348	1.93E-09
Anaerostipes	FC_vs_CON	294.274519	-4.197554403	2.57E-06
Lachnospiraceae UCG−006	FC_vs_CON	412.586107	-4.172077506	1.25E-10
Parabacteroides	FC_vs_CON	136.702842	-4.133868635	1.14E-12
Lachnospiraceae UCG−004	FC_vs_FS	13.1743277	-4.048776446	6.79E-10
Alistipes	FC_vs_CON	24.4990952	-4.005588127	2.58E-09
Acetatifactor	FC_vs_CON	105.120581	-3.925544886	3.50E-09
Escherichia−Shigella	FS_vs_CON	196.323115	-3.910953104	6.08E-11
uncultured Bacteroidales bacterium	FC_vs_CON	16.9449094	-3.869405751	1.52E-07
Tyzzerella 4	FS_vs_CON	4.8313218	-3.857112228	5.90E-11
uncultured	FC_vs_FS	1970.97886	-3.855610183	8.22E-11
uncultured bacterium	FC_vs_CON	29.5323043	-3.798875465	5.11E-09
Ruminococcaceae NK4A214 group	FC_vs_CON	35.1980214	-3.770428401	2.37E-10
Escherichia−Shigella	FC_vs_CON	196.323115	-3.767309695	8.53E-10
Intestinimonas	FC_vs_FS	13.9657251	-3.766726351	5.00E-08
Parasutterella	FC_vs_FS	15.6970085	-3.687651541	2.45E-06
uncultured Bacteroidales bacterium	FC_vs_FS	16.9449094	-3.60834736	7.08E-07
Parasutterella	FC_vs_CON	15.6970085	-3.536437014	1.02E-05
Adlercreutzia	FC_vs_CON	18.9445377	-3.501672362	1.32E-06

Coriobacteriaceae UCG−002	FC_vs_CON	102.389941	-3.266877947	1.02E-05
Tyzzerella 3	FC_vs_FS	52.7342782	-3.21496406	1.12E-06
GCA-900066225	FC_vs_CON	13.1496662	-3.159769794	2.95E-08
uncultured bacterium	FC_vs_CON	8.28627775	-3.133161259	7.27E-06
Intestinimonas	FC_vs_CON	13.9657251	-3.070547053	1.62E-05
Ruminococcaceae UCG−009	FC_vs_FS	27.3004252	-3.046940479	1.07E-06
Staphylococcus	FS_vs_CON	3.90070357	-2.973515836	1.92E-07
Enterococcus	FS_vs_CON	5.68524503	-2.876835461	5.98E-06
uncultured	FC_vs_CON	228.108237	-2.804476839	1.21E-05
Tyzzerella 4	FC_vs_CON	4.8313218	-2.776601587	7.91E-06
Tyzzerella 3	FC_vs_CON	52.7342782	-2.775846732	4.39E-05
Unknown	FC_vs_FS	4288.50063	-2.730573335	2.19E-07
Lachnospiraceae NK4B4 group	FC_vs_CON	19.9719551	-2.698180066	0.00097877
uncultured Firmicutes bacterium	FC_vs_FS	5.80591515	-2.682566894	2.77E-05
uncultured	FC_vs_CON	1970.97886	-2.626968519	1.94E-05
[Eubacterium] fissicatena group	FS_vs_CON	5.11710993	-2.62402099	3.07E-05
Acinetobacter	FS_vs_CON	2.51676391	-2.599637331	5.58E-06
Coprococcus 2	FS_vs_CON	2.27840207	-2.481723318	3.07E-05
Clostridiales bacterium enrichment culture clone 06−1235251−67	FC_vs_FS	6.87410323	-2.446598154	2.77E-05
Anaerotruncus	FC_vs_CON	28.0065901	-2.053291983	0.01017686
uncultured Lachnospiraceae bacterium	FC_vs_CON	4.81583123	-2.036730851	0.00315994
Lachnospiraceae UCG−004	FC_vs_CON	13.1743277	-2.036251602	0.00451245
uncultured bacterium	FC_vs_FS	8.28627775	-2.035791734	0.00468675
GCA−900066225	FS_vs_CON	13.1496662	-1.961953158	0.00038257
uncultured Mollicutes bacterium	FC_vs_FS	4.62196605	-1.929490726	0.00846291
uncultured rumen bacterium	FC_vs_FS	3.79758732	-1.856757316	0.00523879
Unknown	FC_vs_CON	4288.50063	-1.822956469	0.00097877
uncultured	FC_vs_FS	3.8856885	-1.794060745	6.59E-05
Phocea	FS_vs_CON	1.80222932	-1.731540442	0.00189098
uncultured Lachnospiraceae bacterium	FC_vs_FS	4.81583123	-1.635921521	0.01855382
Ruminococcaceae UCG−009	FC_vs_CON	27.3004252	-1.63159425	0.01714721
Acinetobacter	FC_vs_CON	2.51676391	-1.517621202	0.01309167
uncultured bacterium	FS_vs_CON	1.78925779	-1.481726819	0.01287161
Coprococcus 2	FC_vs_CON	2.27840207	-1.400436422	0.03022422
Ruminiclostridium 5	FC_vs_FS	271.524596	-1.310604025	0.00729618
GCA−900066225	FC_vs_FS	13.1496662	-1.197816636	0.04814768
Streptococcus	FS_vs_CON	1.84340814	-1.183844324	0.02908293
uncultured	FC_vs_FS	2.41233768	-1.142820552	0.0290884

Ruminococcaceae UCG−014	FC_vs_FS	674.18926	-1.126082222	0.03741428
uncultured	FC_vs_FS	4.60712959	0.980960401	0.03741428
Anaerofustis	FC_vs_FS	1.44894849	1.102563912	0.04285036
Bacillus	FC_vs_FS	1.39188411	1.105422455	0.03946832
Candidatus Saccharimonas	FC_vs_FS	1.35583732	1.107274449	0.03765589
Anaerofilum	FC_vs_FS	1.34804059	1.107450254	0.03765589
Dietzia	FC_vs_FS	1.30816026	1.108240165	0.03741428
Clostridium sensu stricto 18	FC_vs_FS	1.30816026	1.108240165	0.03741428
uncultured organism	FC_vs_FS	1.30816026	1.108240165	0.03741428
[Ruminococcus] gauvreauii group	FC_vs_FS	1.30816026	1.108240165	0.03741428
Lachnoclostridium 5	FC_vs_FS	1.30816026	1.108240165	0.03741428
Lachnospiraceae NC2004 group	FC_vs_FS	1.30816026	1.108240165	0.03741428
Moryella	FC_vs_FS	1.30816026	1.108240165	0.03741428
Sellimonas	FC_vs_FS	1.30816026	1.108240165	0.03741428
Candidatus Soleaferrea	FC_vs_FS	1.30816026	1.108240165	0.03741428
Haemophilus	FC_vs_FS	1.30816026	1.108240165	0.03741428
Defluviitaleaceae UCG−011	FC_vs_FS	25.9337856	1.121021492	0.02225898
uncultured rumen bacterium	FC_vs_CON	1.46654416	1.126332484	0.03283721
Ruminococcaceae UCG−005	FC_vs_FS	245.305711	1.154586719	0.03741428
Ruminococcus 1	FC_vs_CON	1421.96818	1.170878701	0.04506375
Oscillibacter	FC_vs_CON	591.22098	1.176264449	0.03405798
uncultured bacterium	FS_vs_CON	2.72067845	1.183692057	0.04990854
Tyzzerella	FC_vs_CON	87.3770525	1.244725504	0.02395119
uncultured	FS_vs_CON	2.41233768	1.245642067	0.01587785
uncultured bacterium	FS_vs_CON	29.5323043	1.276985824	0.04990854
unidentified rumen bacterium RF32	FC_vs_FS	2.98292233	1.318179504	0.00478197
Defluviitaleaceae UCG−011	FC_vs_CON	25.9337856	1.324107749	0.00750157
uncultured	FC_vs_CON	4.60712959	1.372995516	0.0052082
Hydrogenoanaerobacterium	FC_vs_FS	1.38027696	1.373524469	0.00712283
Facklamia	FC_vs_FS	1.71257229	1.383734529	0.00527655
Ruminiclostridium 9	FS_vs_CON	218.961501	1.388506297	0.04990854
Ruminococcaceae UCG−009	FS_vs_CON	27.3004252	1.415346229	0.04990854
Enterorhabdus	FS_vs_CON	99.8269249	1.432178269	0.02900559
Family XIII AD3011 group	FC_vs_FS	9.75065878	1.43810261	0.00844407
Rothia	FS_vs_CON	10.1242213	1.446722049	0.00814556
Fournierella	FS_vs_CON	10.8224695	1.451646592	0.04824195
Family XIII AD3011 group	FC_vs_CON	9.75065878	1.453160392	0.0101334
uncultured	FC_vs_FS	1.41146118	1.483150942	0.00318402
uncultured Firmicutes bacterium	FS_vs_CON	5.80591515	1.512693325	0.0196532
Prevotellaceae NK3B31 group	FS_vs_CON	88.9237736	1.521886536	0.02669235
[Eubacterium] nodatum group	FC_vs_FS	40.2564595	1.572278329	0.00070517

uncultured rumen bacterium	FC_vs_FS	1.46654416	1.638420354	0.00075047
Parabacteroides	FS_vs_CON	136.702842	1.684107154	0.0064322
Ruminococcaceae NK4A214 group	FS_vs_CON	35.1980214	1.689263982	0.00153038
uncultured	FS_vs_CON	228.108237	1.694265238	0.01781735
Rothia	FC_vs_CON	10.1242213	1.737132396	0.00061171
GCA−900066575	FS_vs_CON	255.51557	1.75437449	0.01781735
[Eubacterium] coprostanoligenes group	FC_vs_FS	566.387421	1.793344316	0.0033409
Ruminiclostridium 1	FC_vs_CON	4.17427591	1.874776632	0.00033156
unidentified rumen bacterium RF32	FC_vs_CON	2.98292233	1.878159876	0.00017847
Acetatifactor	FS_vs_CON	105.120581	1.879716314	0.00769312
Lachnospiraceae NK4B4 group	FS_vs_CON	19.9719551	1.920290416	0.01788363
Caldicoprobacter	FC_vs_CON	3.93015968	1.923971143	0.00046188
Brevibacterium	FC_vs_CON	1.89614918	1.931591296	8.63E-05
Papillibacter	FC_vs_CON	4.79006649	1.976294183	0.00108651
Faecalibaculum	FC_vs_FS	353.034549	1.984640813	0.01738563
Lachnospiraceae UCG−004	FS_vs_CON	13.1743277	2.012524844	0.00157282
uncultured organism	FC_vs_CON	2.19470567	2.102292434	4.39E-05
Corynebacterium 1	FC_vs_FS	6.08686737	2.351108445	0.00011202
Enterococcus	FC_vs_FS	5.68524503	2.397013259	0.00017567
Brevibacterium	FC_vs_FS	1.89614918	2.427562279	2.89E-07
Yaniella	FC_vs_CON	2.40554171	2.448047862	7.76E-06
[Eubacterium] fissicatena group	FC_vs_FS	5.11710993	2.468846855	7.07E-05
Ruminococcus 2	FC_vs_CON	318.955147	2.479216544	0.00797728
Caldicoprobacter	FC_vs_FS	3.93015968	2.501776208	2.44E-06
Ruminiclostridium 1	FC_vs_FS	4.17427591	2.597630494	3.40E-07
uncultured organism	FC_vs_FS	2.19470567	2.649339441	1.21E-07
uncultured	FS_vs_CON	3.8856885	2.664411264	4.25E-09
Staphylococcus	FC_vs_FS	3.90070357	2.68159796	3.36E-06
Brachybacterium	FC_vs_CON	2.76649668	2.715679448	1.06E-06
Papillibacter	FC_vs_FS	4.79006649	2.838054631	1.39E-06
Yaniella	FC_vs_FS	2.40554171	2.921531599	3.16E-08
Brachybacterium	FC_vs_FS	2.76649668	3.184846508	3.02E-09

CHAPTER 4: Mineral interactions and inflammatory signaling are implicated growth wasting following excess oral iron supplementation in pre-weanling rats

ABSTRACT

Iron supplements are supplied widely to infants despite low rates of iron deficiency in many populations and there are growing concerns regarding adverse health and development effects of excess iron provision. Adverse effects of iron on infant growth and development are poorly understood but may be related to direct iron toxicity in developing organs. Another possibility is that iron overload alters inflammatory signaling and trace mineral metabolism, but these mechanisms have not been fully investigated. To characterize effects of excess iron doses on development, iron status, trace mineral status, and inflammatory signaling, Lewis rat litters were culled to 8 pups (4 males and 4 females) and randomly assigned to daily supplementation groups to receive either vehicle control (CON; 10% *w*/*v* sucrose solution) or ferrous sulfate (FS) iron at one of the following doses: 10, 30, or 90 mg iron/kg body weight—FS-10, FS-30, and FS-90, respectively—from postnatal day (PD) 2 through 9. FS-90 litters, but not FS-30 or FS-10, failed to thrive compared to CON litters and had smaller brains on PD 10. Among the groups FS-90 liver iron levels were highest, as were liver injury scores, and white blood cell counts. Compared to CON, circulating MCP-1 was increased in FS-90 pups. and liver zinc and copper levels. The growth wasting outcomes of excess FS provision in pre-weanling rats may be related to liver injury, inflammation, and altered trace mineral metabolism.

4.1. INTRODUCTION

Iron deficiency (ID) is a common micronutrient deficiency that causes around half of all anemia cases worldwide [1]. Infants are particularly at risk for ID, which can disrupt cognitive development and heighten the risk for infection, in addition to causing anemia [2–4]. The American Academy of Pediatrics recommends supplemental iron (SI) for all infants to prevent ID [5]. Unfortunately, SI can also be

harmful if provided beyond physiological requirements [6–10]. A growing number of studies report adverse effects of SI in iron-replete infants [11–15], but the mechanisms of iron toxicity at this developmental stage are not well understood. Experts in this area including the 2020 Dietary Guidelines Advisory Committee agree that improving the efficacy of SI provision in infants necessitates that future research investigate the mechanisms underlying adverse health and development effects of SI [6,7,16–18].

The effects of excess SI on early growth and neurodevelopment are unclear. Some studies indicate the provision of SI delays growth in iron replete infants. Overall growth delays including in the central nervous system might explain cognitive delays, however, some studies do not show an effect of SI on the growth of iron replete infants [8,11,12,19–22]. The inconsistent growth outcomes are likely related to variation in the form or dose of SI provided in the study, or in the baseline iron status of the study subjects. Iron toxicity may disrupt organ development, but this mechanism has not been fully investigated. Iron may also alter the metabolism of other essential trace minerals. In previous studies, providing SI to infants has negatively affected zinc or copper status [12,23–25]. If excess iron is disruptive to essential trace mineral availability, this may also explain the delays in growth and development.

Ferrous sulfate (FS) is an inexpensive form of SI found in most infant iron drops and infant formulas [26]. Excess FS can have adverse effects on growth and cognitive development [11,13,27–29], but the relationship between FS dose and infant development is unclear [30]. Using an iron supplementation model in pre-weanling rats, we investigated health and development effects of FS. Brain size at postnatal day (PD) 15 increased with daily FS supplementation at 10 mg iron/kg body weight per day, but brain iron stores were not impacted by FS at this dose. This physiological dose was designed to represent the daily iron intake of an infant fed exclusively iron-fortified formula compared to vehicle control [31]. Presently, we report the effects of excess FS dosing on pre-weanling rat health

and development. Excess FS at 90 mg iron/kg body weight caused growth wasting, inflammation, and reduced brain size. Our results indicate that excess FS disrupts postnatal growth and neurodevelopment, and these outcomes may be related to liver iron loading, systemic inflammation, and mineral interactions.

4.2. METHODS

4.2.1. Animal Experiments

Animal experiments were approved by the University of California Davis Institutional Animal Care and Use Committee. Adult male and female Lewis rats (Charles River Laboratories, Wilmington, MA, USA), were housed under standard conditions for the duration of the study: in clear polycarbonate hanging cages at constant temperature (22°C) and humidity (63%) with standard 12 h light cycles, and *ad libitum* access to 18% protein rodent chow (200 mg Fe/kg diet; 2018, Teklad Diets, Madison, WI, USA). Only nulliparous females—8-10 weeks old—were used for breeding experimental litters. On postnatal day (PD) 2 litters were culled to sex-matched litters of 8 pups to control for growth, cross-fostering from litters born within 24 h of each other, as necessary. Litters were assigned randomly to either vehicle control supplementation (CON; 10% *w/v* sucrose; n= 3 litters/group, 24 pups/group), or one of three FS iron doses (n=3 litters/group, 24 pups/group): 10 mg iron/kg body weight (FS-10), 30 mg iron/kg body weight (FS-30), or 90 mg iron/kg body weight (FS-90). Iron was provided as ferrous sulfate heptahydrate (Cat#215422-250G, Sigma-Aldrich, St. Louis, MO, USA) dissolved in 10% (w/v) sucrose in varying concentrations. The lowest dose (10 mg iron/kg) is representative of daily iron intake from formula [31]. The 30 and 90 mg doses provide excess iron, but at sub-toxic levels for adult rats [32]. Oral iron was administered once daily PD 2-9, in the afternoon by hand-pipetting, and body weight (BW) was recorded on PD 2, 4, 6, 8, and 10 (study end; day of necropsy). Supplement volume was calculated according to body weight and ranged from 8-60 µl.

4.2.2. Necropsy and Hematology

On PD 10, litters were separated from dams and fasted for 4-6 h. Pups were weighed and euthanized by decapitation under deep anesthesia (100 mg ketamine × 10 mg xylazine/kg BW). Whole blood was collected from the head cavity into EDTA-treated tubes (Greiner Bio-One, Monroe, NC, USA) and held at 4°C. Whole brains were removed, weighed, and four brain regions were promptly dissected: prefrontal cortex (PFC), striatum (ST), hippocampus (HP), and cerebellum (CE). All brains were dissected by the same researcher for consistency.

Complete blood counts (CBC; n = 3-4/group, 2 litters/group) were completed by the UC Davis School of Veterinary Medicine Clinical Pathology Laboratory within 24 h of blood collection.

4.2.3. Non-heme Iron

Non-heme iron concentrations (n = 14-18/group, 3 litters/group for each tissue) in the liver, kidney, spleen, and the four brain regions were determined by the bathophenanthroline method [33].

4.2.4. Histopathology

Fresh livers (n = 6/group, 3 litters/group) were immersion-fixed in 4% (w/v) paraformaldehyde (PFA) for 24 h at 4°C, then washed in three changes of 1x PBS and stored in 70% ethanol at 4°C. Fixed livers were embedded in paraffin using standard protocols. The UC Davis School Of Veterinary Medicine Anatomic Pathology Laboratory completed sectioning and staining. Liver sections were stained with Perls' Prussian Blue with nuclear fast red counterstain for iron detection, as well as Masson's Trichrome stain for evaluation of liver injury and inflammation.

Masson's Trichrome-stained liver slides were scored for injury and inflammation in a blinded fashion using a NAFLD scoring system for rodents [34]. A veterinary pathologist at the UC Davis School of Veterinary Medicine Comparative Pathology Laboratory assessed and scored steatosis (micro- or macro-vesicular), inflammation, fibrosis, and necrosis. Scores for steatosis, fibrosis, and necrosis were assigned

as follows: 0, parameter absent; 1, <10% affected area; 2, 10-25% affected area; 3, 26-50% affected area; 4, >50% affected area. Distribution of steatosis, fibrosis, and necrosis were classified as random, centrilobular, midzonal, periportal, or diffuse (all zones equally affected). Inflammation was scored according to number of inflammatory foci/field as follows: 0, parameter absent; 1, minimal, scattered, rare (<1 per 20x field); 2, mild (<2 per 20x field); 3, moderate (2 - 4 per 20x field); 4, severe (>4 per 20x field). Presence or absence of degeneration, hypertrophy, and oval cell/biliary hyperplasia was also noted.

4.2.5. Liver Gene Expression

The TRIzol method (Invitrogen™, Carlsbad, CA, USA) was applied to extract RNA from liver tissue. Tissues had been collected into RNA*later* ® (Thermo Fisher Scientific™, Waltham, MA, USA), incubated for an initial 24 h at 4°C, and then stored at -20°C until RNA extraction. A kit was used to reverse transcribe total RNA to cDNA (High-Capacity cDNA Archive Kit, Cat#4374966, Applied Biosystems™, Foster City, CA, USA), which was subsequently stored in EB buffer at 4°C. Real-time PCR reactions were performed using iTaq Universal SYBR Green Supermix (Cat#1725121, Bio-Rad, Hercules, CA, USA), a Bio-Rad CFX96 Real-Time machine, and the following primer sets: *Actb* forward, 3'-GAAATCGTGCGTGACATTAAAGAG-5'; *Actb* reverse, 3'- GCGGCAGTGGCCATCTC -5' [35]; *Hamp* forward 3'-GCTGCCTGTCTCCTGCTTCT-5'; *Hamp* reverse 3'-CTGCAGAGCCGTAGTCTGTCTCGTC-5' [36]. Hepcidin (*Hamp*) gene expression was calculated relative to the CON group using the $2^{-\Delta\Delta Ct}$ method, with *Actb* serving as the housekeeping gene (n = 13-18/group, 3 litters/group).

4.2.6. Serum Chemokine/Cytokine Array

Fresh whole blood was incubated in sterile tubes at room temperature for 30 min, and then centrifuged at 300 rcf for 15 min to isolate serum. Sera were diluted 1:1 in 1x PBS and shipped on dry ice to Eve Technologies Corporation (Calgary, AB Canada). Array services were used (Cat#RD27) for quantifying 27 total chemokines and cytokines (n = 10/group, 3 litters/group): CCL11, EGF, CX3CL1,

IFNγ,IL-1α, IL-1β, IL-2, IL-4, IL-5, IL-6, IL-10, IL-12(p70), IL-13, IL-17A, IL-18, IP-10, CXCL1, TNFα, G-CSF, GM-CSF, CCL2, Leptin, CXCL5, CCL3, CXCL2, CCL5, and VEGF.

4.2.7. Zinc and Copper

Zinc and copper concentrations (n = 9-18/group, 3 litters/group for each tissue) were determined in liver, kidney, spleen, and brain regions—PFC, ST, HP, and CE—by atomic absorption spectrometry using methods described previously [31].

4.2.8. Statistical Analysis

Statistical analysis and plotting were performed with GraphPad Prism (v9.3.1). The study was designed to consider the variation between litters, as well as within litters, while testing for differences among groups. When testing for differences in weight gain among groups, pup body weights were averaged by litter and litters were treated as biological replicates. A two-way repeated measure ANOVA was applied to test for effects of time and supplementation group on litter weight gain and post-hoc Tukey's test detected differences between groups. Samples for all other outcomes besides weight gain were taken randomly from multiple litters in the same group to capture litter variation. The sample size of pups and number of litters represented in each of the outcomes are listed in the corresponding methods above. All datasets were checked for normality using the Shapiro Wilks test. Kruskal-Wallis and Dunn's tests were used for finding overall group effects and differences between groups, respectively, in non-parametric data. $p < 0.05$ determined significance.

4.3. RESULTS

4.3.1. Excess FS Disrupts Growth

Average pup BW increased over time in all litters but was negatively impacted by FS-90 supplementation (Figure 1A). The BW of pups in FS-10 and FS-30 groups were similar to CON. However,

in the FS-90 group BW was 10% lower than CON on PD 4 ($p < 0.05$), and 17% lower on PD 10 ($p < 0.001$). Additionally, FS-90 brains weighed 10% less than CON and FS-10 brains at PD 10 (Figure 1B, $p < 0.001$).

Body weight at PD 10 was lower only in FS-90 males compared to FS-10 and FS-30 males and no difference was found in female body weights at this age (Figure S1A-B). Similarly, brain weight of FS-90 males was lower than CON and FS-10 males, while no significant effects were found to female brain weight (Figure S1C-D).

4.3.2. Hepatic Iron Loading from FS Dosing

To identify tissues impacted by iron loading following excess iron supplementation in pre-weanling rats, non-heme iron levels were quantified in liver, kidney, spleen, and four brain regions including the prefrontal cortex (PFC), striatum (ST), hippocampus (HP), and cerebellum (CE). Liver iron concentration increased in response to FS ($p < 0.0001$; Figure 2a). Relative to CON, liver iron increased 800% in the FS-10 group, 900% in the FS-30 group, and 1,100% in the FS-90 group. In spleen tissue, iron levels were unchanged in the FS-10 group but increased 180% in FS-30 and FS-90 relative to CON ($p < 0.05$). Iron levels in kidney and all four brain regions were unchanged with any iron dose. Iron deposition was undetectable at 40x objective in CON liver sections stained for iron (Figure 2d) but could be visualized under low magnification (10x objective) in FS-group livers. Hepatic iron concentration was inversely correlated to BW ($p = 0.0001$; Figure 2b), but not brain weight ($p = 0.09$; Figure 2c). These results suggest a negative relationship between liver iron stores and growth when excess FS is provided.

Liver hepcidin mRNA expression (*Hamp*) was induced in all FS groups, with the highest expression 50-fold over CON in FS-90 liver tissue ($p < 0.0001$). Liver non-heme iron was significantly correlated to hepcidin expression (Figure 2e-f). Thus, liver iron stores and hepcidin expression both responded to oral iron dosing in pre-weanling rats.

4.3.3. Hematological Effects of Excess FS

Hemoglobin, hematocrit, red blood cell (RBC) count, mean corpuscular volume (MCH), and mean cell hemoglobin concentration (MCHC) were unaffected by iron dose (CBC results shown in Table 1). However, MCH was altered by iron dose ($p < 0.0001$) and was elevated with FS-30 compared to FS-10. Although there was an overall effect of dose on RBC distribution width (RDW) ($p = 0.008$), the comparison between the FS-30 and FS-90 groups and CON was not significant ($0.08 > p > 0.05$).

Corrected WBC count was elevated in FS-90 compared to CON group ($p < 0.05$). Iron dose influenced neutrophil count significantly but the comparison in neutrophil count between FS-90 and CON was not significant ($0.08 > p > 0.05$). No effect of FS was observed on monocyte or lymphocyte counts.

4.3.4. Liver Histopathology

Liver injury and inflammation (n = 6/group) was assessed by a pathologist blinded to the treatment groups and results are depicted in Figure 3. Inflammation was either mild or minimal, and the highest scores were assigned to CON and FS-30 groups. Randomly distributed microvesicular steatosis was observed in all groups, but the FS-90 group received the highest steatosis scores. Periportal fibrosis was present in all groups, but FS-90 also received the highest fibrosis scores. Random necrosis was present in at least a few animals in each group; however, the highest necrosis score was assigned to an FS-30 liver sample. Degeneration and oval cell/biliary hyperplasia were present in all groups. Hypertrophy was not detected in the FS-90 group, although it was detected frequently in CON livers (present in 4/6 samples). It is unclear why liver hypertrophy occurred in the CON group.

4.3.5. Chemokine and Cytokine Response

Serum levels of eotaxin (CCL11), epidermal growth factor (EGF), interleukins (1α, 1β, 2, 4, 5, 6, 10, 12 (p70), 13, 17A, & 18), C-X-C motif chemokine 10 (CXCL10), growth-related alpha-protein (CXCL1), tumor necrosis factor (TNF-α), G-CSF (Granulocyte colony-stimulating factor), C-C motif chemokine 3

(CCL3), and C-C motif chemokine 5 (CCL5) were unaffected by iron dose (Table 2). However, levels of the following proteins were affected by iron dose: fractalkine (CX3CL1), interferon gamma (IFNγ), GM-CSF (Granulocyte-macrophage stimulating factor), C-C motif chemokine 2 (CCL2), leptin, C-X-C motif chemokine 5 (CXCL5), CXCL2 (C-X-C motif chemokine 2), and vascular endothelial growth factor (VEGF).

Fractalkine (CX3CL1), a chemokine expressed mainly by the central nervous system that plays an important role in early brain development [37], was reduced in FS-30 and FS-90 sera compared to CON ($p = 0.0018$). Mean interferon gamma (IFNγ) levels in FS-90 sera were lower than CON but this difference not significant ($0.08 > p > 0.05$). GM-CSF (Granulocyte-macrophage stimulating factor) and C-C motif chemokine 2 (CCL2), a pro-inflammatory chemokine, were elevated in FS-90 compared to FS-10 only ($p < 0.05$); differences observed between FS-90 and CON or FS-30 group means were not significant. Leptin is a hunger-suppressing hormone that is upregulated by inflammation [38]; leptin levels were elevated in FS-30 group compared to FS-10 ($p < 0.05$), but there were no significant differences between other doses. CXCL5 attracts and activates neutrophils [39] and was reduced in FS-90 sera compared to CON ($p < 0.05$). Levels of CXCL2 (C-X-C motif chemokine 2) and vascular endothelial growth factor (VEGF) were lower in FS-30 sera compared to CON ($p < 0.05$), but there were no differences among the other dose groups.

4.3.6. Alterations to Liver Zinc and Copper

Zinc and copper concentrations were quantified in liver, spleen, kidney, PFC, ST, HP, and CE (Figure 4). Only liver zinc and copper concentrations were altered by iron dose; zinc and copper were unaffected by iron in all other tissues. Liver zinc increased with all iron doses ($p < 0.01$), whereas liver copper decreased only with FS-90, the highest iron dose, compared to CON ($p < 0.0001$). Indeed, in the FS-90 livers, zinc concentration was 2-fold that of CON, and copper concentration was one-third that of CON.

4.4. DISCUSSION

Iron, the trace mineral, is essential for growth and metabolism, but excess intake of iron is toxic. Although beneficial to many infants, supplemental iron (SI) provided to iron-replete infants can be detrimental to growth and cognitive development. Iron may disrupt growth by injuring developing tissue through iron overload-related toxicity. Another possibility is that excess iron interrupts the metabolism and transport of other trace minerals that are essential for normal growth. To investigate mechanisms of growth disruption, pre-weanling Lewis rat litters were supplemented from postnatal day (PD) 2 to 10 with excess FS iron doses (10, 30, or 90 mg iron/kg BW) or vehicle control (CON), and growth, tissue iron loading, systemic inflammation, and trace mineral status outcomes were assessed. Pups in the FS-90 group failed to thrive compared to CON; however, FS-30 and FS-10 pups gained weight similarly to CON. The liver was by far the most impacted by iron loading in all FS groups, and the greatest liver iron levels were measured in the FS-90 group. Delay in weight gain and lower brain weights in the FS-90 group may have been associated with liver damage, inflammatory signaling, and altered trace mineral metabolism. Finally, brain weight effects in the FS-90 group did not relate to liver or brain iron levels—suggesting that adverse long-term cognitive-behavioral effects of excess iron may not be related to early brain iron exposure, as previously suspected.

Studies from our group and others show that intestinal iron absorption is elevated during the pre-weanling developmental stage [28,36,40,41], and this makes them more susceptible to iron toxicity. The LD50 for ferrous sulfate in adult rats is estimated to be 780-1100 mg iron/kg BW [42,43]. Excess dosing reduced body weight in surviving adult rats [43]. In comparison, few studies have reported the pre-weanling growth response to excess iron dosing. Considering the elevated absorption in pre-weanling animals, it seems likely that they would be more susceptible to iron toxicity. We report that 90 mg iron/kg BW as FS is sufficient to disrupt growth in Lewis rat pups (Figure 1). Our finding that 10 mg iron/kg BW does not impact weight gain in pre-weanling rats is consistent with our previous study [31]. Other studies in pre-weanling rats did not observe effects on weight gain with 30 or 150 ug per day as

FS, nor with up to 30 mg iron/kg BW as ferrous succinate [40,44,45]. In Holstein calves, weight gain was reduced for those receiving formula fortified with 5000 µg iron/g formula as FS, but not with 2000, 1000, 500, or 100 µg iron/g formula [46]. Another study supplied up to 50 mg iron/kg BW daily as FS to pre-weanling piglets, but weight gain up to weaning was unaffected [28]. Similarly, weight gain was unaffected in piglets that received 8 or 24 mg iron per day as ferric citrate [47]. In our study, brain weight was reduced in the FS-90 group, but not in the other iron groups. Other studies have not measured brain weight following excess iron exposure in pre-weanling animals. In one previous study from our group, FS-10 treatment increased brain weight in pre-weanling rats supplemented up to PD 14 [31]. These results reflect the conclusions of previous experiments in pre-weanling animals, that growth and brain development outcomes of iron supplementation depend on the iron dose. Additionally, the dose that disrupts normal pre-weanling rat growth may be substantially lower than the toxic doses reported for adult rats. Additional experiments would help to define growth and mortality cutoffs for FS at this age.

Whether or not iron absorption is elevated in pre-weanling animals, excess intake might lead to toxic iron loading in developing organs. In our FS dosing experiment, the liver was most affected by iron loading. Spleen and kidney iron levels increased moderately in the FS-30 and FS-90 groups, while iron levels in the brain were similar in all groups. With consideration to the reduced brain weight effects in the FS-90 group, it remains plausible that excess FS disrupts brain development without changing iron levels in major regions of the brain. With the exception of the liver, body iron homeostasis prevents iron loading in most organs. Hepatocytes store excess body iron and produce hepcidin, a hormone that protects against iron overload by suppressing intestinal iron absorption and reducing iron levels in circulation [48]. Current liver iron loading results, as well as a previous iron radioisotope tracing experiment from our group [40], are evidence that hepatocyte iron regulation is intact, and that the liver

takes up most of the excess body iron stores. It remains probable that growth and development outcomes in the FS-90 group are related to excess liver iron loading.

Damage to the liver due to iron loading during early development might explain the growth wasting effects. The highest scores of steatoses and fibrosis were observed in the FS-90 group; however, higher inflammation scores were observed in the FS-30 and CON groups. These findings suggest that FS-10 was protective against inflammation and liver injury, while FS-30 and FS-90 promoted inflammation and liver injury. The reason for the high inflammation scores in CON livers remains unclear, but this outcome is discussed in more detail below as a potential weakness of the study. Few other studies have assessed liver injury and inflammation in rats or mice following excess iron provision during the pre-weanling period. Studies on human hemochromatosis provide some insight surrounding the pathological manifestations of liver iron overload. Genetic hemochromatosis is a liver iron overload disease caused by various mutations resulting in hepcidin deficiency [49]. Histopathological evaluation of hemochromatosis liver samples linked liver iron level to manifestations of liver injury, including necrosis, inflammation, and fibrosis [50]. Future experiments could seek to establish iron status cutoffs that predict the risk for liver injury in pre-weanling animals.

Hemoglobin and hematocrit levels were similar to other values reported at this age [51,52] and were not impacted by excess iron at PD 10, in contrast to previous results from our group [31,45,53]. The FS-30 group had higher MCH values than FS-10, but there was no significant effects among groups for any other RBC parameter (Table 1). [31]. Among the previous studies from our group that found increased hemoglobin with iron, only one measured hemoglobin at PD 10, and the others measured effects at PD 15 and PD 21 [31,45,53]. Another study found no effect on hemoglobin, RBC, or MCV with iron at PD 12 [52]. RBC maturation and concentration increases with postnatal age [51], so it may be likely that iron has a greater impact on these parameters as postnatal age increases. Pigs are at greater risk of anemia than other animal models and require pre-weanling iron injections for normal growth.

Iron supplementation of pre-weanling piglets has consistently increased hemoglobin and hematocrit in controlled experiments [28,54–56]. Iron supplementation experiments in calves and foals have more mixed hematology results [46,57,58]. In addition to model species, variations in study design may result in different effects on hematological parameters, such as the dose and form of iron supplement. Future studies might clarify whether excess iron promotes hematopoiesis in pre-weanling animals. In addition to hematological parameters, measuring plasma iron and transferrin saturation levels in future studies would indicate availability of iron for RBC precursors.

Elevated WBC and neutrophil counts in the FS-90 group indicate systemic inflammation. However, an acute phase response was not observed in serum cytokines and chemokines changes. Elevated serum CCL2, a pro-inflammatory cytokine, was observed in the FS-90 group and CCL2 has been shown to promote steatosis during liver injury [59]. Additionally, CXCL5 was reduced in FS-90 sera vs. CON. Lower serum levels were observed in humans with chronic liver disease, and lower CXCL5 was associated with more severe necroinflammation and fibrosis [60]. Experiments in CXCL5-KO mice demonstrate that CXCL5 enhances neutrophil recruitment toward injured lung tissue by blocking pro-inflammatory chemokine scavenging from circulation [61]. Lower serum CX3CL1 was observed in both the FS-30 group and FS-90 group. Previous research indicates that CX3CL1 is upregulated in hepatocytes and hepatic stellate cells due to liver injury and becomes elevated in serum [62]. This report conflicts with our findings, and we did not measure liver inflammatory gene expression in the present study. To our knowledge, no other studies have reported serum chemokine and cytokine expression following excess iron at this developmental stage. Future studies could evaluate the inflammatory response of hepatocytes, stellate cells, and invading immune cells to identify likely inflammatory signaling mechanisms to explain how excess iron affects early growth wasting.

As mentioned previously, it is also possible that growth wasting outcomes of excess iron are due to mineral interactions. Previous experiments in humans have indicated providing excess iron to infants

may compromise their metabolism and uptake of other essential trace minerals [12,24,63,64], and another study from our group showed that trace mineral stores are impacted by excess iron supplementation [40]. Diverging effects were observed for liver zinc and copper levels with excess iron in the previous study and the present study (Figure 4). Liver zinc was elevated in all FS groups, with the highest levels observed in the FS-90 group. In contrast, liver copper levels were reduced only in the FS-90 group. In the previous study, liver zinc was elevated at PD 10 due to excess FS. In the same study liver copper levels were reduced in the highest FS dose group, while spleen and brain zinc and copper levels were unaffected [40]. Two other studies observed lower serum and tissue copper levels in weanling rats fed excess iron [65,66]. Yet another study in weanling rats did not observe changes in liver copper but found elevated liver zinc and manganese [67]. Liver copper levels and weight gain were reduced in weanling mice that consumed excess iron. The authors noted that copper absorption was not impaired by excess iron; instead, they concluded that copper utilization was disrupted in these mice [68]. Metabolism of iron, zinc, and copper, as well as metabolic interactions among these minerals, may be altered under various states of inflammation, so altered zinc and copper stores in the liver due to excess iron may be the result of local or systemic inflammatory signaling [69,70]. In summary, current and previous evidence indicates that growth wasting outcomes of excess iron may be due to disruptions to zinc or copper metabolism. Furthermore, it is likely that some changes to mineral metabolism are secondary to liver injury and inflammatory signaling.

Iron loading induces the expression of metallothionein (MT), a cellular zinc-binding protein that can also bind copper [71,72]. Specifically, iron upregulates Zip8 and Zip14, which preferentially transport zinc and iron at physiological pH [72]. It is likely that zinc levels in the liver are elevated following FS supplementation due to increased zinc importing and binding activities by these proteins as a result of iron loading. Inflammatory cytokines and chemokines also induce MT expression to sequester zinc and in the liver. Iron and zinc loading due to systemic inflammation would further induce expression of MT

and ZIP proteins, exacerbating iron overload toxicity and compromising the availability of zinc for other growing tissues [71]. Related to growth outcomes, MT-zinc complexes that enter mitochondria can disrupt electron transport chain activities and slow energy production by oxidative phosphorylation [73]. Considering the overlapping impacts of excess iron and inflammation, it may be reasoned that the ongoing iron loading in the liver, injuries induced by iron toxicity, systemic inflammation-induced metal sequestration in the liver, and disruption to zinc metabolism are all contributing to growth wasting in excess iron supplemented rats. The lower levels of liver copper observed with increasing iron doses are likely a consequence of iron decreasing the uptake of copper into the liver; a competitive iron-copper interaction at the level of cellular uptake has been described [74]. The lower level of copper, in turn, is likely to decrease the activity of CuZn-SOD and consequently the protection against free radical-mediated adverse effects.

This study has several strengths, including supplementation design, dosing, and number of pups/litters assessed. The results strengthen previous hypotheses that excess iron disrupts growth and trace mineral metabolism in pre-weanling animal growth and development and provide new data on brain iron and trace mineral loading effects, hematology, and chemokine/cytokine expression. One important limitation to note is regarding the liver pathology results reported of the vehicle control (CON) group. We were surprised to see mild inflammation, steatosis, fibrosis, and necrosis in many of the pups in this group. Liver injury may have resulted from stress due to handling, however, since handling was kept to a brief 2-5 min period per day, this seemed unlikely. Alternatively, it seemed possible that sucrose in the vehicle solution may have adverse effects on the developing liver. As it turns out, previous studies do show that liver injury may arise from early life sucrose exposure [75,76], That being said, much higher doses of sucrose were provided in these studies than the amount we provided in our daily supplement volumes. Regardless, the findings demand that future investigations employing this model include additional control groups: an un-supplemented control group as well as a control

group that receives only water without sucrose, in order to test for both sucrose and the effects of handling on liver injury and inflammation.

Excess daily iron supplementation at 90 mg iron/kg BW as FS is disruptive to weight gain in pre-weanling rats. Growth wasting was related to excess iron loading, but reduced brain weight was not related to changes in brain iron levels. Iron loading in the liver following excess FS may cause liver damage and inflammation and may disrupt zinc and copper metabolism. The results suggest liver damage, inflammation, and mineral interactions may be involved in the growth wasting outcomes of excess iron in pre-weanling rats.

4.5. REFERENCES

1. Kassebaum, N.J. The Global Burden of Anemia. *Hematology/Oncology Clinics of North America* **2016**, *30*, 247–308, doi:10.1016/j.hoc.2015.11.002.
2. Zimmermann, M.B.; Hurrell, R.F. Nutritional Iron Deficiency. *Lancet* **2007**, *370*, 511–520, doi:10.1016/S0140-6736(07)61235-5.
3. East, P.; Doom, J.R.; Blanco, E.; Burrows, R.; Lozoff, B.; Gahagan, S. Iron Deficiency in Infancy and Neurocognitive and Educational Outcomes in Young Adulthood. *Developmental Psychology* **2021**, *57*, 962–975, doi:10.1037/dev0001030.
4. Black, M.M.; Quigg, A.M.; Hurley, K.M.; Pepper, M.R. Iron Deficiency and Iron-Deficiency Anemia in the First Two Years of Life: Strategies to Prevent Loss of Developmental Potential: Nutrition Reviews©, Vol. 66, No. S1. *Nutrition Reviews* **2011**, *69*, S64–S70, doi:10.1111/j.1753-4887.2011.00435.x.
5. Shelov, S.P.; American Academy of Pediatrics *Caring for Your Baby and Young Child: Birth to Age Five*; Bantam: New York, 2009; ISBN 978-0-553-38630-1.
6. Lonnerdal, B. Excess Iron Intake as a Factor in Growth, Infections, and Development of Infants and Young Children. *Am J Clin Nutr* **2017**, *106*, 1681S-1687S, doi:10.3945/ajcn.117.156042.
7. Wessling-Resnick, M. Excess Iron: Considerations Related to Development and Early Growth. *Am J Clin Nutr* **2017**, *106*, 1600S-1605S, doi:10.3945/ajcn.117.155879.
8. Pasricha, S.-R.; Hayes, E.; Kalumba, K.; Biggs, B.-A. Effect of Daily Iron Supplementation on Health in Children Aged 4-23 Months: A Systematic Review and Meta-Analysis of Randomised Controlled Trials. *Lancet Glob Health* **2013**, *1*, e77–e86, doi:10.1016/S2214-109X(13)70046-9.
9. Paganini, D.; Zimmermann, M.B. The Effects of Iron Fortification and Supplementation on the Gut Microbiome and Diarrhea in Infants and Children: A Review. *Am J Clin Nutr* **2017**, *106*, 1688S-1693S, doi:10.3945/ajcn.117.156067.
10. Hare, D.J.; Cardoso, B.R.; Szymlek-Gay, E.A.; Biggs, B.-A. Neurological Effects of Iron Supplementation in Infancy: Finding the Balance between Health and Harm in Iron-Replete Infants. *The Lancet Child & Adolescent Health* **2018**, *2*, 144–156, doi:10.1016/S2352-4642(17)30159-1.
11. Dewey, K.G.; Domellöf, M.; Cohen, R.J.; Landa Rivera, L.; Hernell, O.; Lönnerdal, B. Iron Supplementation Affects Growth and Morbidity of Breast-Fed Infants: Results of a Randomized

Trial in Sweden and Honduras. *The Journal of Nutrition* **2002**, *132*, 3249–3255, doi:10.1093/jn/132.11.3249.
12. Lind, T.; Seswandhana, R.; Persson, L.-A.; Lönnerdal, B. Iron Supplementation of Iron-Replete Indonesian Infants Is Associated with Reduced Weight-for-Age. *Acta Paediatr* **2008**, *97*, 770–775, doi:10.1111/j.1651-2227.2008.00773.x.
13. Lozoff, B. Iron-Fortified vs Low-Iron Infant Formula: Developmental Outcome at 10 Years. *Arch Pediatr Adolesc Med* **2012**, *166*, 208, doi:10.1001/archpediatrics.2011.197.
14. Sazawal, S.; Black, R.E.; Ramsan, M.; Chwaya, H.M.; Stoltzfus, R.J.; Dutta, A.; Dhingra, U.; Kabole, I.; Deb, S.; Othman, M.K.; et al. Effects of Routine Prophylactic Supplementation with Iron and Folic Acid on Admission to Hospital and Mortality in Preschool Children in a High Malaria Transmission Setting: Community-Based, Randomised, Placebo-Controlled Trial. *Lancet* **2006**, *367*, 133–143, doi:10.1016/S0140-6736(06)67962-2.
15. Moya-Alvarez, V.; Cottrell, G.; Ouédraogo, S.; Accrombessi, M.; Massougbodgi, A.; Cot, M. High Iron Levels Are Associated with Increased Malaria Risk in Infants during the First Year of Life in Benin. *Am J Trop Med Hyg* **2017**, *97*, 497–503, doi:10.4269/ajtmh.16-0001.
16. Dietary Guidelines Advisory Committee *Scientific Report of the 2020 Dietary Guidelines Advisory Committee: Advisory Report to the Secretary of Agriculture and the Secretary of Health and Human Services*; U.S. Department of Agriculture, Agricultural Research Service: Washington, DC, 2020; p. 786;.
17. Cai, C.; Granger, M.; Eck, P.; Friel, J. Effect of Daily Iron Supplementation in Healthy Exclusively Breastfed Infants: A Systematic Review with Meta-Analysis. *Breastfeed Med* **2017**, *12*, 597–603, doi:10.1089/bfm.2017.0003.
18. Brannon, P.M.; Stover, P.J.; Taylor, C.L. Integrating Themes, Evidence Gaps, and Research Needs Identified by Workshop on Iron Screening and Supplementation in Iron-Replete Pregnant Women and Young Children. *Am J Clin Nutr* **2017**, *106*, 1703S-1712S, doi:10.3945/ajcn.117.156083.
19. Majumdar, I.; Paul, P.; Talib, V.H.; Ranga, S. The Effect of Iron Therapy on the Growth of Iron-Replete and Iron-Deplete Children. *J Trop Pediatr* **2003**, *49*, 84–88, doi:10.1093/tropej/49.2.84.
20. Petry, N.; Olofin, I.; Boy, E.; Donahue Angel, M.; Rohner, F. The Effect of Low Dose Iron and Zinc Intake on Child Micronutrient Status and Development during the First 1000 Days of Life: A Systematic Review and Meta-Analysis. *Nutrients* **2016**, *8*, doi:10.3390/nu8120773.
21. Gahagan, S.; Yu, S.; Kaciroti, N.; Castillo, M.; Lozoff, B. Linear and Ponderal Growth Trajectories in Well-Nourished, Iron-Sufficient Infants Are Unimpaired by Iron Supplementation. *J Nutr* **2009**, *139*, 2106–2112, doi:10.3945/jn.108.100735.
22. Björmsjö, M.; Hernell, O.; Lönnerdal, B.; Berglund, S.K. Reducing Iron Content in Infant Formula from 8 to 2 Mg/L Does Not Increase the Risk of Iron Deficiency at 4 or 6 Months of Age: A Randomized Controlled Trial. *Nutrients* **2020**, *13*, 3, doi:10.3390/nu13010003.
23. Domellöf, M.; Dewey, K.G.; Cohen, R.J.; Lönnerdal, B.; Hernell, O. Iron Supplements Reduce Erythrocyte Copper-Zinc Superoxide Dismutase Activity in Term, Breastfed Infants. *Acta Paediatr* **2005**, *94*, 1578–1582, doi:10.1080/08035250500252674.
24. Wieringa, F.T.; Berger, J.; Dijkhuizen, M.A.; Hidayat, A.; Ninh, N.X.; Utomo, B.; Wasantwisut, E.; Winichagoon, P. Combined Iron and Zinc Supplementation in Infants Improved Iron and Zinc Status, but Interactions Reduced Efficacy in a Multicountry Trial in Southeast Asia. *J Nutr* **2007**, *137*, 466–471, doi:10.1093/jn/137.2.466.
25. Haschke, F.; Ziegler, E.E.; Edwards, B.B.; Fomon, S.J. Effect of Iron Fortification of Infant Formula on Trace Mineral Absorption: *Journal of Pediatric Gastroenterology and Nutrition* **1986**, *5*, 768–773, doi:10.1097/00005176-198609000-00018.
26. Lönnerdal, B. Trace Element Nutrition of Infants--Molecular Approaches. *J Trace Elem Med Biol* **2005**, *19*, 3–6, doi:10.1016/j.jtemb.2005.03.004.

27. Gahagan, S.; Delker, E.; Blanco, E.; Burrows, R.; Lozoff, B. Randomized Controlled Trial of Iron-Fortified versus Low-Iron Infant Formula: Developmental Outcomes at 16 Years. *J Pediatr* **2019**, *212*, 124-130.e1, doi:10.1016/j.jpeds.2019.05.030.
28. Ji, P.; Lonnerdal, B.; Kim, K.; Jinno, C.N. Iron Oversupplementation Causes Hippocampal Iron Overloading and Impairs Social Novelty Recognition in Nursing Piglets. *J Nutr* **2019**, *149*, 398–405, doi:10.1093/jn/nxy227.
29. Ji, P.; B Nonnecke, E.; Doan, N.; Lönnerdal, B.; Tan, B. Excess Iron Enhances Purine Catabolism Through Activation of Xanthine Oxidase and Impairs Myelination in the Hippocampus of Nursing Piglets. *J Nutr* **2019**, *149*, 1911–1919, doi:10.1093/jn/nxz166.
30. Hare, D.J.; Braat, S.; Cardoso, B.R.; Morgan, C.; Szymlek-Gay, E.A.; Biggs, B.-A. Health Outcomes of Iron Supplementation and/or Food Fortification in Iron-Replete Children Aged 4–24 Months: Protocol for a Systematic Review and Meta-Analysis. *Syst Rev* **2019**, *8*, 253, doi:10.1186/s13643-019-1185-3.
31. McMillen, S.; Lönnerdal, B. Postnatal Iron Supplementation with Ferrous Sulfate vs. Ferrous Bis-Glycinate Chelate: Effects on Iron Metabolism, Growth, and Central Nervous System Development in Sprague Dawley Rat Pups. *Nutrients* **2021**, *13*, 1406, doi:10.3390/nu13051406.
32. National Research Council (US) Subcommittee on Laboratory Animal Nutrition In *Nutrient Requirements of Laboratory Animals*; National Academies Press (US).
33. Torrance, J.D.; Bothwell, T.H. A Simple Technique for Measuring Storage Iron Concentrations in Formalinised Liver Samples. *S Afr J Med Sci* **1968**, *33*, 9–11.
34. Liang, W.; Menke, A.L.; Driessen, A.; Koek, G.H.; Lindeman, J.H.; Stoop, R.; Havekes, L.M.; Kleemann, R.; van den Hoek, A.M. Establishment of a General NAFLD Scoring System for Rodent Models and Comparison to Human Liver Pathology. *PLoS ONE* **2014**, *9*, e115922, doi:10.1371/journal.pone.0115922.
35. Li, Y.; Yu, P.; Chang, S.-Y.; Wu, Q.; Yu, P.; Xie, C.; Wu, W.; Zhao, B.; Gao, G.; Chang, Y.-Z. Hypobaric Hypoxia Regulates Brain Iron Homeostasis in Rats: H YPOBARIC H YPOXIA R EGULATES I RON H OMEOSTASIS. *J. Cell. Biochem.* **2017**, *118*, 1596–1605, doi:10.1002/jcb.25822.
36. Darshan, D.; Wilkins, S.J.; Frazer, D.M.; Anderson, G.J. Reduced Expression of Ferroportin-1 Mediates Hyporesponsiveness of Suckling Rats to Stimuli That Reduce Iron Absorption. *Gastroenterology* **2011**, *141*, 300–309, doi:10.1053/j.gastro.2011.04.012.
37. Nemes-Baran, A.D.; White, D.R.; DeSilva, T.M. Fractalkine-Dependent Microglial Pruning of Viable Oligodendrocyte Progenitor Cells Regulates Myelination. *Cell Reports* **2020**, *32*, 108047, doi:10.1016/j.celrep.2020.108047.
38. Abella, V.; Scotece, M.; Conde, J.; Pino, J.; Gonzalez-Gay, M.A.; Gómez-Reino, J.J.; Mera, A.; Lago, F.; Gómez, R.; Gualillo, O. Leptin in the Interplay of Inflammation, Metabolism and Immune System Disorders. *Nat Rev Rheumatol* **2017**, *13*, 100–109, doi:10.1038/nrrheum.2016.209.
39. Persson, T.; Monsef, N.; Andersson, P.; Bjartell, A.; Malm, J.; Calafat, J.; Egesten, A. Expression of the Neutrophil-Activating CXC Chemokine ENA-78/CXCL5 by Human Eosinophils: CXCL5 Expression by Eosinophils. *Clinical & Experimental Allergy* **2003**, *33*, 531–537, doi:10.1046/j.1365-2222.2003.01609.x.
40. Leong, W.-I.; Bowlus, C.L.; Tallkvist, J.; Lönnerdal, B. Iron Supplementation during Infancy—Effects on Expression of Iron Transporters, Iron Absorption, and Iron Utilization in Rat Pups. *The American Journal of Clinical Nutrition* **2003**, *78*, 1203–1211, doi:10.1093/ajcn/78.6.1203.
41. Frazer, D.M.; Wilkins, S.J.; Darshan, D.; Mirciov, C.S.G.; Dunn, L.A.; Anderson, G.J. Ferroportin Is Essential for Iron Absorption During Suckling, But Is Hyporesponsive to the Regulatory Hormone Hepcidin. *Cellular and Molecular Gastroenterology and Hepatology* **2017**, *3*, 410–421, doi:10.1016/j.jcmgh.2016.12.002.

42. Weaver, L.C.; Gardier, R.W.; Robinson, V.B.; Bunde, C.A. Comparative Toxicology of Iron Compounds. *Am J Med Sci* **1961**, *241*, 262–302.
43. Whittaker, P.; Ali, S.F.; Imam, S.Z.; Dunkel, V.C. Acute Toxicity of Carbonyl Iron and Sodium Iron EDTA Compared with Ferrous Sulfate in Young Rats. *Regulatory Toxicology and Pharmacology* **2002**, *36*, 280–286, doi:10.1006/rtph.2002.1577.
44. Schröder, N.; Fredriksson, A.; Vianna, M.R.; Roesler, R.; Izquierdo, I.; Archer, T. Memory Deficits in Adult Rats Following Postnatal Iron Administration. *Behav Brain Res* **2001**, *124*, 77–85, doi:10.1016/s0166-4328(01)00236-4.
45. Alexeev, E.E.; He, X.; Slupsky, C.M.; Lönnerdal, B. Effects of Iron Supplementation on Growth, Gut Microbiota, Metabolomics and Cognitive Development of Rat Pups. *PLoS One* **2017**, *12*, e0179713, doi:10.1371/journal.pone.0179713.
46. Jenkins, K.J.; Hidiroglou, M. Effect of Excess Iron in Milk Replacer on Calf Performance. *J Dairy Sci* **1987**, *70*, 2349–2354, doi:10.3168/jds.S0022-0302(87)80295-3.
47. Furugouri, K.; Kawabata, A. Iron Absorption in Nursing Piglets. *J Anim Sci* **1975**, *41*, 1348–1354, doi:10.2527/jas1975.4151348x.
48. Wang, C.-Y.; Babitt, J.L. Liver Iron Sensing and Body Iron Homeostasis. *Blood* **2019**, *133*, 18–29, doi:10.1182/blood-2018-06-815894.
49. Pietrangelo, A. Hereditary Hemochromatosis. *Annu. Rev. Nutr.* **2006**, *26*, 251–270, doi:10.1146/annurev.nutr.26.061505.111226.
50. Deugnier, Y.M.; Loréal, O.; Turlin, B.; Guyader, D.; Jouanolle, H.; Moirand, R.; Jacquelinet, C.; Brissot, P. Liver Pathology in Genetic Hemochromatosis: A Review of 135 Homozygous Cases and Their Bioclinical Correlations. *Gastroenterology* **1992**, *102*, 2050–2059, doi:10.1016/0016-5085(92)90331-R.
51. Sewald, K.; Mueller, M.; Buschmann, J.; Hansen, T.; Lewin, G. Development of Hematological and Immunological Characteristics in Neonatal Rats. *Reproductive Toxicology* **2015**, *56*, 109–117, doi:10.1016/j.reprotox.2015.05.019.
52. Dubuque, S.H.; Dvorak, B.; Woodward, S.S.; McCuskey, R.S.; Kling, P.J. Iron-Deficient Erythropoiesis in Neonatal Rats. *Biol Neonate* **2002**, *81*, 51–57, doi:10.1159/000047184.
53. Leong, W.-I.; Bowlus, C.L.; Tallkvist, J.; Lönnerdal, B. DMT1 and FPN1 Expression during Infancy: Developmental Regulation of Iron Absorption. *American Journal of Physiology-Gastrointestinal and Liver Physiology* **2003**, *285*, G1153–G1161, doi:10.1152/ajpgi.00107.2003.
54. Perng, V.; Li, C.; Klocke, C.R.; Navazesh, S.E.; Pinneles, D.K.; Lein, P.J.; Ji, P. Iron Deficiency and Iron Excess Differently Affect Dendritic Architecture of Pyramidal Neurons in the Hippocampus of Piglets. *J Nutr* **2021**, *151*, 235–244, doi:10.1093/jn/nxaa326.
55. Egeli, A.K.; Framstad, T. Effect of an Oral Starter Dose of Iron on Haematology and Weight Gain in Piglets Having Voluntary Access to Glutamic Acid-Chelated Iron Solution. *Acta Vet Scand* **1998**, *39*, 359–365.
56. Dong, Z.; Wan, D.; Li, G.; Zhang, Y.; Yang, H.; Wu, X.; Yin, Y. Comparison of Oral and Parenteral Iron Administration on Iron Homeostasis, Oxidative and Immune Status in Anemic Neonatal Pigs. *Biol Trace Elem Res* **2020**, *195*, 117–124, doi:10.1007/s12011-019-01846-9.
57. Eisa, A.M.A.; Elgebaly, L.S. Effect of Ferrous Sulphate on Haematological, Biochemical and Immunological Parameters in Neonatal Calves. *Vet Ital* **2010**, *46*, 329–335.
58. Kohn, C.W.; Jacobs, R.M.; Knight, D.; Hueston, W.; Gabel, A.A.; Reed, S.M. Microcytosis, Hypoferremia, Hypoferritemia, and Hypertransferrinemia in Standardbred Foals from Birth to 4 Months of Age. *Am J Vet Res* **1990**, *51*, 1198–1205.
59. Baeck, C.; Wehr, A.; Karlmark, K.R.; Heymann, F.; Vucur, M.; Gassler, N.; Huss, S.; Klussmann, S.; Eulberg, D.; Luedde, T.; et al. Pharmacological Inhibition of the Chemokine CCL2 (MCP-1)

Diminishes Liver Macrophage Infiltration and Steatohepatitis in Chronic Hepatic Injury. *Gut* **2012**, *61*, 416–426, doi:10.1136/gutjnl-2011-300304.
60. Tacke, F.; Zimmermann, H.W.; Trautwein, C.; Schnabl, B. CXCL5 Plasma Levels Decrease in Patients with Chronic Liver Disease: CXCL5 Plasma Levels in Liver Disease. *Journal of Gastroenterology and Hepatology* **2011**, *26*, 523–529, doi:10.1111/j.1440-1746.2010.06436.x.
61. Mei, J.; Liu, Y.; Dai, N.; Favara, M.; Greene, T.; Jeyaseelan, S.; Poncz, M.; Lee, J.S.; Worthen, G.S. CXCL5 Regulates Chemokine Scavenging and Pulmonary Host Defense to Bacterial Infection. *Immunity* **2010**, *33*, 106–117, doi:10.1016/j.immuni.2010.07.009.
62. Shimoda, S.; Harada, K.; Niiro, H.; Taketomi, A.; Maehara, Y.; Tsuneyama, K.; Kikuchi, K.; Nakanuma, Y.; Mackay, I.R.; Gershwin, M.E.; et al. CX3CL1 (Fractalkine): A Signpost for Biliary Inflammation in Primary Biliary Cirrhosis. *Hepatology* **2010**, *51*, 567–575, doi:10.1002/hep.23318.
63. Lind, T.; Lönnerdal, B.; Stenlund, H.; Gamayanti, I.L.; Ismail, D.; Seswandhana, R.; Persson, L.-A. A Community-Based Randomized Controlled Trial of Iron and Zinc Supplementation in Indonesian Infants: Effects on Growth and Development. *Am J Clin Nutr* **2004**, *80*, 729–736, doi:10.1093/ajcn/80.3.729.
64. Lind, T.; Lönnerdal, B.; Stenlund, H.; Ismail, D.; Seswandhana, R.; Ekström, E.-C.; Persson, L.-A. A Community-Based Randomized Controlled Trial of Iron and Zinc Supplementation in Indonesian Infants: Interactions between Iron and Zinc. *Am J Clin Nutr* **2003**, *77*, 883–890, doi:10.1093/ajcn/77.4.883.
65. Klevay, L.M. Iron Overload Can Induce Mild Copper Deficiency. *Journal of Trace Elements in Medicine and Biology* **2001**, *14*, 237–240, doi:10.1016/S0946-672X(01)80009-2.
66. Ha, J.-H.; Doguer, C.; Wang, X.; Flores, S.R.; Collins, J.F. High-Iron Consumption Impairs Growth and Causes Copper-Deficiency Anemia in Weanling Sprague-Dawley Rats. *PLoS ONE* **2016**, *11*, e0161033, doi:10.1371/journal.pone.0161033.
67. Vayenas, D.V.; Repanti, M.; Vassilopoulos, A.; Papanastasiou, D.A. Influence of Iron Overload on Manganese, Zinc, and Copper Concentration in Rat Tissues in Vivo: Study of Liver, Spleen, and Brain. *Int J Clin Lab Res* **1998**, *28*, 183–186, doi:10.1007/s005990050041.
68. Ha, J.-H.; Doguer, C.; Collins, J.F. Consumption of a High-Iron Diet Disrupts Homeostatic Regulation of Intestinal Copper Absorption in Adolescent Mice. *American Journal of Physiology-Gastrointestinal and Liver Physiology* **2017**, *313*, G353–G360, doi:10.1152/ajpgi.00169.2017.
69. DiSilvestro, R.A.; Marten, J.T. Effects of Inflammation and Copper Intake on Rat Liver and Erythrocyte Cu-Zn Superoxide Dismutase Activity Levels. *The Journal of Nutrition* **1990**, *120*, 1223–1227, doi:10.1093/jn/120.10.1223.
70. Liuzzi, J.P.; Lichten, L.A.; Rivera, S.; Blanchard, R.K.; Aydemir, T.B.; Knutson, M.D.; Ganz, T.; Cousins, R.J. Interleukin-6 Regulates the Zinc Transporter Zip14 in Liver and Contributes to the Hypozincemia of the Acute-Phase Response. *Proc. Natl. Acad. Sci. U.S.A.* **2005**, *102*, 6843–6848, doi:10.1073/pnas.0502257102.
71. Lynes, M.A.; Hidalgo, J.; Manso, Y.; Devisscher, L.; Laukens, D.; Lawrence, D.A. Metallothionein and Stress Combine to Affect Multiple Organ Systems. *Cell Stress and Chaperones* **2014**, *19*, 605–611, doi:10.1007/s12192-014-0501-z.
72. Wang, C.-Y.; Jenkitkasemwong, S.; Duarte, S.; Sparkman, B.K.; Shawki, A.; Mackenzie, B.; Knutson, M.D. ZIP8 Is an Iron and Zinc Transporter Whose Cell-Surface Expression Is Up-Regulated by Cellular Iron Loading. *Journal of Biological Chemistry* **2012**, *287*, 34032–34043, doi:10.1074/jbc.M112.367284.
73. Koh, J.-Y.; Lee, S.-J. Metallothionein-3 as a Multifunctional Player in the Control of Cellular Processes and Diseases. *Mol Brain* **2020**, *13*, 116, doi:10.1186/s13041-020-00654-w.
74. Arredondo, M.; Martínez, R.; Núñez, M.T.; Ruz, M.; Olivares, M. Inhibition of Iron and Copper Uptake by Iron, Copper and Zinc. Biol. Res. **2006**, 39, doi:10.4067/S0716-97602006000100011.

75. Chicco, A.; Creus, A.; Illesca, P.; Hein, G.J.; Rodriguez, S.; Fortino, A. Effects of Post-Suckling n-3 Polyunsaturated Fatty Acids: Prevention of Dyslipidemia and Liver Steatosis Induced in Rats by a Sucrose-Rich Diet during Pre- and Post-Natal Life. *Food Funct.* **2016**, *7*, 445–454, doi:10.1039/C5FO00705D.
76. D'Alessandro, M.E.; Oliva, M.E.; Fortino, M.A.; Chicco, A. Maternal Sucrose-Rich Diet and Fetal Programming: Changes in Hepatic Lipogenic and Oxidative Enzymes and Glucose Homeostasis in Adult Offspring. *Food Funct.* **2014**, *5*, 446, doi:10.1039/c3fo60436e.

FIGURES

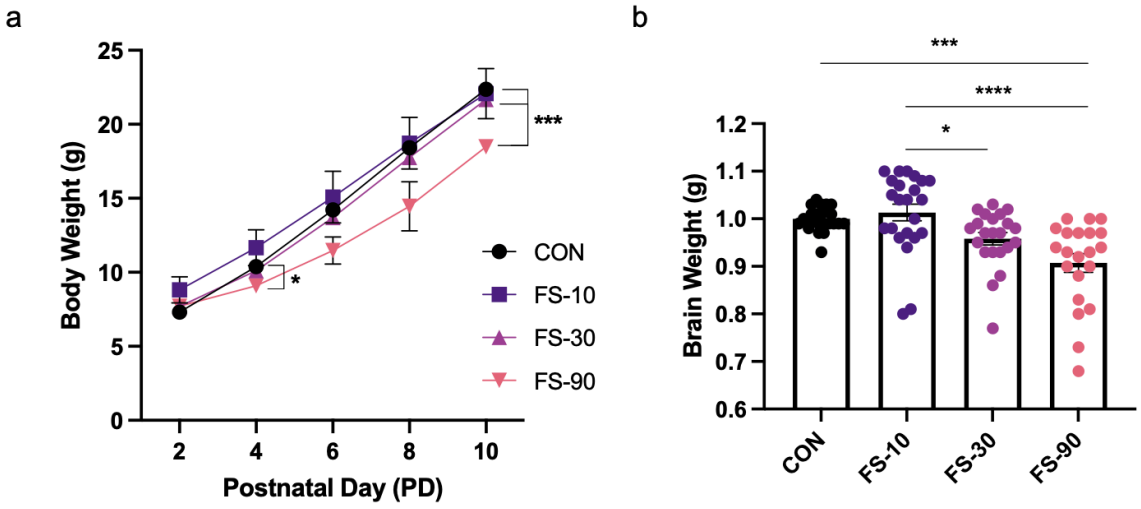

Figure 1. Growth and development are disrupted by excess ferrous sulfate (FS) iron supplementation in pre-weanling rats. (a) Litter weight gain is reduced in FS-90 group across study period—postnatal day (PD) 2-10. Body weight of pups (n = 21-24/group, 3 litters/group) was measured every other day and group means ± SEM are shown. (b) Brain weight at necropsy on PD 10 is reduced with excess FS iron supplementation. Biological replicates (n = 21-24/group, 3 litters/group) are shown as individual data points with mean ± SEM. CON, vehicle control supplementation group; FS-10, 10 mg iron/kg BW; FS-30, 30 mg iron/kg BW; FS-90, 90 mg iron/kg BW. *p*-value summary: *, $p < 0.05$; ***, $p < 0.001$; ****, $p < 0.0001$.

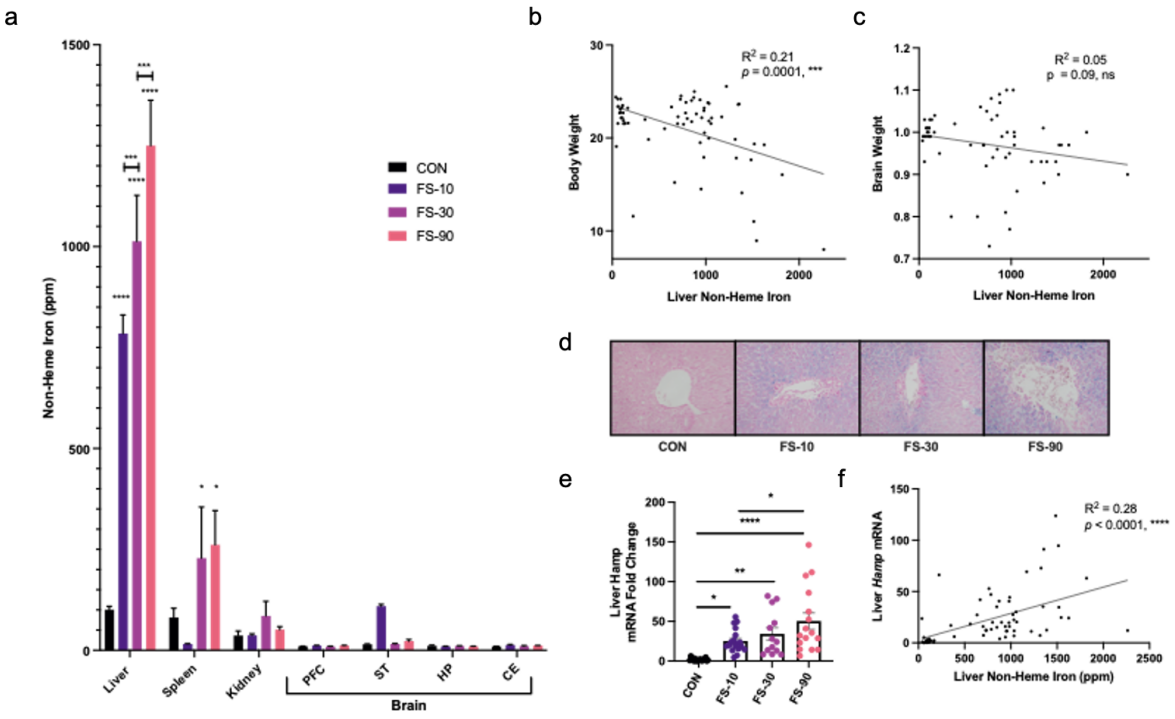

Figure 2. Liver iron loading and hepcidin expression increased with iron dose. (a) Tissue non-heme iron concentration on PD 10 following 8 days of FS dosing from PD 2-9. Data for each tissue (n = 14-18/group, 3 litters/group) are represented as mean ± SEM. (b) Correlation analysis of liver non-heme iron concentration vs. PD 10 body weight and (c) brain weight. (d) Microscope images of Perls' Prussian blue iron-stained liver sections (n=/6 per group), captured with 40x objective lens (representative images shown). (e) Fold-change in liver *Hamp* gene expression, assessed by RT-qPCR. Biological replicates (n = 13-18/group, 3 litters/group) are shown as individual data points with mean ± SEM. (f) Correlation analysis of liver non-heme iron concentration vs. liver *Hamp* expression. *p*-value summary: *, $p < 0.05$; **, $p < 0.01$; ***, $p < 0.001$; ****, $p < 0.0001$.

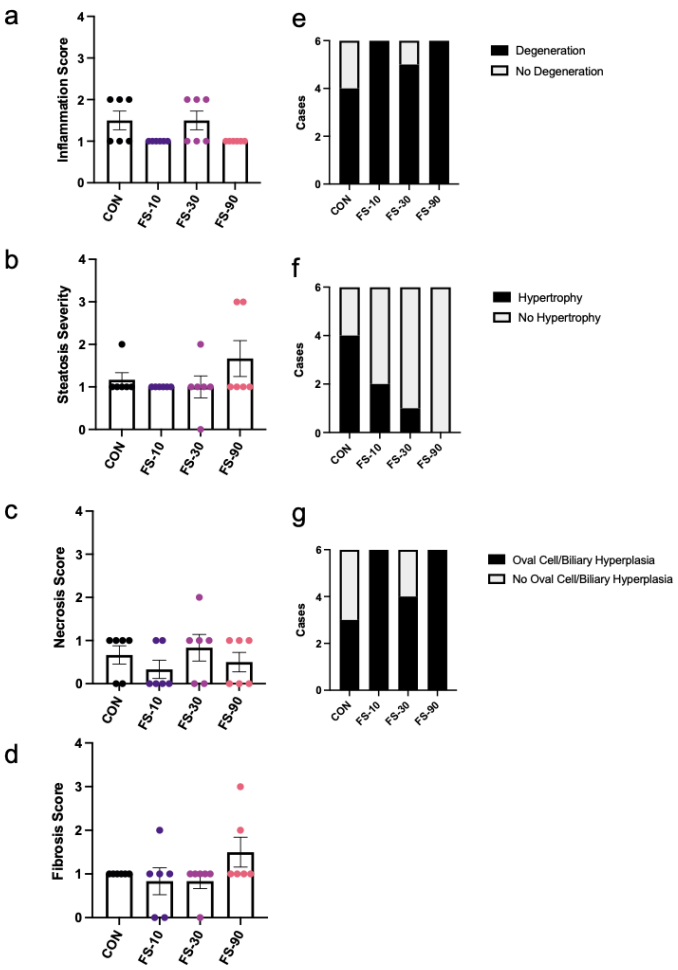

Figure 3. Hepatic inflammation and injury scores from histopathology following excess iron dosing. Scores were assigned by a pathologist blinded to treatment groups. (a-d) Inflammation, steatosis, necrosis, and fibrosis severity scores. Biological replicates (n = 6/group) are shown as individual data points with mean ± SEM. (e-g) Presence of degeneration, hypertrophy, or oval cell/biliary hyperplasia. Data shown as number of cases per group.

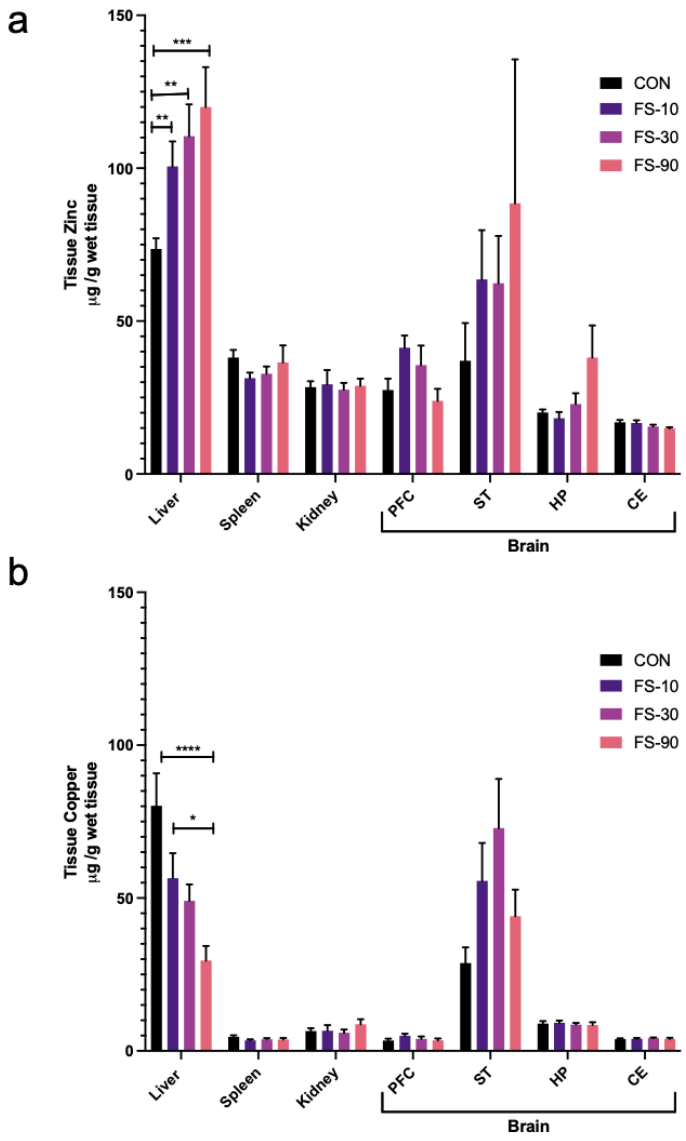

Figure 4. Hepatic zinc and copper levels are altered by excess iron. Tissue zinc (a) and copper (b) were determined with atomic absorption spectroscopy. Data for each tissue (n = 9-18/group, 3 litters/group) are represented as mean ± SEM. *p*-value summary: *, $p < 0.05$; **, $p < 0.01$; ***, $p < 0.001$; ****, $p < 0.0001$.

TABLES

Table 1. Complete blood count (CBC) results.

Result (units)[1]	Group Mean ± Std. Deviation				
	CON	**FS-10**	**FS-30**	**FS-90**	**p-value[2]**
Hemoglobin (g/dL)	8.95 ± 0.44	8.50 ± 0.60	9.15 ± 0.25	9.03 ± 0.31	0.3635
Hematocrit (%)	31.0 ± 2.9	28.3 ± 1.5	30.8 ± 0.50	29.8 ± 3.3	0.4288
RBC (M/µL)	3.62 ± 0.17	3.52 ± 0.23	3.50 ± 0.11	3.50 ± 0.13	0.7836
MCV (fl)	85.5 ± 5.1	80.9 ± 1.4	87.7 ± 2.4	90.4 ± 0.85	0.1436
MCH (pg)[2]	24.8 ± 0.17[a,b]	24.1± 0.25[a]	26.2 ± 0.22[b]	25.8 ± 0.15[a,b]	<0.0001, ****
MCHC (g/dL)	29.1 1.8	29.8 ± 0.60	29.8 ± 0.71	28.6 ± 0.30	0.4185
RDW (%)	20.8 ± 2.2	18.0 ± 1.0	17.3 ± 0.50[†]	17.0 ± 1.0[†]	0.0080, **
WBC/µL	2938 ± 18	4170 ± 110	3403 ± 630	4210 ± 1300	0.1355
WBC/µL (corrected)[2]	2874 ± 19[a]	3910 ± 77[a,b]	3300 ± 640[a,b]	4540 ± 620[b]	0.0095, **
Monocytes (%)	4.75 ± 2.8	6.00 ± 2.7	6.25 ± 2.6	7.25 ± 4.3	0.8003
Monocytes (count)	137 ± 78	244 ± 130	204 ± 81	310 ± 190	0.4937
Lymphocytes (%)	80.0 ± 3.7	78.3 ± 2.5	63.3 ± 30	68.3 ± 6.6	0.0976
Lymphocytes (count)	2300 ± 200	3060 ± 570	2150 ± 1200	2700 ± 610	0.3158
Neutrophils (%)	14.5 ± 2.1	15.0 ± 1.0	29.8 ± 30	23.0 ± 6.9	0.0689
Neutrophils (count)	416 ± 56	589 ± 130	924 ± 82	948 ± 480[†]	0.0486, *

[1]RBC, red blood cells; MCV, mean cell volume; MCH, mean cell hemoglobin; MCHC, mean cell hemoglobin concentration; RDW, red blood cell distribution width; WBC, white blood cells.
[2]Kruskal-Wallis test for effect of FS on mean, n=3-4/group. *p*-value summary: *, $p < 0.05$; **, $p < 0.01$; ****, $p < 0.0001$. [2]Means with different superscripts are significantly different by post-hoc Dunn's test, $p < 0.05$. [†]Comparison to CON mean p-value: $0.08 > p > 0.05$.

Table 2. Serum cytokine and chemokine protein concentrations.

Protein Name	Group Mean (pg/mL) ± Std. Deviation				
	CON	**FS-10**	**FS-30**	**FS-90**	**p-value[1]**
G-CSF	23.5 ± 5.2	23.2 ± 5.9	23.8 ± 4.9	24.1 ± 8.7	0.9907
CCL11	5.44 ± 4.8	5.32 ± 3.9	5.91 ± 4.5	7.19 ± 5.3	0.8525
GM-CSF[2]	9.87 ± 12[a,b]	0.00 ± 0.0[a]	3.98 ± 8.4[a,b]	17.4 ± 21[b]	0.0184, *
IL-1α	226 ± 200	164 ± 120	200 ± 74	289 ± 240	0.4027
Leptin[2]	39800 ± 5500[a,b]	28,800 ± 9,200[a]	55,500 ± 11,000[b]	46,300 ± 38,000[a,b]	0.0445, *
CCL3	63.5 ± 10	49.2 ± 7.7	58.2 ± 11	51.0 ± 18	0.0533
IL-4	0.770 ± 1.6	0.00 ± 0.0	0.385 ± 1.2	1.75 ± 3.2	0.2649
IL-1β	23.6 ± 7.2	18.8 ± 6.4	20.4 ± 8.7	144 ± 320	0.0594
IL-2	11.8 ± 14	18.2 ± 24	23.4 ± 12	24.5 ± 30	0.1524
IL-6	58.6 ± 190	0.00 ± 0.0	58.6 ± 190	319 ± 740	0.0856
EGF	37.2 ± 42	22.7 ± 20	14.8 ± 11	34.0 ± 42	0.7772
IL-13	0.669 ± 1.1	0.858 ± 1.9	1.20 ± 3.1	0.599 ± 1.9	0.7739
IL-10	78.0 ± 29	62.1 ± 22	55.0 ± 16	254 ± 540	0.2956
IL-12p70	22.7 ± 18	15.8 ± 14	32.7 ± 17	19.2 ± 28	0.1264
IFNγ	289 ± 110	209 ± 140	311 ± 95	180 ± 95[†]	0.0359, *
IL-5	31.9 ±16	27.8 ± 17	43.1 ± 21	48.6 ± 26	0.1014
IL-17A	14.2 ± 2.7	11.6 ± 3.2	12.5 ± 2.6	14.1 ± 7.7	0.3261
IL-18	900 ± 320	987 ± 290	986 ± 400	1310 ± 400	0.0654
CCL2[2]	1,640 ± 190[a,b]	1,330 ± 190[a]	1,640 ± 320[a,b]	1820 ± 620[b]	0.0274, *
IP-10	361 ± 40	343 ± 38	320 ± 60	341 ± 81	0.1078
CXCL1	145 ± 140	116 ± 140	153 ± 73	79.3 ± 100	0.3601
VEGF[2]	211 ± 21[a]	192 ± 34[a,b]	167 ± 18[b]	193 ± 44[a,b]	0.0138, *
CX3CL1	227 ± 18[a]	209 ± 22[a,b]	188 ± 22[b]	190 ± 25[b]	0.0018, **
CXCL5[2]	10,000 ± 2,100[a]	8,670 ± 1,400[a,b]	8,480 ± 1,500[a,b]	7,150 ± 1,500[b]	0.0047, **
CXCL2[2]	24.2 ± 19[a]	4.46 ± 10[a,b]	0.00 ± 0.0[b]	18.1 ± 27[a,b]	0.0076, **
TNFα	4.94 ± 1.5	5.06 ± 1.2	4.58 ± 1.5	4.08 ± 1.1	0.3831
CCL5	57,800 ± 12,000	62,500 ± 19,000	52,800 ± 9,100	49,200 ± 16,000	0.2522

[1]Kruskal-Wallis or ANOVA test for effect of FS on mean, n=10/group. *p*-value summary: *, $p < 0.05$; **, $p < 0.01$. [2]Means with different superscripts are significantly different by post-hoc Dunn's or Tukey's test, $p < 0.05$. [†]Comparison to FS-30 mean p-value: $0.08 > p > 0.05$.

SUPPLEMENTARY FIGURES

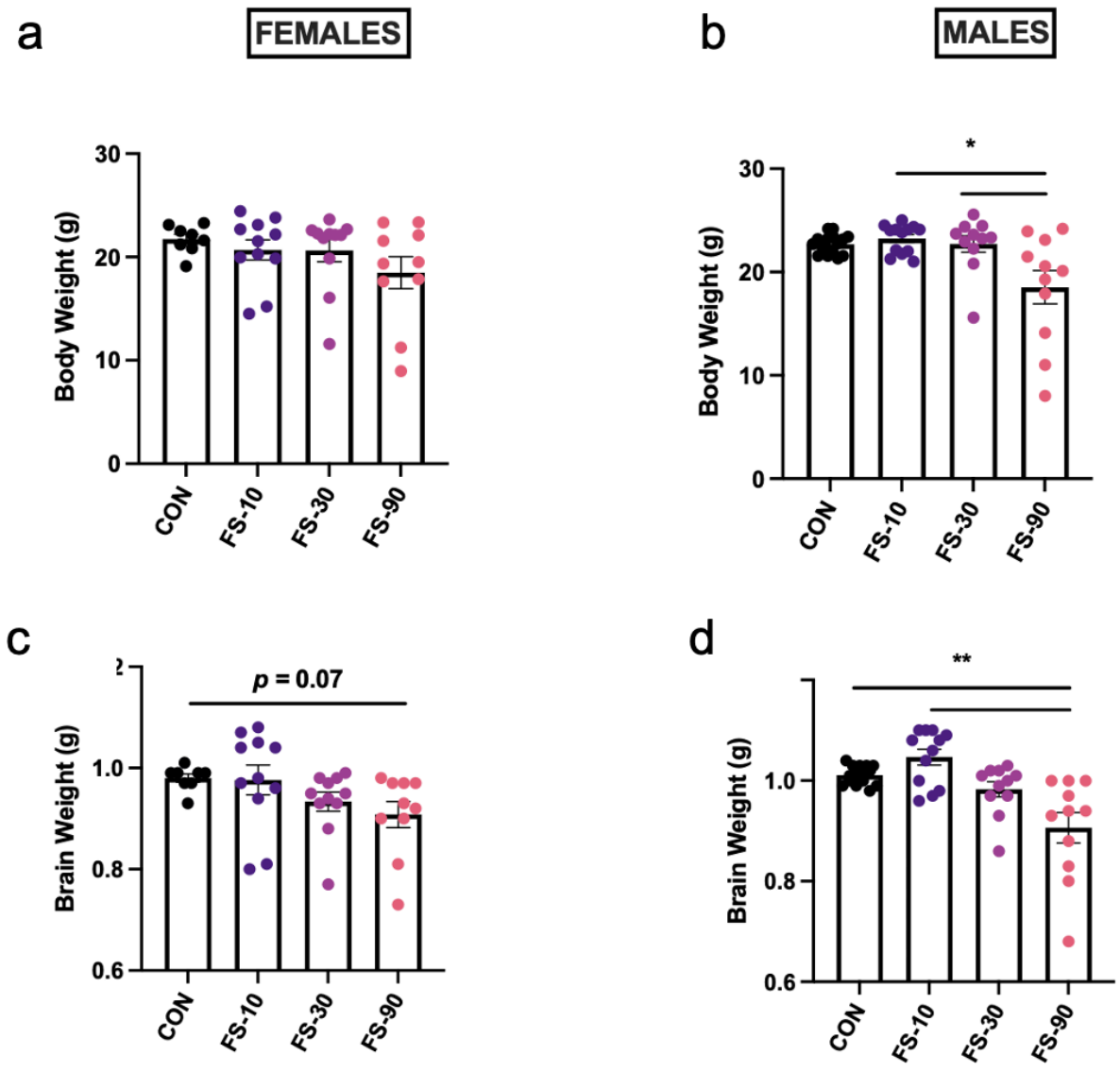

Supplementary Figure 1. Growth and development are disrupted only in male pups that received excess FS. (a-b) Litter weight gain is reduced in FS-90 males but not females at study end point, PD 10. (c-d) Brain weight at necropsy on PD 10 is reduced in males but females that received excess FS. Means ± SEM are shown. *p*-value summary: *, $p < 0.05$; **, $p < 0.01$.